Characterization of water repellency for natural soil and hydrophobized sand: Development of a hydrophobized capillary barrier system for surface water control at solid waste landfills

Japanese title:

自然土壌及び疎水性添加砂の撥水性特性：廃棄物処分場における地表水制御の
ための疎水性キャピラリーバリヤシステムの開発

by

Yodhasinghege Nadeeka Senani Wijewardana

B. Sc. Agricultural, Technology and Management (University of Peradeniya) 2009

M. Phil. Integrated Water resources Management (PGIA, University of Peradeniya) 2012

DISSERTATION

Submitted in partial fulfillment of the requirement for the degree of

DOCTOR OF PHILOSHOPHY

in

International Graduate Program on Environmental Science and Infrastructure Engineering

to the

Graduate school of science and Engineering

SAITAMA UNIVERSITY

Approved by

Prof. Ken Kawamoto, Academic supervisor and committee chairman

Prof. Norio Tanaka, Committee member

Dr. Masahiko Osada, Committee member

Dr. Shingo Asamoto, Committee member

September 2015

ACKNOWLEDGMENT

TABLE OF CONTENTS

LIST OF FIGURES

LIST OF TABLES

Chapter 1

1. GENERAL INTRODUCTION

Environmental and social problems related to solid waste dump sites are common in most of developing countries since they are practicing open dumping as a final disposing method. Therefore, waste directly expose to environment and will emit the greenhouse gases as well as problem to the people's health who living in near to the dumping area. Moreover during the rainy season, production of landfill leachate will contaminate both surface and groundwater resources. In Sri Lanka, almost all the open dumps are operated as unmanaged and uncontrolled due to lack of technology, high cost of operation and maintenance and running out of capacity etc. (Sewwandi et al., 2012). Therefore, it is important to introduce simple and low cost capping system to the waste sites and it will help to create aesthetic appearance too in addition to solving the above problems.

Modern engineered capping systems are technically effective, but they do not provide a feasible solution for landfills located in developing countries due to economic and technical constraints. In Table 1.1 is summarizing the basic requirements for fulfilment of capping systems: use of site specific materials, low-cost technology, sustainable long-term performance and also environment friendly (Subedi et al., 2012). Recently earthen covers such as capillary barrier and evapotranspirative covers have been proposed as technically feasible and low cost method (Nakafusa et al., 2011; Khire et al., 2000; Simon and Muller, 2004).

1.1 Capillary barrier cover systems

Capillary barrier cover system (CBCS) consists fine-over-coarse grain layers, which help to prevent water infiltration and control seepage into solid waste landfills. Capillary barrier effect is mainly govern by the contrast in hydraulic conductivity (K) between the fine and coarse grain layers at similar suction heads which exist near the fine-coarse grain layer interface. Fig. 1.1a represent the variation of K during the wetting process in two layers. At the beginning of wetting process/ or infiltration of fine layer has a finite K, whereas the K of the coarse layer is very small and would be immeasurable. With continuing of infiltration process, water content of the fine grain layer will increase gradually and suction will be reduced. So that, K of fine layer will increased gradually and K of coarse layer will remain immeasurably small until its

water entry head is overcome. Therefore, water will not move from the fine layer into the coarse layer. So water will be diverted along the fine-coarse interface and it will enhance the diversion length (L) when it's sloped (Fig. 1.1b).

Table 1.1 Requirements for capillary barrier cover systems summarized from Sharma and Reddy (2004), Simon and Müller (2004) and Benson and Khire (1995) (after Subedi et al., 2012).

No	Item	Key points	Description
1	Site specific	Use of locally available materials	Construction materials are easily available in rural areas
2	Low cost	Less investments and maintenance cost	Use of available construction materials is proved to be cost effective
3	Sustainable	Durable and long-term performance	Design system performs well for controlling infiltration and surface water seepage for desired periods
4	Environmentally friendly	Use of environmental friendly materials and technologies	Construction materials are nontoxic and do not harm human health or the environment
5	Engineered	Easy construction	Proposed system is easy to construct with locally available manpower and skills

(a)   **(b)**
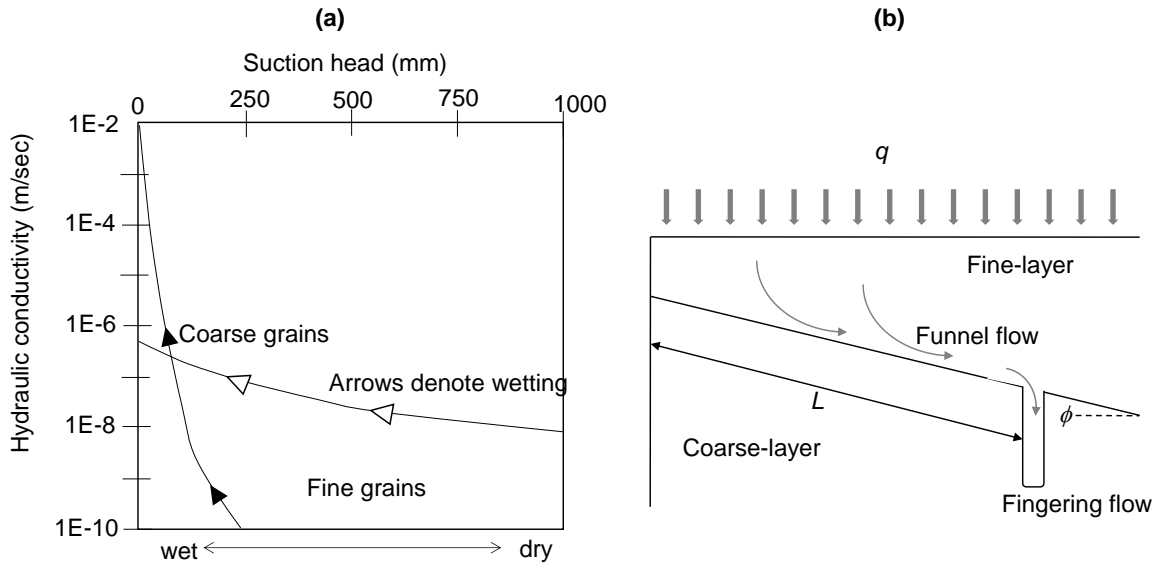
Figure 1.1 (a) Typical hydraulic conductivity of fine and coarse grains which can produce capillary barrier effect and (b) function of capillary barrier.

1.2 Theoretical Considerations

Mechanism of lateral diverting of water in CBCS has been discussed (Ross 1990; Stormont 1996; Parent and Cabral. 2006. Ross (1990) developed analytical relationships for the L and the diversion capacity (Q_{max}) of a capillary barrier (Eq.1.1) based on quasi-linear approximation for unsaturated and saturated hydraulic conductivities. The Ross's equation can be used to calculate the L (Eq. 1.2).

$$Q_{max} < K_s \tan \phi / \alpha \tag{1.1}$$

$$L < K_s \tan \phi / q \alpha \tag{1.2}$$

Where K_s is saturated hydraulic conductivity, α = sorptive number/ Gardner's α ($K(\psi) = K_s \exp(\alpha\psi)$ (Philip 1969; Gardner 1958), ψ = matric suction, ϕ = down dip angle and q = infiltration rate. There are more extended form of equations available to calculate L of CBCS (Kung, 1990 (Eq. 1.3); Steenhuis et al., 1991 (Eq. 1.4); Stormont, 1995 (Eq. 1.5)). Stormont. (1995) can be used in case of anisotropy K.

$$L = \frac{K_s \, \sigma_w \sin 2\emptyset}{q \rho_w g} \left(\frac{1}{r} - \frac{1}{R} \right) \qquad (1.3)$$

$$L = \tan \phi \left[\frac{1}{\alpha} \left(\frac{K_s}{q} - 1 \right) + \frac{K_s}{q} \left(h_a - h_w \right) \right]$$
(1.4)

$$L = \frac{K_{s,xx} \tan \emptyset}{q} \left[\frac{1}{\alpha} \right] \left(1 - \frac{q \cos \xi}{K_{s,zz} \cos \emptyset} \right) + (h_a - h_w) + \left(\frac{K_{s,xx} - K_{s,zz}}{K_{s,zz}} \right) \tan \emptyset \cos \xi b \qquad (1.5)$$

where, σ_w: surface tension of water, ρ_w: density of water, g: acceleration of gravity, r: the smallest pore in the top-layer (fine), R: the largest pore in the sub-layer (coarse), h_a: air-entry suction in the top-layer (cm), h_w: water-entry suction in the sub-layer (cm), b = thickness of fine-layer and θ and ξ = down dip contact angles and contact angle for vertical direction's hydraulic conductivity component respectively.

There are number of possibilities for increasing the L of CBCS. One of technique is to construct fine layer with a soil which has a great hydraulic conductivity (Stormont 1996). Limitation of a more conductive soils are explained by Stormont. (1996) as (1) the soil may not be readily available, increasing the cost of the capillary barrier; (2) the soil may not serve as an adequate rooting medium; (3) the storage capacity of the soil may be relatively small; and (4) the soil might not be possess the necessary unsaturated transport characteristics to develop a capillary break with the underlying material. Therefore, hydrophobized CBCS has been proposed by Dell'Avanzi et al., 2010 and Subedi et al., 2012 to increase diversion length, L or to enhance the impermeable properties.

1.3 Application of Hydrophobized Capillary Barrier Cover System

Impermeable properties of CBCS might be loss due to continue infiltration and especially in rainy periods. Application of water repellent grains into coarse layer (CL) will enhance the impermeable properties (Dell'Avanzi et al., 2010; Subedi et al., 2012).

Water repellent grains can be prepared by mixing-in or solvent-in hydrophobic agents (Subedi et al., 2012) such as polytetrafluorethylene (Dell'Avanzi et al., 2010), stearic acid

(Leelamanie et al., 2008; González-Peñaloza et al., 2013), oleic acid (Subedi et al., 2012), and dichloromethylsilane (Bachmann and McHale, 2009).

Figure 1.2 illustrated the hydrophobized CBCS and process of water diversion. Non hydrophobic grains absorb water quickly and hydrophobic grains surface will help to persist water drops on surface without infiltrating. Therefore, it is advantageous to divert water easily along the fine-coarse interface.
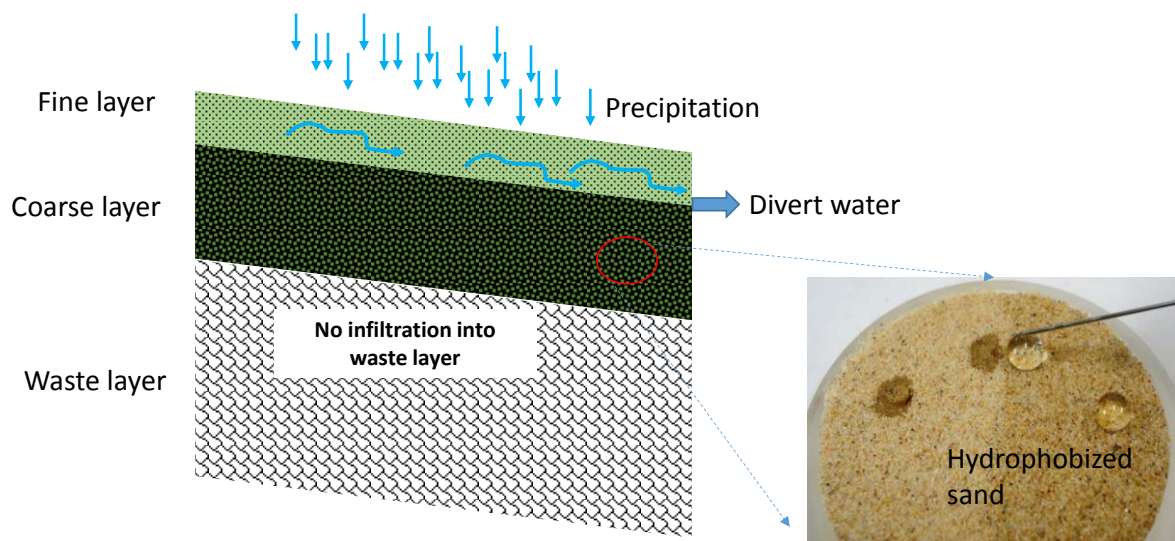
Figure 1.2 Schematic diagram of hydrophobized capillary barrier cover system.

The degree of water repellence can be tested using different test methods such as water drop penetration time (WDPT) (King, 1981), molarity of an ethanol droplet test (MED) (Roy and McGill, 2002) and sessile drop method (SDM) (Bachmann et al., 2000a; Bachmann et al., 2000b). Using above methods we can evaluate either water drop persistency (time, sec.) or soil-water initial contact angle. Figure 1.3 show the degree of hydrophobicity for different size of grains. There is an optimum content that can be produced maximum hydrophobicity.

5
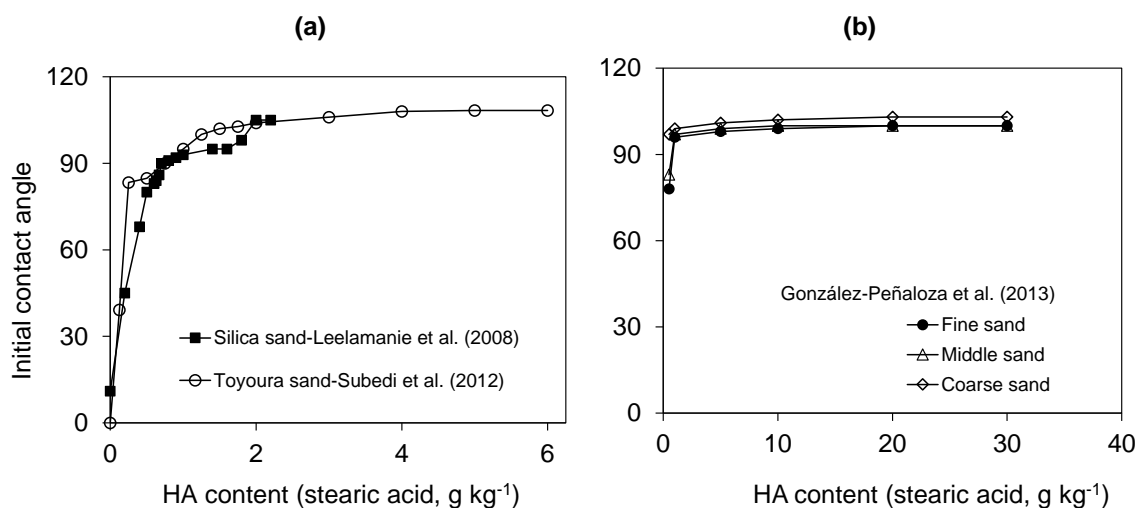
Figure 1.3 Degree of hydrophobicity for sands with different hydrophobic agent contents.

1.4 Scope and objectives

In this PhD study, mainly focused on grain size selection for hydrophobized capillary barrier and parallel to that characterize the soil-water repellency for different soil types to understand the behavior of soil water repellency characteristics curve. The three specific objectives of this Ph.D. study were (i) Characterizing of Water Repellency for Hydrophobized Grains with Different Geometry and Size, (ii) Soil-Water Repellency Characteristic Curves for Soil Profiles with Organic Carbon Gradients, and (iii) Qualitative assessment of water repellent soil using XPS measurements.

The structure of the Ph.D. dissertation including the focus and content of each of the four chapters following this introductory chapter is given below (Fig. 1.4):

Chapter 1 is the **GENERAL INTRODUCTION** including background, research motivation and objectives of this study.

Chapter 2 is the study on **CHARACTERIZATION OF WATER REPELLENCY OF HYDROPHOBIZED GRAINS WITH DIFFERENT GEOMETRIES AND SIZES.** Recently, earthen cover systems are most popular application in solid waste management sector to use as final cover system. Capillary barrier cover system (CBCS) is one of the most cost effective application for CBCS to prevent water infiltration into the waste site. But, country

6

like Sri Lanka receiving a high amount of precipitation throughout the year. So, impermeability of CBCS can be a problem, therefore to increase the performance a hydrophobized CBCS might be a use full technique. Therefore, six grains type were evaluated to use as a CBCS coarse layer materials.

Chapter 3 is the identification and characterization of soil water repellency under the title of **SOIL-WATER REPELLENCY CHARACTERISTIC CURVES FOR SOIL PROFILES WITH ORGANIC CARBON GRADIENTS.** Soil samples were collected from Japan and New Zealand sampling sites under different vegetation type. Soil samples were prepared with different soil-moisture content and degree of soil-water repellency was measured using three common methods. They are water drop penetrating time (WDPT), Molarity of ethanol droplet method and sessile drop method (SDM). Results were compared with ratio of clay/soil organic carbon. As a main findings, soil water repellency parameters were introduced based on soil water repellency characteristics curves. Suggested parameters were compared with soil organic carbon content.

Chapter 4 is the qualitative study of soil organic matter under the title of **CHEMICAL CHARACTERIZATION (C, N AND O) OF WATER REPELLENT SOIL USING X-RAY PHOTOELECTRON SPECTROSCOPY MEASUREMENTS.** Selected soil samples from Japan and New Zealand were studied with X-ray photoelectron spectroscopy. We found that, there is an effects from soil organic carbon content on soil water repellency and it is important to study the surface carbon, nitrogen and oxygen composition of water-repellent soil compare to the non-repellent soils.

Chapter 5 is the **SUMMARY, CONCLUSIONS AND PERSPECTIVES** of this study.

CHAPTER 1
GENERAL INTRODUCTION

THEME I: *APPLICATION OF WATER REPELLENCY*

CHAPTER 2
CHARACTERIZATION OF WATER REPELLENCY OF HYDROPHOBIZED GRAINS WITH DIFFERENT GEOMETRIES AND SIZES

THEME II: *IDENTIFICATION AND CHARACTERIZATION OF SOIL WATER REPELLENCY*

CHAPTER 3
SOIL-WATER REPELLENCY CHARACTERISTIC CURVES FOR SOIL PROFILES WITH ORGANIC CARBON GRADIENTS

CHAPTER 4
CHEMICAL CHARACTERIZATION (C, N AND O) OF WATER REPELLENT SOIL USING XPS MEASUREMENTS

CHAPTER 5
SUMMARY, CONCLUSIONS AND PERSPECTIVES

Figure 1.4 Structure of this dissertation

1.5 References

Bachmann, J., McHale, G., 2009. Superhydrophobic surfaces: A model approach to predict contact angle and surface energy of soil particles. Eur. J. Soil Sci. 60:420–430. doi:10.1111/j.1365-2389.2008.01118.x.

Bachmann, J., Ellies, A., Hartge, K.H., 2000a. Development and application of a new sessile drop contact angle method to assess soil water repellency. Journal of Hydrology, 231-232: 66–75.

Bachmann, J., Horton, R., van der Ploeg, R. R. and Woche, S., 2000b. Modified sessile drop method for assessing initial soil–water contact angle of sandy soil. Soil Sci. Soc. Am. J. 64: 564-567.

Dell'Avanzi, E., Guizelini, A. P., da Silva, W. R., Nocko, L.M., 2010. Potential use of induced soil-water repellency techniques to improve the performance of landfill's alternative final cover systems. p. 461–466. In O. Buzzi et al. (ed.) Unsaturated soils. Vol. 1. Experimental studies in unsaturated soils and expansive soils. CRC Press, Boca Raton, FL.

Gardner, W.R., 1958. Some steady state solutions of the unsaturated moisture flow equation with application to evaporation from a water table. Soil Sci., 85: 3228-3232.

González-Peñaloza, F. A., Zavala, L. M., Jordán, A., Bellinfante, N., Bárcenas-Moreno, G., Mataix-Solera, J., Granged, A.J.P., Granja-Martins, F.M., Neto-Paixão, H.M., 2013. Water repellency as conditioned by particle size and drying in hydrophobized sand. Geoderma, 209-210, 31–40. doi:10.1016/j.geoderma. 2013.05.022.

Khire, M., Benson, C., Bosscher. P., 2000. "Capillary Barriers in Semi-Arid and Arid Climates: Design Variables and the Water Balance," Journal of Geotechnical and geoenvironmental Engineering, ASCE, 126(8), 695-708.

King, P.M., 1981. Comparison of methods for measuring severity of water repellence of sandy soils and assessment of some factors that affect its measurement. Australian Journal of Soil Research, 19:275–285.

Kung, K.J.S., 1990. Preferential flow in a sandy vadose zone 2. Mechanisms and implications. Geoderma 46, 59–71.

Leelamanie, D.A.L., Karube, J., Yoshida. A., 2008. Relative humidity effects on contact angle and water drop penetration time of hydrophobized fine sand. Soil Science and Plant Nutrition, 54: 695-700.

Nakafusa, S., Kobayashi, K., Morii, T., Takahashita, Y., 2001. Estimation of water diversion provided by capillary barrier of soils, Unsaturated Soils: Theory and Practice 2011 Jotisankasa, Sawangsuriya, Soralump and Mairaing (Eds). Kasetsart University, Thailand.

Parent, S.E., Cabral, A., 2006. Design of inclined covers with capillary barrier effect. Geotechnical and geological engineering. 24: 689-710. DOI 10.1007/s10706-005-3229-9.

Philip, J.R., 1969. Theory of infiltration, Adv. Hydrosci., 5, 215-296.

Ross, B., 1990. The diversion capacity of capillary barriers, Water Resour. Res., 26, 625-2629.

Roy, J.L., McGill. W.B., 2002. Assessing soil water repellency using the molarity of ethanol droplet (MED) test. Soil Sci. 167: 83–97. doi:10.1097/00010694-200202000-00001.

Sewwandi, B.G.N., Takahiro, K., Kawamoto, K., Hamamoto, S., Shingo Asamoto, S., Sato, H., 2012. Characterization of Landfill Leachate From Municipal Solid Wastes Landfills In Sri Lanka. International Conference on Sustainable Built Environment, Kandy, Sri Lanka.

Simon, F.G., Müller. W.W., 2004. Standard and alternative landfill capping design in Germany. Environmental science policy 7: 277-290.

Steenhuis, T.S., Parlange, J.-Y., Kung, K.-J.S., 1991. Comment on "The diversion capacity of capillary barriers" by Benjamin Ross. Water Resour. Res., 27: 2155-2156.

Stormont, J.C., 1996. The effectiveness of two capillary barriers on a 10% slope. Geotechnical and geological engineering. 14(4), 243–267.

Stormont, J.C., 1995. The effect of constant anisotropy on capillary barrier performance, Water Resour. Res., 31, 783-785.

Subedi, S., Kawamoto, K., Jayarathna, L., Vithanage, M., Moldrup, P., de Jonge, L.W., Komatsu. T., 2012. Characterizing time dependent contact angle for sands hydrophobized with oleic and stearic acids. Vadose zone Journal, 11 (1), doi:10.2136/vzj2011.0055.

Wijewardana, Y.N.S., Kawamoto, K., Moldrup, P., Komatsu, T., Kurukulasuriya, L. C., Priyankara, N. H. 2015. Characterization of Water Repellency for Hydrophobized Grains with Different Geometry and Size. Environmental earth science (Accepted).

Chapter 2

2. CHARACTERIZATION OF WATER REPELLENCY OF HYDROPHOBIZED GRAINS WITH DIFFERENT GEOMETRIES AND SIZES

ABSTRACT

Capillary barrier cover systems (CBCSs) are useful and low-cost earthen cover systems for preventing water infiltration and controlling seepage at solid waste landfills. A possible technique to enhance the impermeable properties of CBCSs is to make water repellent grains by mixing the earthen cover material with a hydrophobic agent (HA). In this study, six different grains with different geometries and sizes were used to prepare dry hydrophobized grains by mixing with different contents of oleic acid (OA) as a HA. Wet hydrophobized grains were prepared by adjusting the water content (θ_g; kg kg^{-1}) of dry hydrophobized grains. To characterize the water repellency (WR) of dry and wet hydrophobized grains, initial solid-water contact angles (α_i) were measured using the sessile drop method (SDM). Based on SDM results from the α_i-HA content and α_i-θ_g curves, useful WR indices were introduced as "$Area_{\_dry}$" and "$Area_{\_wet}$" (areas under the α_i-HA content and α_i-θ_g curves), "$HA_{\_zica}$" and "θ_{g_zica}" (maximum HA content and θ_g at which WR disappears), and "$\alpha_{i,\ peak}$" and "$HA_{\_\alpha i,\ peak}$" (peak α_i in the α_i-HA content curve and corresponding HA content to $\alpha_{i,\ peak}$). Pearson correlation analysis was performed to identify correlations between proposed WR indices and basic grain properties. Results showed that WR indices correlated well to d_{50} and coefficient of uniformity (C_u) and regression equations for WR indices were obtained as functions of d_{50} and C_u ($r^2 > 0.7$).

2.1 Introduction

A landfill capping system for solid waste landfills is a key component in engineered solid waste landfills (Purdy and Horton 1999; Simon and Müller 2004). An appropriate design of the landfill capping system is important to prevent infiltration of precipitation into the waste, minimize leachate generation from the landfill sites (Koerner and Daniel 1992), and isolate waste from the environment (Pease and Stormant 1996; Yanful et al., 2006). Moreover, a landfill capping system is necessary for preventing bio-intrusion and controlling landfill gas emissions (Bozkurt et al., 2001). Modern engineering capping systems such as geo-membranes, geotextiles, and geo-synthetic clay liners are technically effective (Koerner and Daniel 1997), but, they are not acceptable for waste landfills in developing countries due to economic and technical constraints (Sharma and Reddy 2004; Simon and Müller 2004; Subedi et al., 2012). Therefore, earthen cover systems (Benson and Khire 1995) including evapotranspirative covers (Scanlon et al. 2005) and capillary barrier cover systems (CBCSs) (Tidwell et al., 2003; Morris and Stormont 1998) have been studied in recent years as acceptable and low-cost techniques for waste landfills in developing countries.

CBCS consists of a fine grain layer over a coarse grain layer. Percolated water from the top surface is retained in the interface between these layers without penetrating into the coarser-grained layer due to capillary force in the fine-grained layer. Then the water retained in the fine-grained layer can be removed by evapotranspiration (Khire et al., 2000) and/or diverted to drainage along the inclined interface of the layers (Ross 1990; Steenhuis et al., 1991; Stormont 1995). As examined by Dell' Avanzi et al. (2010) and Subedi et al. (2012), a possible technique to enhance the abilities of a capillary barrier and control seepage is to make the coarse-grained materials water repellent by mixing or coating them with hydrophobic agents (HAs).

Various HAs have been tested to alter the hydrophobicity of grain surfaces: silicone resins, amine acetates, fluoro-chemicals (Fink 1970), polyoxyalkylated diethylenetriamine (Alexandrova et al., 2011), dichlorodimethylsilane (DCMS) (Liu et al., 2012), polytetrafluorethylene (Dell' Avanzi et al., 2010), stearic acid (Leelamanie et al., 2008; Subedi et al., 2012; González-Peñaloza et al., 2013), and oleic acid (Subedi et al., 2012). They reported that the hydrophobized grains were fully effective to repel the water, based on the results of tests of water repellency (WR) such as water drop penetration time (King 1981), molarity of an ethanol droplet test (Roy and McGill 2002) and sessile drop method (SDM) (Bachmann et al., 2000a, b). These studies were carried out by using materials of one or several different sizes

(Leelamanie et al., 2008-silica sand; Subedi et al., 2012-fine sand; González-Peñaloza et al., 2013-quartz sand). However, the effects of grain size and geometry on the WR characteristics of hydrophobized grains have not yet been fully investigated even though such information is necessary to select suitable materials for designing an appropriate hydrophobized CBCSs.

Furthermore, one of the practical concerns of using hydrophobized grains under natural conditions is the reduction of WR due to the variation in water content under repeated infiltration and water redistribution processes, implying that the abilities of capillary barrier and seepage control in the CBCS will change with time due to the change in WR of the hydrophobized grains. Several researchers have examined the effects of water content (Karunarathna et al., 2010) on the WR characteristics for natural soil samples. For example, de Jonge et al. (1999) and Kawamoto et al. (2007) measured the degree of WR for soil samples with different water contents. They found nonlinear relationships between the degree of WR and water content of most tested soil samples, indicating that the increase in water content does not simply cause the reduction in WR. However, quantitative assessments of the effects of water content on WR characteristics of hydrophobized grains are very limited. Liu et al. (2012) reported a reduction in the soil-water contact angle (thus, degree of WR) for hydrophobized grains (natural sand mixed with DCMS) with increasing water content. Further studies are needed for evaluating the effects of water content on hydrophobized grains and their performance in the CBCS.

This study focused on WR for grains hydrophobized with oleic acid and specific objectives were to: (i) examine the effects of a hydrophobic agent content and water content on WR (ii) suggest new WR indices for dry and wet hydrophobized grains and (iii) discuss relationships between suggested WR indices and tested grain sizes and geometry for the material selection in the CBCS.

2.2 Materials and Methods

2.2.1 Description of tested materials

Commercial grains with round shapes: Accusand 40/50 (0.105-0.425 mm, Unimin Corp., USA) and glass bead (0.075-0.25 m, Potters-Ballotini Co., Ltd., Japan) were used as the first group of tested materials (Table 2.1). Natural grains of Toyoura sand (0.105-0.25 mm, Toyoura

Keiseki Kogyo Co., Ltd., Japan) and Narita sand (0.105-0.84 mm, sampled from the surface layer of an earthen dam in Nagara Town, Chiba, Japan) with less round shapes were used as the second group of test materials. Narita sand was used after sieving into three different grain size fractions as Narita small (0.105-0.25 mm), Narita middle (0.25-0.425 mm) and Narita large (0.425-0.84 mm) (Table 2.1). Figure 2.1a shows grain size distributions for six tested materials. Microscope photographs (VHX-1000, KEYENCE, Osaka, Japan) of materials used are shown in Figs.2.1b to 2.1g at 100x magnification. Physical properties of grain samples are shown in Table 2.1. The N_2 adsorption surface area (SSA_{N2}) was measured using a Surface Area and Porosity Analyzer (TriStar II series, Micromeritics Instrument Corp, GA, USA) for all grains (Table 2.1). Measurement was based on the theory developed by Brunauer et al. 1938. Air-dried grain samples were vacuum dried in a sample chamber at 105 °C for 24 h to remove inert gas and moisture adsorbed on grains surfaces. Sub samples weighing 0.5 g each were used immediately to measure SSA_{N2} in triplicate.
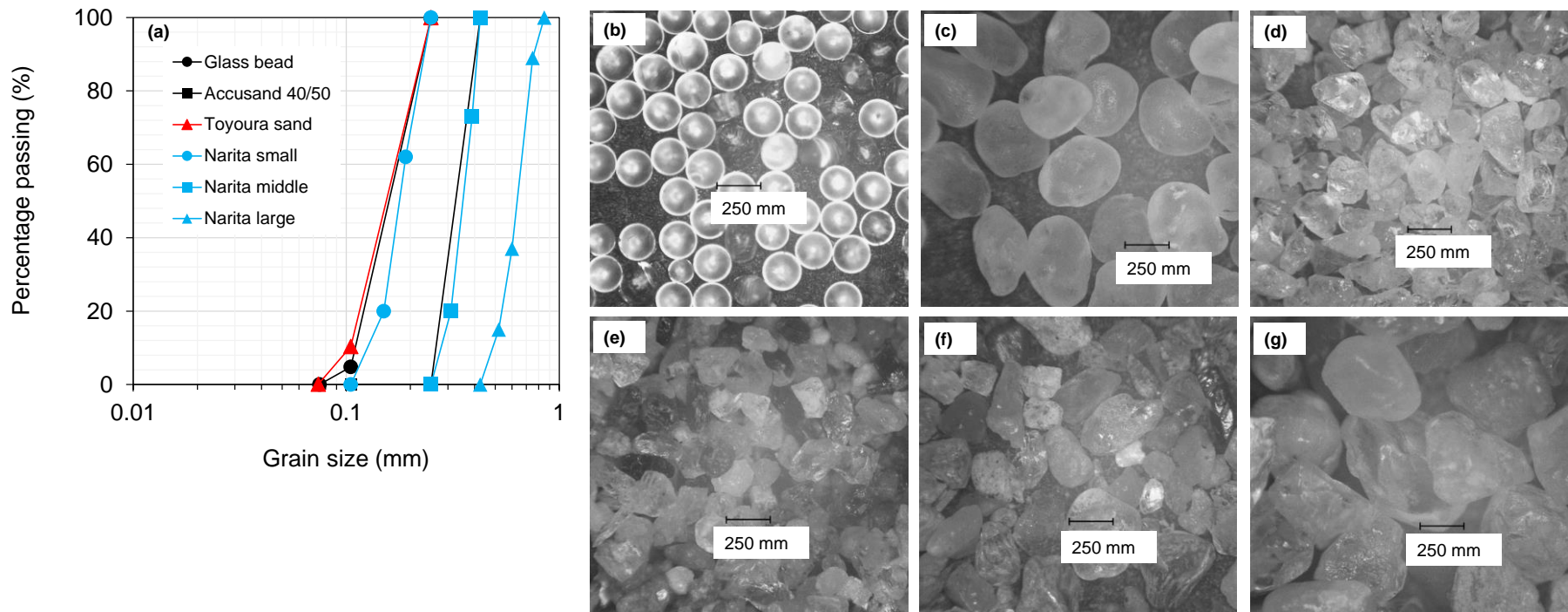
Figure 2.1 Grain size distribution of tested materials (a) and photographs of grains samples (100x); (b) Glass bead, (c) Accusand 40/50, (d) Toyoura sand, (e) Narita small, (f) Narita middle, (g) Narita large.

Table 2.1 Physical properties of used materials; mean diameters at percentage pass 50 % (d_{50}), uniformity of coefficient (C_u), roundness (R_n), sphericity (S_p), dry bulk density (ρ_d), particle density (ρ_s), porosity (ϕ) and N_2 adsorption surface area (SSA_{N2}).

	Material (mm)	d_{50} (mm)	C_u	R_n[†]	S_p[†]	ρ_d g cm^{-3}	ρ_s g cm^{-3}	$\emptyset$	Quartz content (%)	SSA_{N2} (m^2 g^{-1})
Commercial grains	Glass bead (0.075-0.25)	0.15	1.70	1.00	1.00	1.53	2.55	0.40	70-73	5.7 ±0.61)
	Accusand 40/50 (0.105-0.25)	0.35	1.30	0.80	0.80	1.77	2.66	0.32	99.8	5.3 (±0.69)
Natural grains	Toyoura sand (0.105-0.25)	0.17	1.80	0.20	0.75	1.58	2.64	0.40	75.0	2.4 (±0.16)
	Narita small (0105-0.25)	0.19	1.46	0.35	0.73	1.62	2.70	0.40	34.0	11 (±0.35)
	Narita middle (0.25-0.425)	0.35	1.39	0.35	0.73	1.58	2.63	0.40	34.0	8.8 (±0.56)
	Narita large (0.425-0.84)	0.64	1.33	0.35	0.73	1.56	2.60	0.40	34.0	7.7 (±0.4)

[†] Data from Naveed et al. (2011).

2.2.2   Preparation of hydrophobized grains by mixing with oleic acid

Oleic acid (OA, molar mass of 282.46 g mol^{-1}, density of 0.895 g cm^{-3}, Kanto Chemical Corp, Tokyo, Japan) was used as a hydrophobic agent (HA) to make hydrophobized materials by a mixing-in method (Subedi et al., 2012). OA is a mono-unsaturated omega-9 fatty acid consisting of CH_3 and CH_2 groups, a carboxyl groups (COOH) and a vinyl CH group (double bond CH=CH). OA is rich in coconut oil which is a low-cost and easily available material in developing countries in wet tropical regions and is expected to be highly utilized in producing hydrophobized grains for CBCSs.

First, all six different materials were washed with a low-foaming neutral cleansing agent, and then rinsed thoroughly with distilled water several times following the procedure of Subedi et al. (2012). The washed grains were air dried and stored under climate controlled condition (20 $^{\circ}$C and 50 % RH) for two weeks. Air-dry grains were mixed with different content of OA (0 g kg^{-1} to 35 g kg^{-1}). All the OA mixed samples were then stored in sealed plastic bags under the same controlled climate condition. Those samples were labeled as "dry hydrophobized grains".

Water content of the selected OA mixed samples (1 and 5 g kg^{-1}) were adjusted by adding a known amount of distilled water. The water adjusted samples were mixed well and stored in plastic bags under the climate controlled condition. We labeled these moisture adjusted samples "wet hydrophobized grains". All biological or chemical processes during the storage period were ignored in this study because samples were used within 2-days after preparation.

2.2.3   Contact angle measurements by sessile drop method (SDM)

SDM enables determination of the contact angle (α) between the grain surface and a water drops (Bachmann et al., 2000a; Leelamanie and Karube 2007; Subedi et al., 2012) to characterize the degree of WR. Samples were prepared for SDM, by either an adhesive tape method or a repacked sample method. The adhesive tape method is a standard sample preparation method for SDM, and a monolayer of grains was created by spreading grain on a tape and then removing the excess grains (Bachmann et al., 2000a, b; Subedi et al., 2012). The adhesive tape method, however, was difficult to use for dry hydrophobized grains which are

OA mixing-in amount > 20 g kg^{-1} and for wet hydrophobized grains (oily and wettable surfaces). To overcome the above limitation in sample preparation, repacked samples were used in a cylindrical rings with the constant bulk density (ρ_d) given in Table 2.1.

After completing preparation of the sample grain surface, a digital microscope was focused on to the grain surface. Then microphotographs of the contact angle between water droplet and grain surface were recorded using the digital microscope (VHX-1000, KEYENCE, Osaka, Japan). Each sample measurement was repeated five times and the precision of the replication was $\pm 2.5^o$. All SDM were done under climate controlled conditions (20 ^{o}C and 55-65 % RH).

The sizes of the water droplets used in SDM should be considered along with different grain sizes (Liu et al., 2012; Diehl 2013; Wijewardana et al., 2014). Bachmann et al. (2000a) set a reference drop size of 10 µL for sand (0.063 –2 mm) and 2 µL for other materials (clay and silt), Buczko and Bens (2006) used 20 µL, Lamparter et al. (2010) used 1 µL, Liu et al. (2012) used 30 µL and Chau et al. (2014) used 4 µL. Based on these findings and preliminary studies, 20 µL was used for the Narita large fraction and 10 µL for the other grains.

2.3 Results and Discussion

2.3.1   Characterization of water repellency of dry hydrophobized grains

Changes in the initial contact angle (α_i) with increasing HA content, hereafter labeled the α_i - HA content curve, for different grain size fractions are shown in Figs. 2.2a (0-35 g kg^{-1}) and 2.2b (enlarged view of 0-10 g kg^{-1}). Samples of 0 g kg^{-1} (without HA) were wettable for all tested samples which had a zero initial contact angle, zica ($\alpha_i = 0^o$). With increasing HA content from 0.125 to 1.0 g kg^{-1}, α_i values measured for Toyoura sand, glass bead, Narita small and Narita middle sand increased from 0° to ~100°. The Narita large sand showed the maximum α_i of 84° at HA = 5.0 g kg^{-1}, and Accusand 40/50 showed the maximum α_i of 76° at HA = 1.0 g kg^{-1}. After the maximum α_i, Narita small, Narita middle and Toyoura sand showed plateau regions (almost constant α_i values) in the α_i - HA content curve from HA = 1 to 10 g kg^{-1}. On the other hand, Narita large sand had a plateau region only up to HA ~ 6 g kg^{-1} and, thereafter, the α_i values decreased with increasing HA content. Compared to the natural grains (Toyoura and Narita sands), commercial grains (Accusand 40/50 and glass beads) behaved differently.

18

Neither Accusand 40/50 nor glass bead showed plateau regions similar to Toyoura and Narita sands as shown in Fig. 2.2a. The α_i for commercial grains decreased drastically after reaching the maximum α_i values and became zero (non-WR) when the HA content greater than 8-9 g kg^{-1}. It is noted that Narita large sand and Accusand 40/50 did not show the $\alpha_i > 90^o$ at any HA content. According to past WR studies (King 1981; Dekker and Jungerius 1990), dry hydrophobized samples of Narita large sand and Accusand 40/50 can be considered as sub-critical water repellent materials ($0 < \alpha_i < 90^o$).
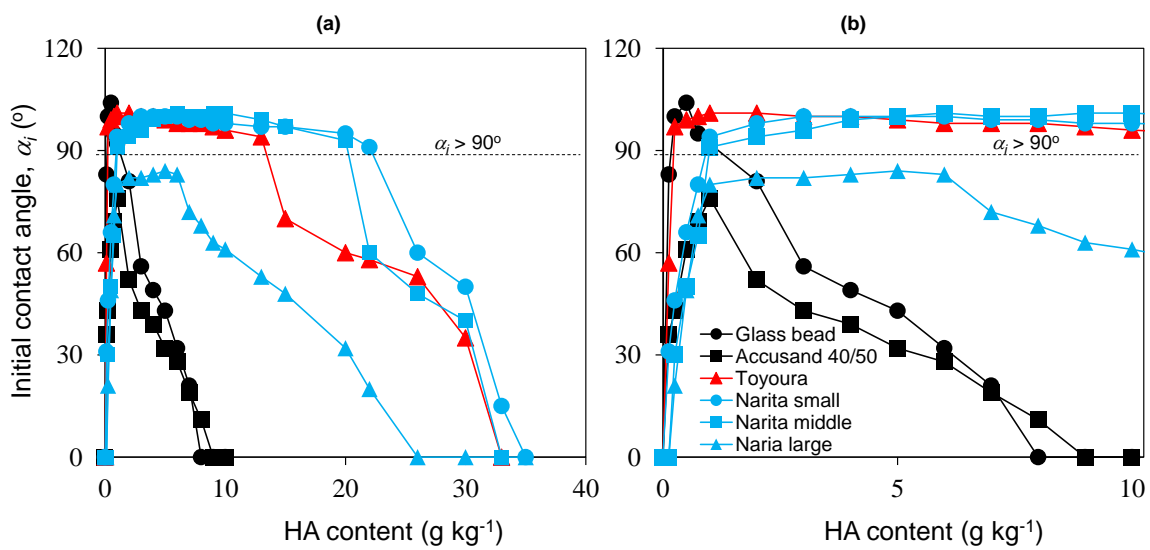
Figure 2.2 Variation of initial contact angle (α_i) with increasing HA content; α_i - HA content curve (a) 0 to 35 g HA per 1 kg of air dry material and (b) close-up view of initial contact angle variation for 0 to 10 g kg^{-1}.

2.3.2 Development of water repellency indices for dry hydrophobized grains

Several past studies have characterized WR curves for naturally water repellent soils (de Jonge et al., 1999; Regalado and Ritter 2005; Kawamoto et al., 2007). They introduced several indices that characterize WR curves (WR as a function of either soil-water content or soil-water potential) such as area below the WR curve and the soil-water content which gives WR peak, and so on. Similar to these approaches, WR indices for characterizing water repellency characteristics curves (WRCCs) for dry hydrophobized grains, i.e., α_i - HA content curve, have also been discussed.

19

Based on the present study and previously published data (Leelamanie et al., 2008; Subedi et al., 2012; González-Peñaloza et al., 2013), two types of curves can be identified for the α_i - HA content relationships: Type I and Type II (Fig. 2.3). The Type I curve shows an increase in the α_i values with HA increment (Region I), reaching to peak α_i and continuing to an apparent maximum α_i (Region II), and then a decrease in the α_i with HA increment (Region III) (see also Fig. 2.5a). Natural grains in this study, according to published data from Leelamanie et al. (2008), Subedi et al. (2012) and González-Peñaloza et al. (2013) belong to the Type I curve. On the other hand, the Type II curve has a single peak α_i without a Region II (see also Fig. 2.5b). Therefore, commercial grains with highly rounded shapes are categorized as Type II curves.
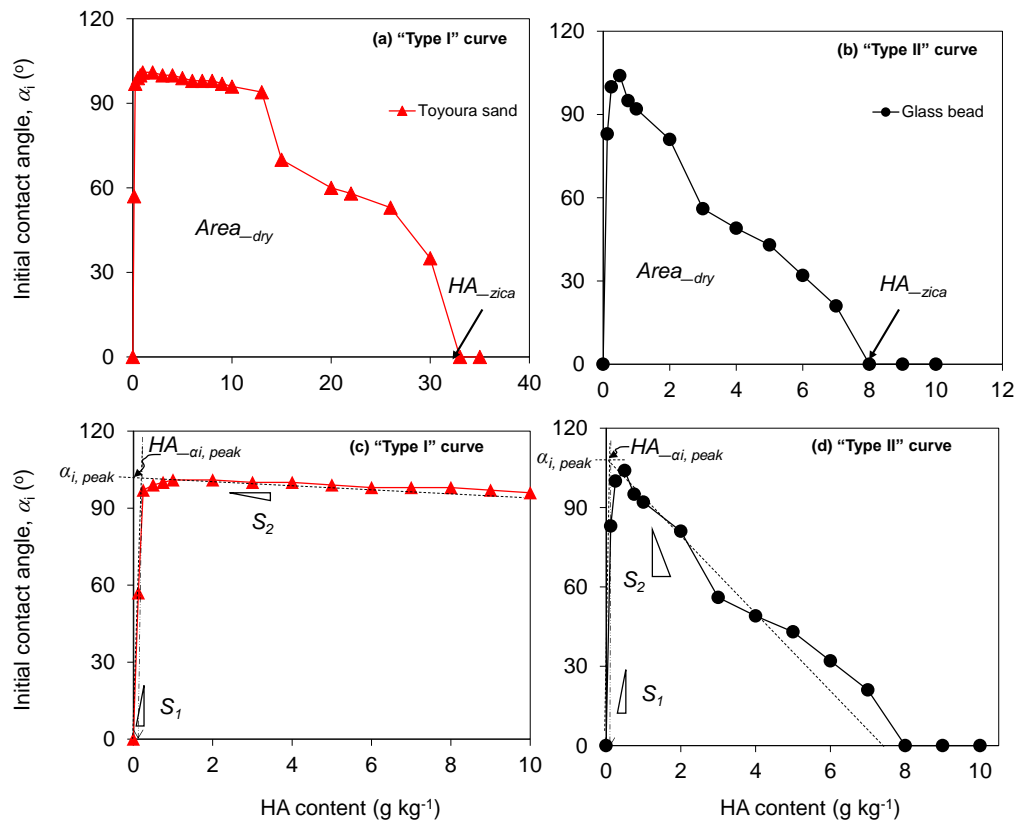
Figure 2.3 Schematic diagram for representing WR indices derived from α_i-HA content curve for dry hydrophobized grains; (a) *Area_dry* and *HA_zica* for "Type I" curve, (b) *Area_dry* and *HA_zica* for "Type II" curve, (c) S_1, S_2, $\alpha_{i, peak}$ and *HA_αi, peak* for "Type I" curve and (d) S_1, S_2, $\alpha_{i, peak}$ and *HA_αi, peak* for "Type II" curve.

Six WR indices of both Type I and II curves that characterize well the shapes of WRCCs for dry hydrophobized grains can be recognized (Fig. 2.3). They are (i) the area under the α_i -

20

HA content curve, "$Area_{\_dry}$", (ii) the maximum HA content at which WR disappears, "$HA_{\_zica}$", (iii) and (iv) slopes of increases and decreases in the α_i - HA content curve, "S_1" and "S_2", (v) HA content that gives a peak α_i value (the point where two tangents of the S_1 and S_2 slopes cross), "$HA\_\alpha_{i,\ peak}$", and (vi) the peak α_i value corresponding to the $HA\_\alpha_{i,\ peak}$, "$\alpha_{i,\ peak}$". According to the schematic illustration in Fig. 2.3, the $\alpha_{i,\ peak}$ does not always correspond to the maximum α_i value. All values of WR indices calculated from measurements are summarized in Table 2.2. Very low $Area_{\_dry}$ for Accusand 40/50 and glass bead were found compared to the Toyoura and Narita sands. As well as, low values of $HA_{\_zica}$ for glass bead and Accusand 40/50 were 8 and 9 g kg^{-1}, respectively. The $HA_{\_zica}$ of Toyoura sand and Narita sands varied between 26 - 35 g kg^{-1}.

Among the derived WR indices, $Area_{\_dry}$, $\alpha_{i,\ peak}$ and $HA\_\alpha_{i,\ peak}$ are important for optimizing the material selection for hydrophobized CBCSs. $Area_{\_dry}$ represents the hydrophobic capacity of dry hydrophobized materials. As well, $\alpha_{i,\ peak}$ and $HA\_\alpha_{i,\ peak}$ can be used for selecting cost effective materials that give a maximum WR (higher $\alpha_{i,\ peak}$ value) with a smaller amount of HA (lower $HA\_\alpha_{i,\ peak}$ value).

Figure 2.4 shows relationships between those WR indices in this study and calculated values for selected past studies. It is interesting that a unique linear relationship can be seen between $Area_{\_dry}$ and $HA_{\_zica}$ ($r^2 = 0.91$, n = 6) (Fig. 2.4a), implying that less rounded grains will result in higher values of $Area_{\_dry}$ and $HA_{\_zica}$ compared to the highly rounded grains. Further understanding is needed because our present study investigated only six samples. Figures 2.4b and 2.4c show the relationships of $\alpha_{i,\ peak}$ and S_1 to $HA\_\alpha_{i,\ peak}$. Published data on materials hydrophobized with stearic acid (Leelamanie et al., 2008; Subedi et al., 2012; González-Peñaloza et al., 2013) are also plotted in Figs. 2.4b and 2.4c. The $\alpha_{i,\ peak}$ values became rather constant irrespective of variation in $HA\_\alpha_{i,\ peak}$ (Fig. 2.4b). This indicates that variation of $\alpha_{i,\ peak}$ is independent of the type of HA that will give a different $HA\_\alpha_{i,\ peak}$. S_1 values decreased exponentially with increasing in $HA\_\alpha_{i,\ peak}$ (Fig. 2.4c). Finer grains will give an $\alpha_{i,\ peak}$ with a lower $HA\_\alpha_{i,\ peak}$ and coarser grains need a comparatively higher $HA\_\alpha_{i,\ peak}$ content to produce $\alpha_{i,\ peak}$. Therefore, grain size and surface roughness will affect S_1 value and $HA\_\alpha_{i,\ peak}$.

Table 2.2 Pearson correlation (r) among water repellency indices and physical properties (no. of sample, n = 4); C_u, d_{50} and SSA_{N2} (Excluding the rounded materials; Glass bead and Accusand 40/50). Correlations demarcated with square that are used to regression equations.

| Materials | WR indices for dry hydrophobized grains | | | | | | WR indices for wet hydrophobized grains | | | |
	$Area\_{dry}$ (rad. g kg⁻¹)	HA_{zica} (g kg⁻¹)	S_1 (°/ g kg⁻¹ HA)	S_2	$α_{i,\ peak}$ (°)	$HA\_α_{i,\ peak}$ (g kg⁻¹)	$Area\_{wet}$ (rad. kg kg⁻¹) 1 g kg⁻¹ HA	5 g kg⁻¹ HA	$θ_{g\_zica}$ (kg kg⁻¹) 1 g kg⁻¹ HA	5 g kg⁻¹ HA
Glass bead	6.5	8.0	172	22.5	106	0.25	3.3 x 10⁻²	1.9 x 10⁻³	25 x 10⁻³	6.5 x 10⁻³
Accusand 40/50	5.2	9.0	58	15.1	76	1.0	0.5 x 10⁻²	0.8 x 10⁻³	11 x 10⁻³	2.8 x 10⁻³
Toyoura	39	33	388	0.25	97	0.25	1.7 x 10⁻²	8.4 x 10⁻³	19 x 10⁻³	9.5 x 10⁻³
Narita small	47	35	86	0.25	94	1.25	2.8 x 10⁻²	28 x 10⁻³	25 x 10⁻³	24 x 10⁻³
Narita middle	43	33	93	0.1	93	1.0	2.5 x 10⁻²	20 x 10⁻³	22 x 10⁻³	19 x 10⁻³
Narita large	22	26	89	0.11	79	1.25	1.5 x 10⁻²	6.5 x 10⁻³	19 x 10⁻³	9.6 x 10⁻³
Calculated values for recently published data										
Subedi et al. (2011) (Toyoura sand)							11 x 10⁻²		10 x 10⁻²	
Liu et al. (2012) (natural sand)							4.8 x 10⁻²		3.3 x 10⁻²	
Leelamanie et al. (2008) (Silica sand)			120	2.22	82	0.5				
Subedi et al. (2012) (Toyoura sand)			329	0.25	101	0.25				
González-Peñaloza et al. (2013) (Quartz sand)										
Fine sand (0.05 - 0.25 mm)			36	0.06	99	1.0				
Middle sand (0.25 - 0.5 mm)			28	0.01	100	2.0				
Coarse sand (0.5 - 2.0 mm)			4	0.08	101	5.0				
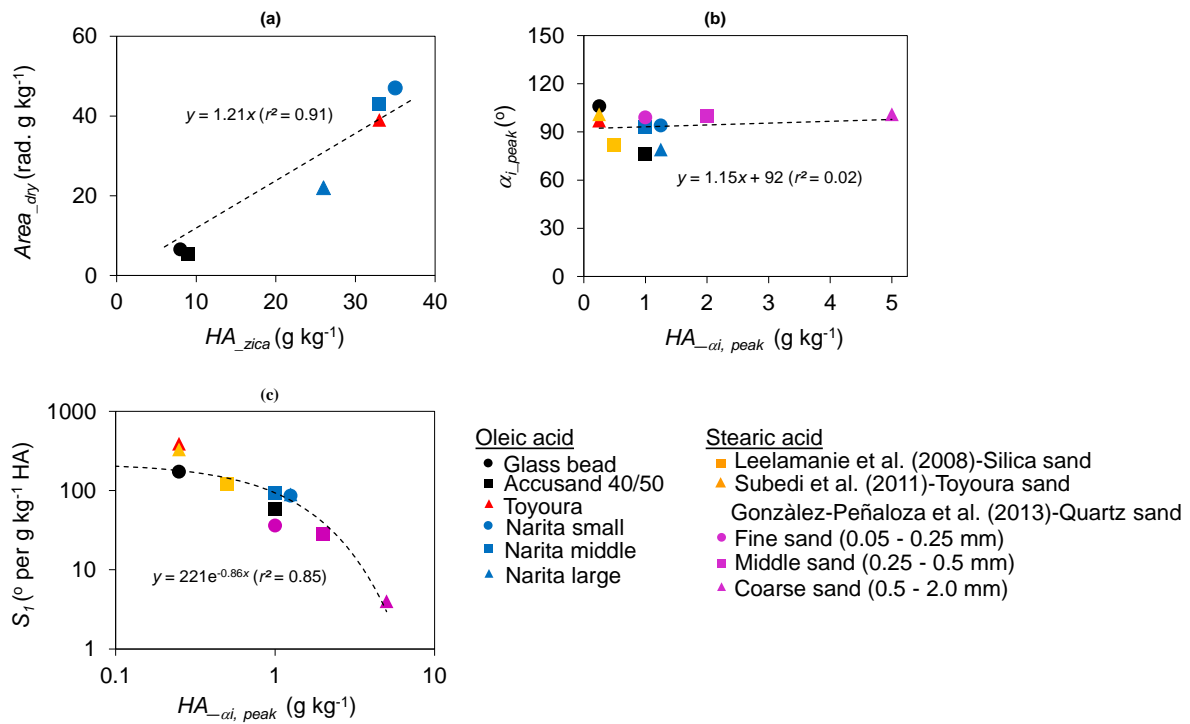
Figure 2.4 Relationship between water repellency indices for dry hydrophobized grains; (a) $Area_{dry}$ and HA_zica, (b) $\alpha_{i, peak}$ and $HA\_\alpha_{i, peak}$, (c) S_1 and $HA\_\alpha_{i, peak}$. The calculated WR indices value for Leelamanie et al. (2008), Subedi et al. (2011) and Gonzàlez-Peñaloza et al. (2013) are included for fitting in Fig. 4b and 4c.

2.3.3 *Mechanism of HA coating and attraction of water molecule at different regions in αi - HA content curve*

Graber et al. (2009) explored the role of fatty acids in soil WR and proposed a conceptual model for a water repellent soil surface. They also explained that surface wetting and persistence of WR will depend on the chemistry of the soil and soil solution. Leelamanie et al. (2007) illustrated the presence of clay in hydrophobic sand, and they assumed HA is sitting on the grain surface as a monolayer at maximum WR (Maximum α_i). To characterize hydrophobic and hydrophilic functional groups, fourier-transform infrared spectral studies were done by Ellerbrock et al. (2005) using natural forest soils and Subedi et al. (2012) using hydrophobized grains. In those studies, ratios of hydrophobic (CH⁻) to hydrophilic (CO⁻) functional groups were analyzed and positive relationships were found between the ratios and HA contents.

Combining all the above studies, we created a diagram to explain the mechanism of HA coating on a grain surface for two types of curves in different regions (Fig. 2.5). In both Type

I and II curves of Region I grains were partially coated with HA and they give α_i values of $0 < \alpha_i < \alpha_{i\_peak}$. HA-coated samples will produce an α_{i_peak} at an optimum coating ($HA\_\alpha_{i,\,peak}$) that can be assumed to coat the surface with an HA monolayer.

Type I of Region II and both Types I and II of Region III can be understood as accumulations of HA on the grain surface forming HA multilayers. The formation of HA multilayers on the grain surface decreases water repellency, resulting in the gradual formation of micelles, i.e., hydrophilic heads of HA towards the outside, that are likely to attract water molecules. At the end of Region III, especially close to HA_{zica}, many micelles exist as a result of excess HA. As shown in Fig. 2.3, WR curves for natural sands in this study and published data were categorized them into Type I while commercial grains with rounded shapes were categorized into Type II. This indicates that the surface roughness of grains affected the formation of HA multilayers and a rough grain surface might hinder the formation of micelles with hydrophilic heads.
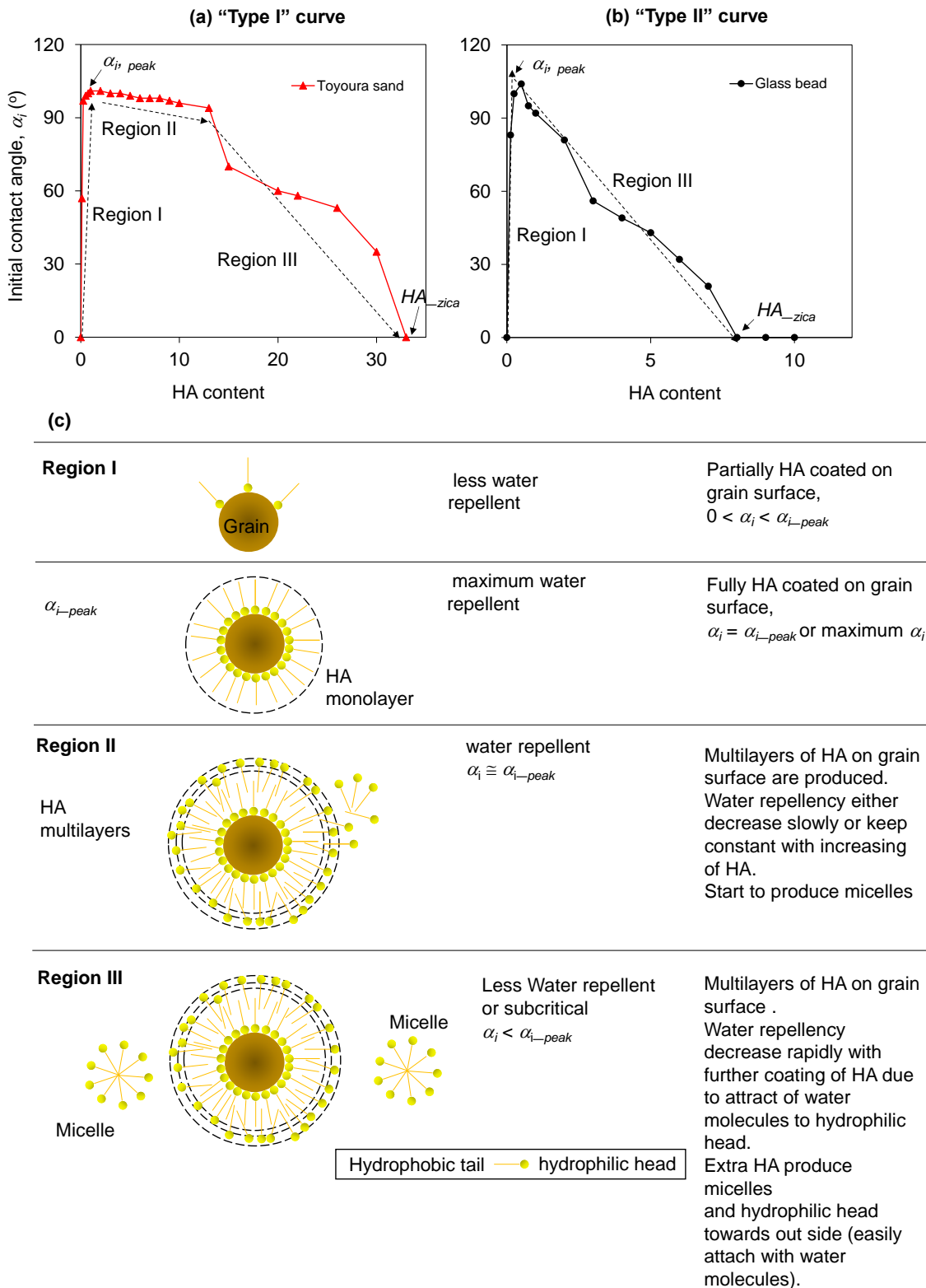
Figure 2.5 Mechanism of HA coating on grain surface at different regions in (a) Type I, (b) Type II curves and (c) schematic diagram for HA coating for different region in αi - HA content curve.

25

2.3.4 *Characterization of water repellency for wet hydrophobized grains*

Based on the α_i-HA relationship shown in Fig. 2.2, two HA contents, i) 1 g kg^{-1} (the highest α_i region/shoulder region) and ii) 5 g kg^{-1} (the representative HA sample of the plateau region), were selected to study the effects of the water content on WR of hydrophobized grains. The gravimetric water content (θ_g) of dry hydrophobized grains was changed by adding distilled water, as described in Materials and Methods. Figure 6 shows the measured α_i - θ_g curves for 1 g kg^{-1} (Fig. 2.6a) and 5 g kg^{-1} (Fig. 2.6b). For all tested materials, the α_i values decreased with increasing in θ_g. Based on results from SDM contact angles for 13 soil samples, Chau et al. (2014) proposed four curve patterns: Type A (contact angles decrease rapidly with increased water content), Type B (contact angles decrease slowly with increased water content), Type C (contact angles are stable until a certain water content is reached, thereafter contact angles decrease slowly with increased water content) and Type D (as water content increases past 0 %, the contact angle initially increased, followed by a decrease in contact angle). According to their proposal, our tested materials were Type B for Accusand 40/50, Narita large, Toyoura sand, and glass bead (5 g kg^{-1}) and Type C for Narita small, Narita middle sand and glass bead (1 g kg^{-1}) curves. Liu et al. (2012) studied the relationship between contact angle and θ_g for natural sand coated with DCMS having a Type C curve. Subedi et al. (2011) also studied the effect of water content on sand samples in a stearic acid solvent (Toyoura sand) and the α_i - θ_g relationships shows the Type B curve (Fig. 2.6). In these published data, WR disappeared, at content over 0.03 and 0.1 kg kg^{-1}, respectively, whereas WR in the present study's materials disappeared between 0.01 and 0.025 kg kg^{-1}. Therefore, to produce WR in a moist condition, the type of HA is important when we make hydrophobized grains for CBCS.
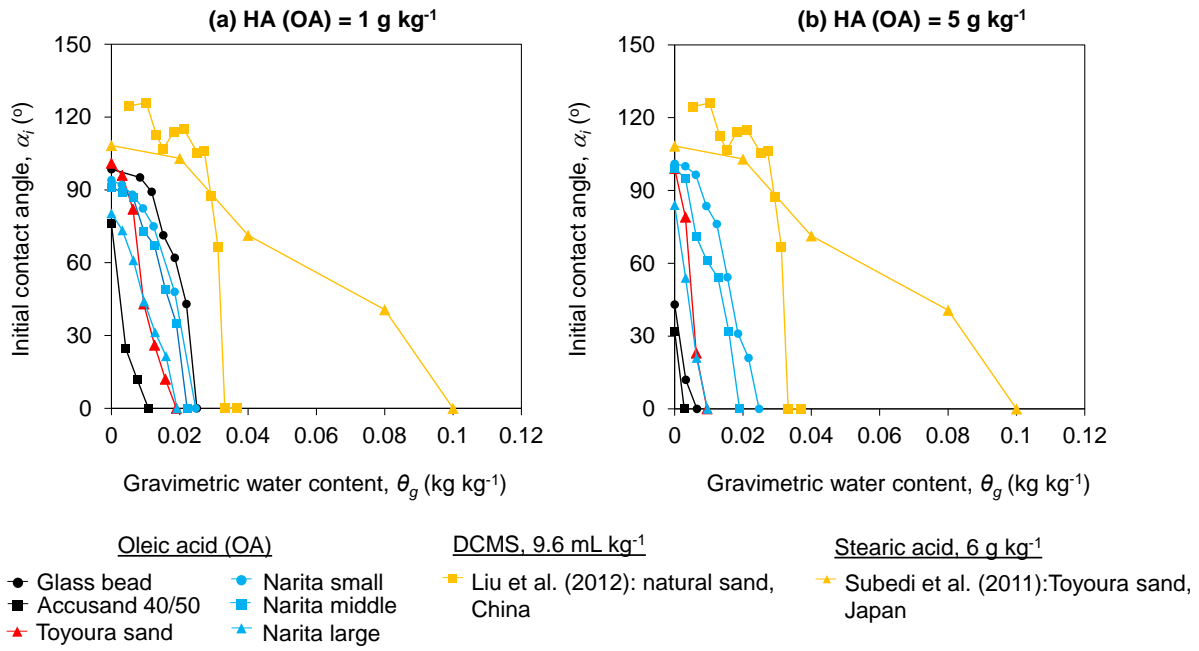
Figure 2.6 Effect of gravimetric water content (θ_g) on initial contact angle (α_i); α_i-θ_g curve for (a) 1 g kg^{-1} and (b) 5 g kg^{-1} of HA mixed samples. Published data of Liu et al. (2012) using DCMS for natural hydrophilic sand and Subedi et al. (2011) using stearic acid for Toyoura sand are also shown.

2.3.5 Development of water repellency indices for wet hydrophobized grains

Figure 2.7a shows a schematic diagram of two WR indices from the α_i - θ_g curve for wet hydrophobized grains. The WR indices are (i) the area under the α_i - θ_g curve, "$Area\_wet$", and (ii) the maximum θ_g at which WR disappears, "θ_{g_zica}". Calculated WR indices for wet hydrophobized grains are shown in Table 2.2. The values of $Area\_wet$ and θ_{g_zica} were lower for 5 g kg^{-1} HA mixed samples compared to those at 1 g kg^{-1}. This can be further explained by the mechanism of HA coating (Fig. 2.5) in different regions where it produces HA micelles. These micelles have hydrophilic heads towards outside and are highly likely to attract water molecules. So, highly HA-coated (5 g kg^{-1}) wet samples rapidly become hydrophilic compared to the less highly HA-coated (1 g kg^{-1}) wet samples.

For comparison, the calculated values of $Area\_wet$ for DCMS reported by Liu et al. 2012 and stearic acid reported by Subedi et al. (2011) were plotted as a function of θ_{g_zica} in Fig. 2.7b. Irrespective of different sizes and geometries of grains and different HAs, there is a unique linear relationship between $Area\_wet$ and θ_{g_zica} [$y = 1.13x$ ($r^2 = 0.97$)]. Further studies are

27

needed, however, to determine if the linear relationship is applicable to characterize WR for wet grains hydrophobized with other HAs.

OA content, 1 g kg^{-1}	● Glass bead	■ Accusand 40/50
	▲ Toyoura	● Narita small
	■ Narita middle	▲ Narita large
OA content, 5 g kg^{-1}	○ Glass bead	□ Accusand 40/50
	△ Toyoura	○ Narita small
	□ Narita middle	△ Narita large
DCMS, 9.6 mL kg^{-1}	■ Liu et al. (2012)-natural sand, China	
Stearic acid, 6 g kg^{-1}	▲ Subedi et al. (2011)-Toyoura sand, Japan	
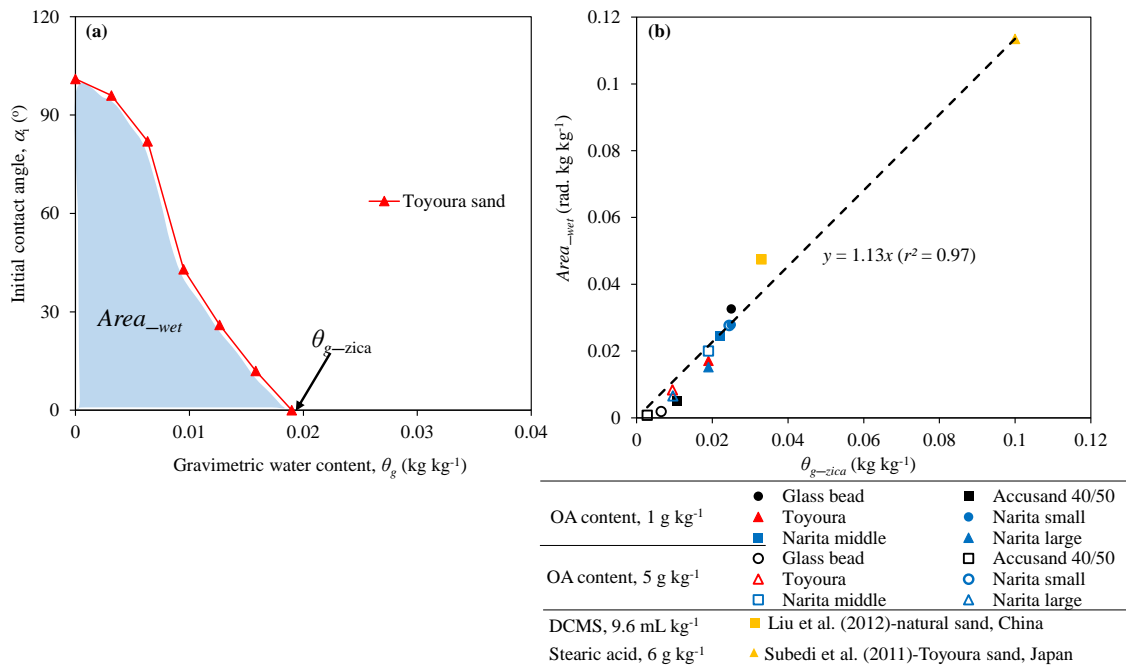
Figure 2.7 (a) Schematic diagram; two water repellency (WR) indices for wet hydrophobized grains based on α_i - θ_g curve. Indices are *Area_wet* (area under the α_i - θ_g curve) and θ_{g_zica} (the maximum θ_g at which WR disappears) and (b) relationship between *Area_wet* and θ_{g_zica} for 1 g kg^{-1} and 5 g kg^{-1} HA mixed samples. The calculated WR indices values for Subedi et al. (2011) and Liu et al. (2012) are included for liner regression analysis.

2.3.6   *Correlations among water repellency indices, grain size, and geometry*

In order to evaluate correlations among WR indices and physical properties of grains including size and geometry, Pearson correlation (*r*) analysis was carried out (Table 2.3). In the analysis, eight WR indices and physical properties for grains such as d_{50}, C_u and specific surface area (SSA_{N2}) were used. The data for commercial grains with round shapes (Accusand 40/50 and glass bead) were excluded from the analysis because their data became irregular compared to those for other tested materials.

Results show that all WR indices for dry hydrophobized grains; $Area_{\_dry}$, $HA_{\_zica}$, $\alpha_{i,peak}$, $HA\_\alpha_{i,peak}$, S_1 and S_2, are relatively highly correlated to d_{50} ($|r| > 0.51$). The WR indices for wet hydrophobized grains, $Area_{\_wet}$ and θ_{g_zica}, are also well correlated to d_{50} ($|r| > 0.42$). As shown in Table 2.3, among the WR indices, $Area_{\_dry}$ and $HA_{\_zica}$ are highly correlated to $Area_{\_wet}$ and θ_{g_zica} ($|r| > 0.68$).

Both d_{50} and C_u are simple physical properties of grains that can be obtained from grain size distribution tests and are commonly used for the material/grain selection in the field of geotechnical engineering. It is important to identify correlations between WR indices and grain properties especially for the material selection to develop hydrophobized CBCSs. In this study, either one or two parameter regression equations are suggested using d_{50} and C_u considering an easy application. Equations (1) - (5) for dry hydrophobized grains and Equations (6) - (7) for wet hydrophobized grains are listed below. Note that equations with r^2 values > 0.7 are shown.

$$Area_{\_dry} = 53.4 - 44.7\,d_{50}\ (r^2 = 0.77) \tag{Eq. 1}$$

$$Area_{\_dry} = 110 - 67.3\,d_{50} - 32.9\,C_u\ (r^2 = 0.97) \tag{Eq. 2}$$

$$\alpha_{i,peak} = 102 - 35\,d_{50}\ (r^2 = 0.93) \tag{Eq. 3}$$

$$\alpha_{i,peak} = 102 - 35.4\,d_{50} - 0.40\,C_u\ (r^2 = 0.94) \tag{Eq. 4}$$

$$HA_{\_\alpha i,peak} = 4.90 - 0.57\,d_{50} - 2.52\,C_u\ (r^2 = 0.91) \tag{Eq. 5}$$

$$Area_{\_wet} = \begin{cases} 8.59 \times 10^{-2} - 3.85 \times 10^{-2}\,d_{50} - 3.46 \times 10^{-2}\,C_u\ (r^2 = 0.99)\ [1\ \mathrm{g\,kg^{-1}}] \\ 9.82 \times 10^{-2} - 4.54 \times 10^{-2}\,d_{50} - 4.49 \times 10^{-2}\,C_u\ (r^2 = 0.99)\ [5\ \mathrm{g\,kg^{-1}}] \end{cases} \tag{Eq. 6}$$

$$\theta_{g\_zica} = \begin{cases} 5.23 \times 10^{-2} - 1.75 \times 10^{-2}\,d_{50} - 1.68 \times 10^{-2}\,C_u\ (r^2 = 0.96)\ \ [1\ \mathrm{g\,kg^{-1}}] \\ 1.24 \times 10^{-2} - 6.29 \times 10^{-2}\,d_{50} - 5.82 \times 10^{-2}\,C_u\ (r^2 = 0.99)\ \ [5\ \mathrm{g\,kg^{-1}}] \end{cases} \tag{Eq. 7}$$

Equations with a single parameter, d_{50}, [Eqs. (1) and (3)] as well as equations with a two parameters, d_{50} and C_u, [Eqs. (2) and (4)] were well correlated to two WR indices for dry hydrophobized grains, $Area_{\_dry}$ and $\alpha_{i,peak}$. For other WR indices for dry and wet hydrophobized grains, on the other hands, equations with a single parameter, d_{50}, did not give sufficient correlations and equations with two parameters, d_{50} and C_u, [Eqs. (5) and (7)] were needed.

Table 2.3 Pearson correlation (r) among water repellency indices and physical properties (no. of sample, n = 4); C_u, d_{50} and SSA_{N2} (Excluding the rounded materials; Glass bead and Accusand 40/50). Correlations demarcated with square that are used to regression equations.

	WR indices for dry hydrophobized grains						WR indices for wet hydrophobized grains				Basic properties		
	$Area_{dry}$	$HA_{\_zica}$	$\alpha_{i,\,peak}$	$HA_{\_\alpha i,\,peak}$	S_1	S_2	$Area_{\_wet}$ (1 g kg^{-1})	$Area_{\_wet}$ (5 g kg^{-1})	θ_{g_zica} (1 g kg^{-1})	θ_{g_zica} (5 g kg^{-1})	C_u	d_{50}	SSA_{N2}
$Area_{dry}$	1.00												
$HA_{\_zica}$	0.99	1.00											
$\alpha_{i,\,peak}$	0.89	0.93	1.00										
$HA_{\_\alpha i,\,peak}$	-0.16	-0.28	-0.60	1.00									
S_1	0.07	0.21	0.52	-0.97	1.00								
S_2	0.51	0.62	0.65	-0.45	0.56	1.00							
$Area_{\_wet}$ [1 g/kg]	0.85	0.77	0.51	0.37	-0.46	0.20	1.00						
$Area_{\_wet}$ [5 g/kg]	0.81	0.74	0.46	0.44	-0.49	0.26	0.99	1.00					
θ_{g_zica} [1 g/kg]	0.75	0.68	0.38	0.51	-0.53	0.28	0.96	0.99	1.00				
θ_{g_zica} [5 g/kg]	0.77	0.69	0.39	0.50	-0.56	0.17	0.99	1.00	0.99	1.00			
C_u	0.30	0.44	0.69	-0.93	0.97	0.74	-0.23	-0.25	-0.29	-0.34	1.00		
d_{50}	-0.88	-0.94	-0.97	0.53	-0.51	-0.81	-0.52	-0.50	-0.45	-0.42	-0.71	1.00	
$SSA_{\_N2}$	0.37	0.47	0.75	-0.97	0.91	0.46	-0.16	-0.24	-0.33	-0.31	0.91	-0.66	1.00

Further studies are necessary to identify the correlations between WR indices and grain properties because our test results were obtained from limited data for four types of natural grains. The proposed equations in this study, however, easily give WR characteristics for both dry and wet hydrophobized grains. Therefore, the equations are recommended to quickly assess the material/grain selection to develop hydrophobized CBCSs.

2.4 Conclusions

The degree of water repellency (WR) for selected, hydrophobized grain materials was evaluated as the solid-water initial contact angle (α_i) as a function of the content of the applied hydrophobic agent (oleic acid) and the water content (θ_g). The α_i - HA and α_i - θ_g curves were measured for six different types of grains with varying geometries and sizes. Eight WR indices were introduced to fully characterize the α_i - HA and α_i - θ_g curves. Pearson correlation analysis revealed significant relationships between the WR indices and basic grain properties such as d_{50} and coefficient of uniformity (C_u), both in the cases of natural grains (non-round), dry and wet, hydrophobized grains. Because the relationships identify WR characteristics for both dry and wet, hydrophobized grains, the relationships seem highly useful for optimal material/grain selection when developing and designing hydrophobized capillary barrier cover systems.

2.5 References

Alexandrova, L., Nedyalkov, M., Khristov, K., Platikanov, D., 2011. Thin wetting film from aqueous solution of polyoxyalkylated DETA (Diethylenetriamine) polymeric surfactant. Colloids and Surfaces A: Physicochemical and Engineering Aspects, 382 (1-3):88–92.

Bachmann, J., Ellies, A., Hartge, K.H., 2000a. Development and application of a new sessile drop contact angle method to assess soil water repellency. Journal of Hydrology, 231-232: 66–75.

Bachmann, J., Horton R., van der Ploeg R.R., Woche S., 2000b. Modified sessile drop method for assessing initial soil–water contact angle of sandy soil. Soil Sci. Soc. Am. J. 64: 564-567.

Benson, C.H., Khire M.V., 1995. Earthen cover for semi-arid climates. In R.J. Dunn and U.P. Singh. (ed.) Landfill closures environmental protection and landfill recovery. ASCE special publication, 201-217, GSP No. 53.

Bozkurt, S., Sifvert, M., Moreno, L., Neretnieks, I., 2001. The long- term evolution of and transport processes in a self-sustained final cover on waste deposits. The Science of the Total Environment, 271: 145-168.

Brunauer, S., Emmett, P.H., Teller, E., 1938. Adsorption of gases in multimolecular layers. Journal of the American chemistry society, 60: 309-319, doi:10.1021/ ja01269a023.

Buczko U., Bens O., 2006. Assessing soil hydrophobicity and its variability through the soil profile using two different methods. Soil Sci. Soc. Am. J. 70: 718-727.

Chau H.W., Biswas A., Vujanovic V., Si B.C., 2014 Relationship between the severity, persistence of soil water repellency and the critical soil water content in water repellent soils. Geoderma, 221-222: 113-120.

de Jonge L.W., Jacobsen O.H, Moldrup P., 1999. Soil Water Repellency: Effects of Water Content, Temperature, and Particle Size. Soil Sci. Soc. Am. J. 63(3): 437-442.

Dekker LW., Jungerius P.D., 1990. Water repellency in the dunes with special reference to the Netherlands. Catena Suppl. 18: 173–183.

Dell'Avanzi, E., Guizelini, A.P., da Silva, W.R., Nocko, L.M., 2010. Potential use of induced soil-water repellency techniques to improve the performance of landfill's alternative final cover systems. In O. Buzzi et al. (ed.), unsaturated soils: Experimental studies in unsaturated soils and expansive soils. 1: 461–466.CRC Press, Boca Raton, FL.

Diehl, D., 2013. Soil water repellency: Dynamics of heterogeneous surfaces. Colloids and Surfaces A: Physicochemical and Engineering Aspects, 432:8–18.

Ellerbrock, R.H., Gerke, H.H., Bachmann, J., Goebel, M.-O., 2005. Composition of organic matter fractions for explaining wettability of three forest soils. Soil Sci. Soc. Am. J. 69: 57–66.

Fink, D.H., 1970. Water repellency and infiltration resistance of organic film coated soils. Soil Sci. Soc. Am. Proc. 34: 189–194

González-Peñaloza, F.A., Zavala, L.M., Jordán, A., Bellinfante, N., Bárcenas-Moreno G., Mataix-Solera, J., Granged, A.J.P., Granja-Martins F.M., Neto-Paixão H.M. 2013. Water repellency as conditioned by particle size and drying in hydrophobized sand. Geoderma, 209-210: 31–40.

Graber, E.R., Tagger, S., Wallach, R., 2009. Role of Divalent Fatty acid salts in soil water repellency. Soil Sci. Soc. Am. J. 73 (2): 541-549.

Kawamoto, K., Moldrup, P., Komatsu, T., de Jonge, L.W., Oda, M., 2007. Water Repellency of Aggregate Size Fractions of a Volcanic Ash Soil. Soil Sci. Soc. Am. J. 71 (6): 1658-1666.

Karunarathna, A.K., Moldrup, P., Kawamoto, K., de Jonge, L.W., Komatsu T., 2010. Two-Region Model for Soil Water Repellency as a Function of Matric Potential and Water Content. Vadose Zone Journal, 9(3): 719-730.

Khire, M., Benson, C., Bosscher, P., 2000. "Capillary Barriers in Semi-Arid and Arid Climates: Design Variables and the Water Balance," Journal of Geotechnical and Geo-environmental Engineering, ASCE, 126(8): 695-708.

King, P.M., 1981. Comparison of methods for measuring severity of water repellence of sandy soils and assessment of some factors that affect its measurement. Australian Journal of Soil Research, 19: 275–285.

Koerner, R.M., Daniel, D.E., 1992. Better cover ups. Civil Engineering. 55-57

Koerner, R.M., Daniel D.E. 1997. Final covers for solid waste landfills and abandoned dumps. ASCE Press, New York.

Lamparter, A., Bachmann, J., Woche, S.K., 2010. Determination of Small-Scale Spatial Heterogeneity of Water Repellency in Sandy Soils. Soil Sci. Soc. Am. J. 74(6), 2010-2012. doi:10.2136/sssaj2010.0082N.

Leelamanie, D.A.L., Karube J., 2007. Effects of organic compounds, water content and clay on water repellency of a model sandy soil. Soil Sci. Plant Nutr. 53: 711–719.

Leelamanie, D.A.L., Karube, J., Yoshida, A., 2008. Relative humidity effects on contact angle and water drop penetration time of hydrophobized fine sand. Soil Science and Plant Nutrition, 54: 695-700.

Liu, H., Ju Z., Bachmann, J., Horton, R., Ren, T., 2012. Moisture-Dependent Wettability of Artificial Hydrophobic Soils and Its Relevance for Water Desorption Curves. Soil Sci. Soc. Am. J. 76 (2): 432-349.

Morris, C.E., Stormont, J.C., 1998. Evaluation of numerical simulations of capillary barrier field tests. Geotechnical and Geological Engineering, 16: 201–213.

Naveed, M., Hamamoto, S., Kawamoto, K., Sakaki, T., Takahashi, M., Komatsu, T., de Jonge L.W., lamandé, M., Moldrup, P. 2011. Gas dispersion in granular porous media under air-dry and wet condition. Soil Sci. Soc. Am. J. 76: 845-852.

Pease, R.E., Stormont J.C., 1996. Increasing the diversion length of capillary barriers. In: Proceeding of the HSRC/WERC joint Conference on the Environment, Albuquerque, New Mexico.

Purdy, S.C.E.G., Horton, E. 1999. Value engineering in a landfill cap design- A case study. Proceedings of sardinia, 7th International waste management and landfill symposium., CISA, cagliari, Italay 4-8 Oct, 1999.

Regalado, C.M., Ritter, A., 2005. Characterizing Water Dependent Soil Repellency with Minimal Parameter Requirement. Soil Sci. Soc. Am. J. 69 (6): 1955-1966.

Ross, B., 1990. The diversion capacity of capillary barriers, Water Resour. Res. 26: 2625-2629.

Roy, J.L., McGill W.B., 2002. Assessing soil water repellency using the molarity of ethanol droplet (MED) test. Soil Sci. 167: 83–97.

Scanlon, B.R., Reedy, R.C., Keese, K.E., Dwyer, S.F., 2005. Evaluation of evapotranspirative covers for waste containment in arid and semiarid regions in the southwestern USA. Vadoze zone J., 4: 55-71.

Sharma, H.D., Reddy, K.R., 2004. Geo-environmental engineering: Site remediation waste containment, and emerging waste management technologies. John Wiley & Sons, Hoboken, NJ.

Simon, F.G., Müller W.W., 2004. Standard and alternative landfill capping design in Germany. Environmental science policy 7: 277-290.

Steenhuis, T.S., Parlange, J –Y., Kung, K.J.S., 1991. Comment on "The diversion capacity of capillary barriers" by Benjamin Ross, Water Resour. Res., 27: 2155-2156.

Stormont, J.C., 1995. The effect of constant anisotropy on capillary barrier performance, Water Resour. Res., 31: 783-785.

Subedi, S., Kawamoto K., Kuroda T., Moldrup P., Komatsu T., 2011. Effect of water content on the water repellency for hydrophobized sands. H53A-1372, American Geophysical Union Fall Meeting 2011.

Subedi, S., Kawamoto, K., Jayarathna, L., Vithanage, M., Moldrup, P., de Jonge, L.W., Komatsu T., 2012. Characterizing time dependent contact angle for sands hydrophobized with oleic and stearic acids. Vadose zone Journal, 11 (1), doi:10.2136/vzj2011.0055.

Tidwell, V.C., Glass, R.J., Chocas, C., Barker, G., Orear., L. 2003. Visualization experiment to investigate capillary barrier performance in the context of a Yucca Mountain emplacement drift. J. of contaminant hydrology, 62-63: 287-301.

Wijewardana, Y.N.S., Kawamoto, K., Komatsu T., Hamamoto S., Subedi S., Moldrup P., 2014. Characterization of time-dependent contact angles for oleic acid mixed sands with different particle size fractions. Unsaturated soils: Research and Applications (UNSAT 2014), N. Khalili, A, Russell and A. Khoshghalb (eds), 255-260, ISBN 978-1-1-138-00150-3.

Yanful, E.K., Mousavi, S.M., Lin-Pei, De Souza., 2006. A numerical study on soil cover performance. Journal of environmental management, 81: 72-92.

Chapter 3

3. SOIL-WATER REPELLENCY CHARACTERISTIC CURVES FOR SOIL PROFILES WITH ORGANIC CARBON GRADIENTS

ABSTRACT

Soil water repellency (SWR) reduces water infiltration into soils due to the presence of hydrophobic organic materials on mineral grain surfaces. The relationship between the degree of SWR and the volumetric soil-water content (θ) is given by the soil-water repellency characteristic curve (SWRCC). The objectives of this study are (i) to characterize SWR comparing three common methods; the water drop penetration time (WDPT) test, the molarity of an ethanol droplet (MED) method, and the sessile drop method (SDM); (ii) to evaluate the applicability of the *Dexter index* (ratio of clay to soil organic carbon, SOC) to identify water-repellent soils, and (iii) to find relationships between SWRCC parameters and SOC content. At six sites in Japan (forest) and New Zealand (pasture), soil was sampled at different depths with SOC contents between 1 and 26 %. SWR of soils adjusted to a wide range of water contents was measured. The WDPT, MED, and SDM generally agreed well in predicting the water content range where SWR occurred, and there was close agreement between average MED and SDM at similar θ. Generally, SWR was only found within the top 20 cm of the soil profiles and for a *Dexter index* ≤ 11, but the *Dexter index* failed to separate water-repellent from non-repellent soils. Four SWRCC parameters were introduced: (i) area under the curve ($S_{WR(\theta)}$); (ii) θ at the maximum SWR ($\theta_{WR\text{-}max}$), (iii) θ where SWR ceased ($\theta_{non\text{-}WR}$), and (iv) the maximum SWR ($CA_{i\text{-}max}$). The $CA_{i\text{-}max}$ was relatively constant with SOC while Langmuir type equations provided the best description (r^2 of 0.5 - 0.7) for the three other SWR parameters as a function of SOC.

3.1 Introduction

Soil water repellency (SWR) is a phenomenon that prevents water infiltration into soils due to the presence of hydrophobic organic materials on the soil grain and aggregate surfaces (DeBano, 2000; Doerr et al., 2000; Buczko and Bens, 2006; Urbanek et al., 2007). Some authors have discussed the hydrophobic properties associated with organic matter coating on soil particles leading to SWR (Ma'shum and Farmer, 1985; Horne and McIntosh, 2000; Leelamanie and Karube, 2014a). The severity of SWR depends primarily on the nature of the organic matter, followed by the soil's water content (King, 1981; Dekker and Ritsema, 1997; de Jonge et al., 1999; Doerr et al., 2000) and its wetting and drying history (Arye et al., 2007; Lamparter et al., 2009). The governing mechanism of surface hydrophobicity is associated with the reconfiguration or reorientation of amphipathic organic matter compounds when they interact with water (Leelamanie and Karub, 2007; Regalado et al., 2008). When soils are wet, polar groups of the organic matter interact with water molecules, but as soils dry out these polar groups interact with each other (Nowak et al., 2013; Doerr et al., 2000). Vogelmann et al. (2013) found that the threshold water content below which hydrophobic soils became hydrophilic varied between 0.36 and 0.57 cm^3 cm^{-3}. Therefore, it is important to identify critical water contents (Dekker et al., 2001; Chau et al., 2014), which are site- and soil-specific, under which soils are water-repellent.

The relationship between the degree of SWR and the soil volumetric water content (θ) is termed as soil water repellency characteristic curve (SWRCC). Different methods were used to measure SWR such as the water drop penetrating time (WDPT) test (King 1981; Van't Woudt, 1959), the molarity of ethanol droplets method (MED) (Roy and McGill, 2002; Kawamoto et al., 2007) and the sessile drop method (SDM) (Bachmann et al., 2000; Subedi et al., 2012). Results of the WDPT test assess the persistence of SWR. The MED method uses the surface tension of ethanol-water mixtures of different molarities to indirectly determine the contact angle. It only works for hydrophobic soils with contact angles greater than 90º (Carrillo et al., 1999). Specifically, the SDM can be used to measure sub-critical SWR (King, 1981; Chau et al., 2014), where the soil-water contact angle is between 0º and 90º.

Potential correlations between measured SWR and different soil properties, such as soil organic carbon (SOC) content (de Jonge et al., 1999; Kawamoto et al., 2007; Rodríguez-Alleres et al., 2007), water content (Karunarathna et al., 2010a, b; de Jonge et al., 1999; Kawamoto et al., 2007) and particle size (de Jonge et al., 1999; Rodriguez-Alleres et al., 2007) have been

analyzed. The team of de Jonge et al. (1999) found single peak and double peak behavior for SWR curves in relation to water content, while Karunarathna et al. (2010a) identified three basic types of curves for single peak behaviors. Their type I curve behavior is characterized by increasing SWR with reducing θ until a maximum SWR at a certain θ (θ_{WR-max}) is reached, and thereafter non-linearly decreasing SWR towards the potential SWR at air-dry θ (θ_{AD}). Type II is the opposite of the type I curve: SWR ceases at a given θ, which is larger than the $\theta_{AD.}$ The soil is fully wettable at θ_{AD}. Type III curve soils are not water-repellent at any θ between field θ to θ_{AD}.

Doerr et al. (2006) analyzed the relationships of SWR with the soils' clay contents, organic matter contents and soil moisture contents (%) for different soil sampling depths under different land-use systems. They concluded that land use and soil moisture contents are reliable predictors for SWR. Also, Vogelmann et al. (2013) generally concluded that in hydrophobic soils, the repellency index and persistence of SWR decreased with depth, reduced organic carbon contents, and increased water contents. Importantly, vegetation type, plant species (McIntosh and Horne, 1994) and the activity of fungal and microbial species (Hallett et al., 2001) could also contribute to the development of SWR in soils. Most published studies have based their conclusions on the relationship between SWR and other basic soil properties only on one or two, mostly indirect SWR characterization methods. In addition, most studies did not evaluate the occurrence of sub-critical SWR. But even sub-critical SWR may reduce water infiltration and promote preferential flow and surface runoff (Clothier et al., 2000). Therefore, in this study, we used three methods including a direct SWR assessment method to estimate SWR, and related the degree of SWR to different θ; ranging from field moist to air-dry conditions.

Japan and New Zealand have many naturally water-repellent soils. For example, in a comprehensive survey on the occurrence of SWR under pasture in the North Island of New Zealand, Deurer et al. (2011) found that SWR to be widely prevalent in pastoral soils independent of soil order. Andosols, which are soils formed from volcanic tephra (WRB, 2006), are important in both countries. They are generally quite young and very fertile. Most Japanese forest soils are Andosols. Some of New Zealand pastoral lands are on Andosols, but Cambisols, which are medium developed and fine-textured soils (WRB, 2006), are also important soils for New Zealand agriculture and specially for pasture productivity (Müller et al. 2014a,b).

Only a few studies on the occurrence of SWR in Andosols have been conducted (Kawamoto et al., 2007; Jordan et al., 2009; Karunarathna et al., 2010a, b; Leelamanie et al., 2014a, 2014b; Neris et al., 2013). For example, Kawamoto et al. (2007) studied SWR in volcanic ash soil samples from Fukushima, Japan and concluded that hydrophobicity of aggregates changed with θ. Neris et al. (2013) measured infiltration and runoff in Andosols in the Canary Islands of Spain under pine forests and rainforests. The type of forest controlled the amount of infiltration and runoff. Under pine forests, infiltration was lower than under rainforest. Jordan et al. (2009) also studied the occurrence and hydrological effects of SWR in volcanic soils under different land uses. Results revealed that runoff was enhanced in water-repellent forest soils (average runoff coefficients between 15.7 and 19.9 %) compared with hydrophilic or slightly water-repellent soils, where runoff rates were lower (between 1.0 and 11.7 %). Similarly, Müller et al. (2010) found that SWR reduced the infiltration rate and increased runoff in New Zealand Andosols. Moreover, Leelamanie and Karube (2007) concluded that hydrophilic organic compounds may increase water repellency when combined with hydrophobic organic compounds.

Ellerbrock et al. (2005) and Schnabel et al. (2013) studied SWR of Cambisols. Ellerbrock et al. (2005) introduced the relatively soil type independent factor "*G*", which is the function of SOC/clay ratio. They found that the relation between the two parameters was exponential. Schnabel et al. (2013) did not find a relationship between SWR and the basic physical or chemical properties of the soils. But for their study they concluded that the bare soil surface was hydrophilic independent of whether it was located below a tree canopy or in the open. Therefore, it seems necessary to discuss further the relationships between SWR and SOC for different land use types.

Organic carbon is normally present in soils as soil organic matter (Dexter et al., 2008) and it affects most physical soil properties (Ball et al., 2000; Wallis and Horne, 1992; Täumer et al., 2005). Dexter et al. (2008) developed a concept showing a correlation between clay content and complex organic carbon (COC) and called it *Dexter number*, *n* where *n* is 1 g of organic carbon associated with *n* g of soil. Further, the authors found that non-complexed clay (NCC, clay that disperses easily in water) and complexed clay (CC, clay associated with organic carbon) occur at *n* values of about 10, which was termed as saturation line (Dexter et al., 2008). So, soil samples above the saturation line are CC, and those below the line are NCC. The applicability of the *Dexter concept*, hereafter called *Dexter plot* to differentiate between

water-repellent and non-water-repellent soils (de Jonge et al., 2009) was also assessed in our study.

The objectives of this study are (i) to characterize SWR using three common methods; the water drop penetration time (WDPT) test, the molarity of ethanol droplet (MED) method and the sessile drop method (SDM); (ii) to assess the applicability of the *Dexter concept* to differentiate water-repellent soils from non-water-repellent soils; and (iii) to analyze the relationship between SWR parameters calculated from SWRCCs and SOC.

3.2 Materials and Methods

3.2.1   Soil sampling and soil properties

Soil samples were collected from Japan (JP) and New Zealand (NZ) representing the soil orders Andosols and Cambisols. Figure 3.1 shows the distribution of the soil sampling locations in JP and NZ. The sites in JP were located in Nishigo, Fukushima (37° 08' N 140° 09' E), Hiruzen, Okayama (35° 16'N 133° 37'E) and Tochigi, Nikko (36° 41'N 139° 4'E), and in NZ they were in Ngahinapouri, Waikato (37° 53'S 175° 12'E), Waihora, Waikato (38° 36'S 175° 74'E) and Whatawhata, Waikato (37° 28'S 175° 3'E). For the last site, high and low fertility fields were sampled; this terminology is based on a long-term phosphorus experiment: the "high fertility" field received 100 kg of Phosphorus per ha and year for 20 years and the "low fertility" field did not received any mineral phosphorous fertilizer during the same time period (Schipper et al., 2009). All JP soil sampling locations were under forest, and the NZ sampling sites were under pasture. The dominant plant species at the sites are listed in Table 3.1. Soil profiles for each site are aligned with each sampling location in Fig. 3.1. Table 3.2 is shown the soil sampling depths, as well as the average of the measured soil physical and chemical properties. All measurements were done in triplicate.

Particle size distribution was performed by the hydrometer method (Gee and Burder 1986) and sieve analysis (Kettler et al., 2001). Soil texture varied but most of the soil samples were sandy clay loam texture (international soil science society - *ISSS* standards). The Soil organic carbon (SOC) and soil organic nitrogen (SON) contents were estimated using ground samples in an automatic CN-analyzer (FLASH 2000 CHNS/O Analyzers, Thermo Scientific, Thermo Fisher Scientific, Inc. (NYSE:TMO)). Using the measured SOC and SON, the C/N

ratio was calculated for all samples. EC and pH were measured using a two-channel type digital meter (EC pH meter WM-32EP, DKK-TOA Corporation, Japan), and soil core samples were used for field dry bulk density determination. Dry bulk density was determined dividing the oven dry total soil core mass by soil core volume.

3.2.1   Soil water retention curves

The soil water retention curve expresses the relationship between water content (either gravimetric or volumetric) and the degree of saturation with suction. The Eq. 3.1 represent the Durner (1994) soil water retention model.

$$S_e = \sum_{i=1}^{k} w_i \left[\frac{1}{1+(\alpha_i.|\psi|)^{n_i}} \right]^{mi} \qquad \text{[Eq. 3.1]}$$

where S_e is effective saturation, defined as $S_e = (\theta-\theta_r) / (\theta_s-\theta_r)$ with θ_s and θ_r being the saturated and residual water contents (Durner, 1994). α, n and m are parameters describing the curve (conditions; $\alpha > 0$, $n > 1$, $m = 1\text{-}1/n$). Kawamoto et al. (2007) measured bimodal ($k = 2$; $\alpha_{1,2}$, $n_{1,2}$, $m_{1,2}$, $w_{1,2}$) soil water retention curves for Japanese volcanic soils, and concluded that the two sets of parameters corresponded to the intra-aggregate and inter-aggregate pores, and that w_1 and w_2 values represented the intra-aggregate and inter-aggregate soil pore distribution, respectively.

Soil water retention curves for soil samples sieved to < 2 mm were determined using a combination of three methods to identify the soil structure (Kawamoto et al., 2007; Karunarathna et al., 2010a): The hanging water column method was used for the pF-range from 0 to 2, a pressure chamber was used for pF- vales between 2 and 4, and a water potential meter (WP4- T, Decagon Devices, Inc., WA; $\pm$ 5% accuracy at pF > 4) was used for pF values larger than 4, where pF [$= \log (|\psi|$; soil water potential in cm H_2O)]. All curve fitting parameters were obtained from the soil water retention data by using the SOLVER tool in Microsoft Excel (Wraith and Or, 1998; Resurreccion et al., 2008).
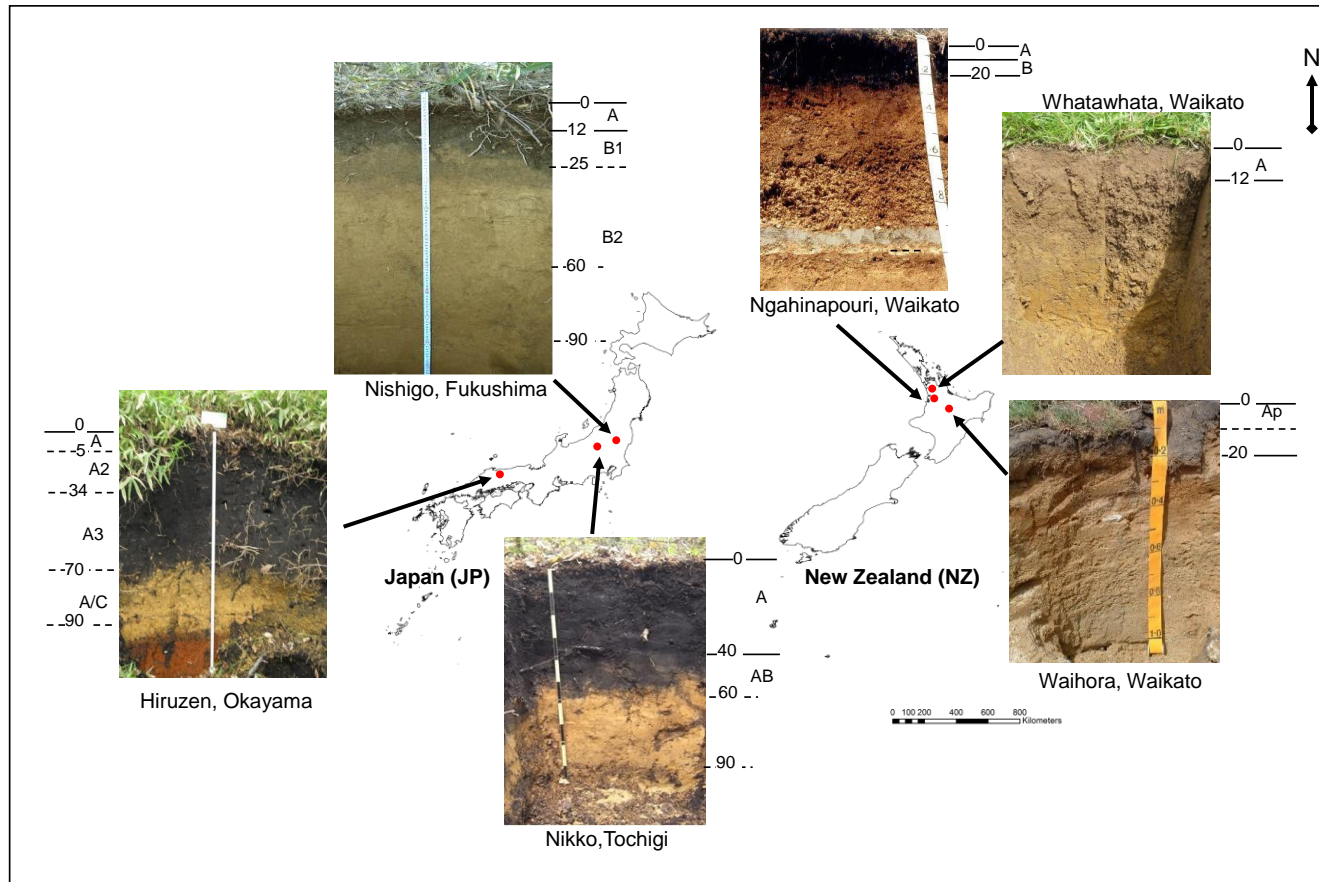
Figure 3.1 Soil sampling locations in Japan:- Nishigo, Fukushima, Hiruzen, Okayama and Tochigi, Nikko and New Zealand:- Ngahinapouri, Waikato, Waihora, Waikato and Whatawhata, Waikato. Soil profiles of the sampling sites in Japan and in New Zealand are aligned with the sampling places.

Table 3.1 Land use type, soil order and plant species for the sampling sites included in this study.

	Sampling locations	Soil order[*]	Land use	Vegetation	References
Japanese (JP) soil sampling sites	Nishigo, Fukushima	Andosols	Forest	*Pinus densiflora,* bamboo grass and various under	Kawamoto *et al.* (2007) Hiradate *et al.* (2006)
	Hiruzen, Okayama	Andosols	Forest	Fagus crenata, Quercus crispula, Acer sieboldianum, Eleutherococcus sciadophylloides	
	Nikko, Tochigi	Andosols	Forest	*Quercus serrate, Sasaella ramase, Pinus densiflora*	
New Zealand (NZ) soil sampling sites	Ngahinapouri, Waikato	Andosols	Pasture	*Lolium perenne, Trifolium pratense, Plantago species.*	Muller *et al.* (2014) Welten et al. (2013) Barkle *et al.* (2011) Aslam *et al.* (2009)
	Waihora, Waikato	Andosols	Pasture	*Lolium perenne and Trifolium species , Bromus species and other lower quality grasses and weeds*	
	Whatawhata, Waikato	Cambisols	Pasture	*Lolium perenne, Agrostis tenuis, Bromus hordacius, Trifolium pratense, Asteracea species Rumex species*	

Table 3.2 Soil physical and chemical properties for the different sampling depths of the Japan (JP) and New Zealand (NZ) sites as included in this study (three replicates were used for each measurements and value represent the average).

	References	Sampling Site	Depth (cm)	Horizon	Soil texture†	Bulk density (g cm⁻³)	Particle density (g cm⁻³)	Clay (%)	Silt (%)	Sand (%)	SOC (%)	SON (%)	C/N	pH	Electrical conductivity (mS cm⁻¹)
JP soils		Nishigo, Fukushima	0-5	A	Sandy loam	0.56	2.45	10.8	14.8	72.3	9.2	0.6	14.8	4.4	0.180
			5-10	A	Clay loam	0.56	2.51	19.1	27.0	53.8	4.9	0.3	15.3	4.6	0.076
			10-15	B1	Loam	0.56	2.55	14.8	29.2	56.0	3.3	0.3	10.5	4.6	0.047
			15-24	B2	Sandy loam	0.56	2.62	13.5	17.7	82.3	2.6	0.3	8.4	4.5	0.032
	Kawamoto et al. (2007)	Nishigo, Fukushima	0-5	A	Clay loam	0.56	2.42	17.8	27.4	54.8	12.3	0.8	16.3	4.9	-
			3-6	A	Clay loam	0.56	2.47	19.9	27.8	52.3	9.2	0.6	16.7	4.9	-
			5-10	A	Sandy loam	0.56	2.54	9.3	22.6	68.0	7.1	0.4	17.5	5.1	-
			10-15	B	Loam	0.56	2.56	10.3	25.0	64.7	4.6	0.3	15.6	5.4	-
		Hiruzen, Okayama	0-3	A		0.38	2.03	-	-	-	26.3	1.4	19.3	4.0	0.144
			3-6	A		0.38	2.06	-	-	-	22.4	1.2	19.1	3.5	0.107
		Nikko, Tochigi	0-5	A	Sandy clay	0.40	2.15	27.2	14.9	57.8	21.0	1.2	17.8	4.7	0.280
			5-34	A2	Sandy clay loam	0.40	2.36	19.6	12.0	68.4	15.6	0.8	20.1	4.8	0.290
			34-70	A3_top	Sandy clay	0.45	2.39	27.6	14.8	57.6	14.7	0.7	21.6	4.3	0.217
				A3_bottom	Sandy clay loam	0.45	2.43	24.0	16.9	69.1	12.6	0.6	21.8	4.7	0.230
			70-90	A/C	Sandy clay loam	0.45	2.51	15.5	18.5	66.0	5.7	0.8	7.0	4.9	0.167
		Aichi (cypress)	0-2	A	Sandy clay loam	0.65	2.28	23.3	8.5	68.2	14.1	0.8	18.5	4.2	0.097
			2-4	A	Sandy clay loam	0.66	2.37	21.0	10.3	68.5	11.6	0.8	15.3	4.1	0.084
			4-6	A	Sandy loam	0.73	2.41	12.3	6.9	80.8	8.8	0.6	15.8	4.0	0.082
			6-8	A	Sandy loam	0.75	2.48	18.0	8.8	73.1	8.6	0.7	12.9	4.1	0.070
			8-10	AB	Sandy loam	0.72	2.53	13.9	11.7	74.4	6.3	0.5	13.5	4.3	0.056
			10-15	AB	Sandy loam	0.78	2.52	17.4	12.5	70.2	5.7	0.4	14.2	4.4	0.051
			15-20	AB	Sandy loam	0.77	2.59	15.8	13.2	71.0	3.9	0.3	13.7	4.6	0.048
	Karunarathna et al. (2010)	Aichi (oak)	0-2	A	Sandy clay loam	0.65	2.27	22.6	14.7	62.7	6.9	0.3	21.4	4.2	-
			2-4	A	Sandy loam	0.76	2.47	19.0	13.1	67.9	4.7	0.2	20.2	4.1	-
			4-6	AB	Sandy loam	0.79	2.57	14.1	13.2	72.7	3.0	0.2	18.8	4.1	-
			6-8	AB	Sandy loam	0.79	2.58	15.5	7.3	77.2	2.3	0.1	20.1	4.1	-
			8-10	AB	Sandy loam	0.81	2.64	14.6	9.1	76.3	2.1	0.1	17.7	4.3	-
			10-15	AB	Sandy loam	0.81	2.63	13.0	9.9	77.1	1.9	0.1	19.0	4.4	-
			15-20	B1	Sandy loam	-	2.65	15.3	12.3	72.4	1.4	0.1	19.8	4.6	-
			20-25	B1	Sandy loam	-	2.68	15.4	11.0	73.6	0.9	0.04	20.7	4.9	-
			30-35	BC	Sandy loam	-	2.69	13.1	8.7	78.2	0.6	0.04	15.3	4.9	-
NZ soils		Ngahinapouri, Waikato	0-5	A	Sandy loam	1.03	2.16	11.2	12.9	76.0	8.7	0.6	15.3	6.0	0.160
			5-10	A	Sandy loam	1.03	2.44	10.2	7.4	82.4	3.7	0.4	9.4	6.2	0.078
			10-20	B	Sandy clay loam	1.03	2.50	15.2	6.5	84.8	2.2	0.4	9.8	5.9	0.048
		Waihora, Waikato	0-5	Ap	Sandy clay loam	0.72	2.12	15.3	10.8	73.9	12.1	0.6	20.9	5.3	0.077
			5-10	Ap	Sandy loam	0.78	2.34	10.1	9.8	80.1	5.6	0.5	12.3	5.5	0.031
			10-20	Ap~Bs	Sandy clay loam	0.79	2.19	17.8	5.6	76.6	1.4	0.1	10.0	5.3	0.050
		Whatawhata, Waikato	0-12 (high fertility)	A	Light clay	1.0	2.36	34.3	40.9	24.8	4.7	0.5	8.9	4.6	0.121
			0-12 (low fertility)	A	Light clay	0.9	2.17	29.6	21.9	48.5	9.2	1.2	7.9	4.5	0.164

† ISSS standards

3.2.2   Soil sample preparation for SWR measurements

Soil samples were sieved to < 2 mm, and all small plant debris was manually removed from the sieved soils. Soil water contents below the natural field water contents (FWC) were prepared following the methodology described in Kawamoto et al. (2007), *i.e.*, the soil samples were oven dried at 60°C for different time intervals. The samples were stored in sealed plastic bag and equilibrated for two days prior to the measurements. The gravimetric water content was measured by oven-drying at 105°C overnight and converted to θ (cm^3 cm^{-3}) by multiplying it with the field dry bulk density (Table 3.2).

The moisture adjusted soil samples were used to measure the degree and persistence of SWR applying the WDPT test (Bisdom et al., 1993; Subedi et al., 2012), the MED method (Roy and McGill, 2002) and the SDM (Bachmann et al., 2000; Subedi et al., 2012). For all methods, soil samples were repacked to their field dry bulk density in cylindrical rings of 5 cm diameter and 1 cm height. The MED test measures the liquid surface tension of an aqueous ethanol droplet (50 ± 5 μL, five replicates) on the sample surface that infiltrates the sample in 5 s, (γ, N m^{-1}) (Karunarathna et al., 2010a). The measured γ were then converted into degrees using cos $\alpha = (\gamma_{90}{}^{o}/\gamma_w)^{0.5}-1$ (Carrillo et al., 1999). The same droplet sizes were used in the SDM and the WDPT test (Subedi et al., 2012), which were conducted in triplicates. After placing the water droplets, the microphotographs of the initial contact angle ($t = 0$ seconds) between the water droplet and the soil surface were recorded with a digital microscopic camera system (VHX-1000, KEYENCE Corp., Osaka, Japan) with 100x magnification., At the same time the WDPT was measured in seconds.

3.3 Results and Discussion

3.3.1   Soil water retention curves for Japanese and New Zealand soils

Measured soil water retention data and fitted curves (Van Genuchten, 1980; Durner, 1994) for the Japanese and New Zealand soils are shown in Fig. 3.2 (data shown only for selected soil sampling depths). All New Zealand soil water retention data were well fitted with the unimodal equation (Eq. 3.1), while the multimodal ($k = 2$ subsystems, Durner. 1994) soil water retention equation (Eq. 3.1) (Van Genuchten, 1980; Durner, 1994) was a better fit for the Japanese water retention data. In the Eq. 3.1, the θ$_s$ was assumed to equal the total porosity of the soil samples.
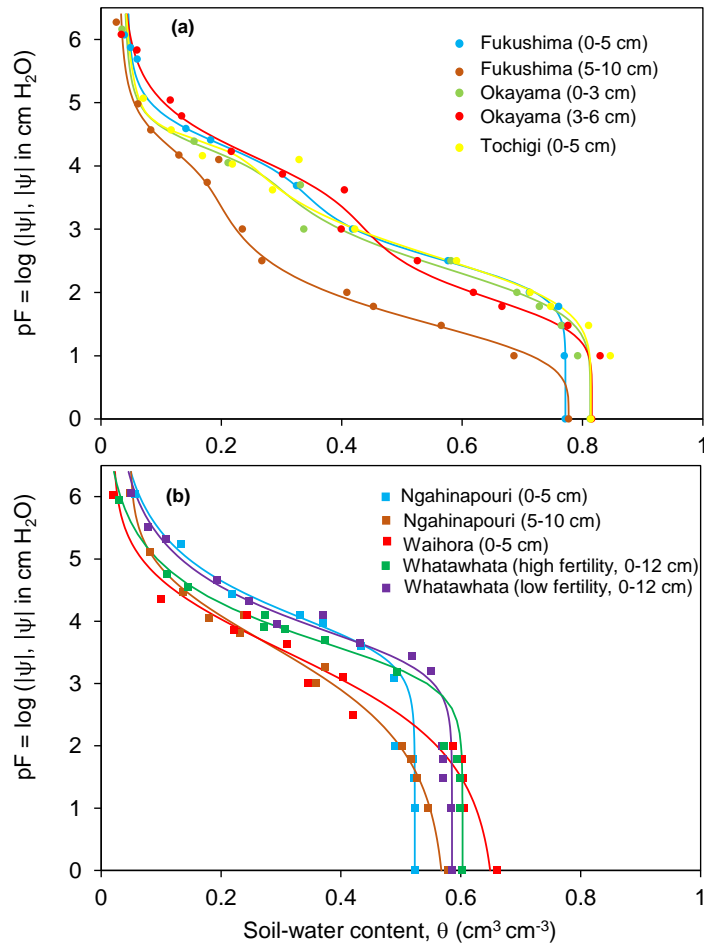
Figure 3.2 Soil water retention (SWR) curves for selected soil samples: (a) Japan soils and (b) New Zealand soils. Symbols show the measured soil water retention data and solid lines show the curves fitted by the Durner (1994) equations.

Estimated parameters are summarized in Table 3.3. The θ_{AD} of the Japanese soils varied between 0.02 and 0.03 cm^3 cm^{-3} and the corresponding pF values for ambient equilibrated soil samples ranged from 5.60 to 6.27. For the New Zealand soil samples, the θ_{AD} ranged between 0.01 and 0.05 cm^3 cm^{-3} with corresponding pF values between 5.94 and 6.06.

Table 3.3 Obtained parameter values for Japanese and New Zealand soil water retention curves

Japan	Depth (cm)	θ_s	θ_r	w_1	α_1	n_1	w_2	α_2	n_2	m_1	m_2
		-- cm³cm⁻³ --			cm⁻¹						
Nishigo, Fukushima	0-5	0.772	0.044	0.63	0.396	8.33	0.37	0.229	14.97	0.880	0.933
	5-10	0.777	0.026	0.84	0.633	4.19	0.16	0.233	14.79	0.762	0.932
	10-15	0.786	0.038	0.87	0.652	3.87	0.13	0.223	14.93	0.742	0.933
Hiruzen, Okayama	0-3	0.813	0.035	0.76	0.411	5.77	0.24	0.233	20.33	0.827	0.951
	3-6	0.816	0.034	0.52	0.516	6.26	0.48	0.238	9.944	0.840	0.899
Nikko, Tochigi	0-5	0.814	0.032	0.82	0.379	5.71	0.17	0.226	32.84	0.825	0.970
	5-34	0.831	0.022	0.37	0.863	3.81	0.63	0.285	7.620	0.738	0.869
New Zealand				α	n	m					
Ngahinapouri, Waikato	0-5	0.523	0.020	0.000	1.452	0.312					
	5-10	0.578	0.048	0.000	0.463	2.903					
	10-15	0.588	0.048	0.004	1.298	0.229					
Waihora, Waikato	0-5	0.661	0.020	0.000	0.488	2.050					
	5-10	0.666	0.005	0.018	1.336	0.252					
	10-20	0.639	0.025	0.014	1.445	0.308					
Whatawhata, Waikato (high fertility)	0-12	0.603	0.002	0.001	1.475	0.322					
Whatawhata, Waikato (low fertility)	0-12	0.585	0.020	0.000	1.460	0.315					

3.3.1 *Characterizations of soil water repellency for different soil depths*

Figure 3.3 shows the variations of SWR for all water-repellent soil samples using the WDPT, MED and SDM methods at different θ. Those soil samples not included in Fig. 3.3 were not repellent at any θ (six samples). The WDPT results were grouped into the following five classes based on Bisdom et al. (1993): wettable (< 5 s), slightly water-repellent (5–60 s), strongly water-repellent (60–600 s), severely water-repellent (600–3600 s) and extremely water-repellent (>3600 s). The soil samples from Fukushima (0–5 cm) and Okayama (0–3 cm) were extremely water-repellent at some θ, while the other Japanese soil samples varied between being wettable (< 5s) and severely water-repellent (600–3600 s) from FWC to θ_{AD}. Generally, the soil samples from the Ngahinapouri (0–5 and 5–10 cm) and Whatawhata high fertility sites were not as water-repellent as the soil samples from the Waihora and the Whatawhata low - fertility sites at medium θ (Fig. 3.3).

According to the SDM results, generally, all samples were wettable at FWC (Fig. 4). With the exception of a few samples (Fukushima 5–10 cm, Tochigi 0–5 cm, and Ngahinapouri 5–10 cm), all other samples were water-repellent at θ_{AD}. The degree of SWR of the soil samples from FWC to θ_{AD} gradually increased, and then decreased with further decreasing θ which followed the findings of Karunarathna et al. (2010a). In particular, the Ngahinapouri soils had high initial contact angle (CA_i) comparable to those measured for the other soils at medium θ (~0.1 to 0.2 cm^3 cm^{-3}). However, the Ngahinapouri soils had a lower persistence of SWR according to WDPT results.

The measured CA_i by MED and SDM were similar for the JP soils, but not for the NZ soils (Fig. 3.3). An explanation might be the different surface energy levels between the NZ and JP soils due to the different qualities of SOC, possibly driven by different vegetation types (Doerr et al., 2006; Martínez-Zavala and Jordán-López 2009; Jordán et al., 2009). In particular, all JP soils were collected from forests, and all NZ soils were under pasture. In addition, the pasture was grazed by animals, which can also affect the propensity of soils to develop hydrophobicity. For example, Schnabel et al. (2013) concluded that grassland intensively grazed with high stocking densities led to hydrophobic surface soil conditions. The chemical characterization of the soils' SOC could possibly help to explain the differences observed.

Water-repellent soil samples shown in Fig. 3.3 grouped into three SOC classes as (i) < 4 %, (ii) 4-10 % and (iii) >10 % of SOC. Then the measured CA_i from MED and SDM for

similar θ (within 0.01 cm^3 cm^{-3}) plotted in 1:1 plot as shown in Fig. 3.4. Fig. 3.4 clearly shows the difference of measured CA_i across different SOC intervals. Further, MED and SDM angles agreed well at average measurements and SDM is a more sensitive measure than MED also at high SWR.
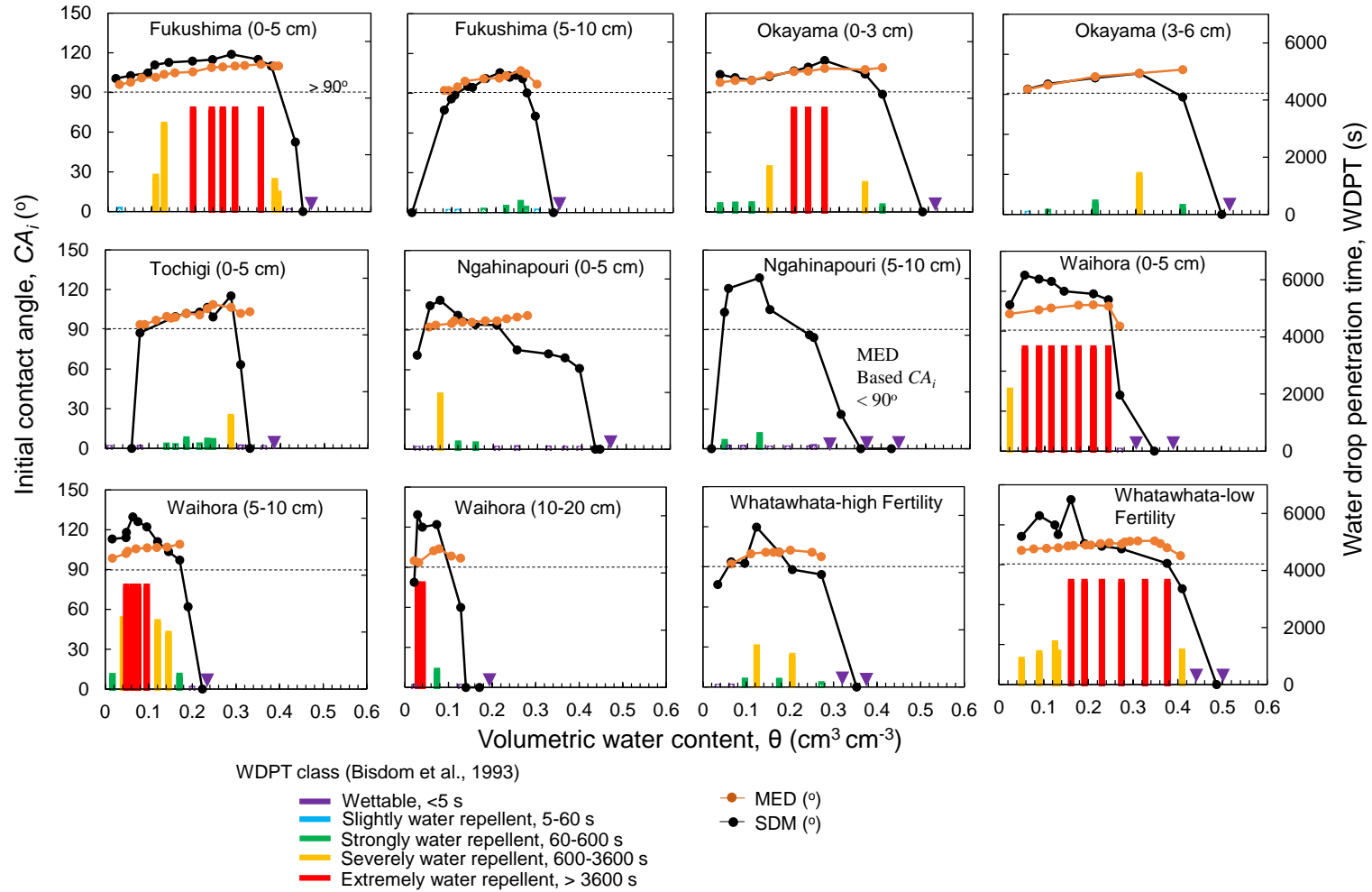
Figure 3.3 Characterization of soil water repellency for soils using the sessile drop method (SDM), the molarity of ethanol droplet (MED) and the water drop penetration time (WDPT) methods with changing volumetric water contents of soil samples. Zero WDPT data points are shown as small triangles.
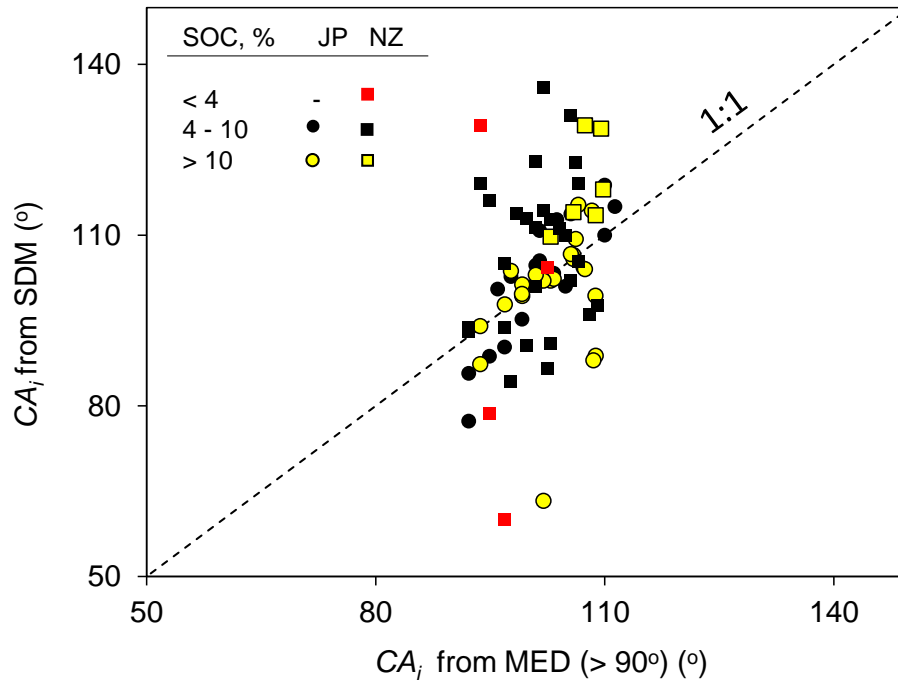
Figure 3.4 Soil-water contact angle measured by SDM and MED for Japanese and New Zealand soil samples (at same θ within 0.01 cm^{-3} cm^{-3}) and they were grouped at various SOC intervals (< 4 %, 4-10 % and > 10 % of SOC).

3.3.2 Applicability of clay/SOC ratio to identify water-repellent soils

All measured soils samples were grouped as water-repellent ($CA_i > 90°$), sub-critical water-repellent ($0 < CA_i < 90°$) and non-water-repellent ($CA_i = 0°$) based on the SDM values of maximum CA_i ($CA_{i\text{-max}}$) and on the SDM values of air-dry soils CA_i ($CA_{i\text{-AD}}$).

Figures 3.6a (based on $CA_{i\text{-max}}$) and 6b (based on $CA_{i\text{-AD}}$) show the relationship between clay content (%) and SOC content (%) for all soils. Saturation lines were drawn for the *Dexter index* at $n = 8$ (de Jonge et al., 1999) and $n = 10$ (Dexter et al., 2008; de Jonge et al., 2009; Karunarathna et al., 2010a). The $n = 10$ line marks the division between COC and NCOC (Dexter et al., 2008). de Jonge et al. (2009) first suggested using the *Dexter index* and saturation line to evaluate whether soil is water-repellent or non-water-repellent.

51

Karunarathna et al. (2010a) concluded that a *Dexter index* of 8 accurately separated water-repellent soils from non-repellent soils. In our study, the same *Dexter index* successfully differentiated between water-repellent and non-water-repellent soils at the maximum water-repellency (Fig. 3.6a), with the exception of the Tochigi soil samples. These soils were non-water-repellent even though they had SOC contents between 12 and 16% SOC (open symbols in Fig 3.6a). It has to be noted that these soil samples might not have been representative samples for respective soil depths. The sampling depths of the Tochigi soil were 5–34 cm, 34–70 cm and 70–90 cm (Table 3.2). This means that each of the soil samples represented a large proportion of the soil profile, and the heterogeneity of the measured sample might have been high.

At θ_{AD}, all soil samples were sub-critically water-repellent or non-water-repellent with the exception of the Fukushima, Waihora and Whatawhata topsoils. In the previous study by Karunarathna et al. (2010a), the positioning of the soil samples was not checked at air-dry conditions in the *Dexter plot*. We show here for the first time that the saturation line was not applicable to demarcate the border between water-repellent soils and non-repellent soils at θ_{AD} (Fig. 3.6b).
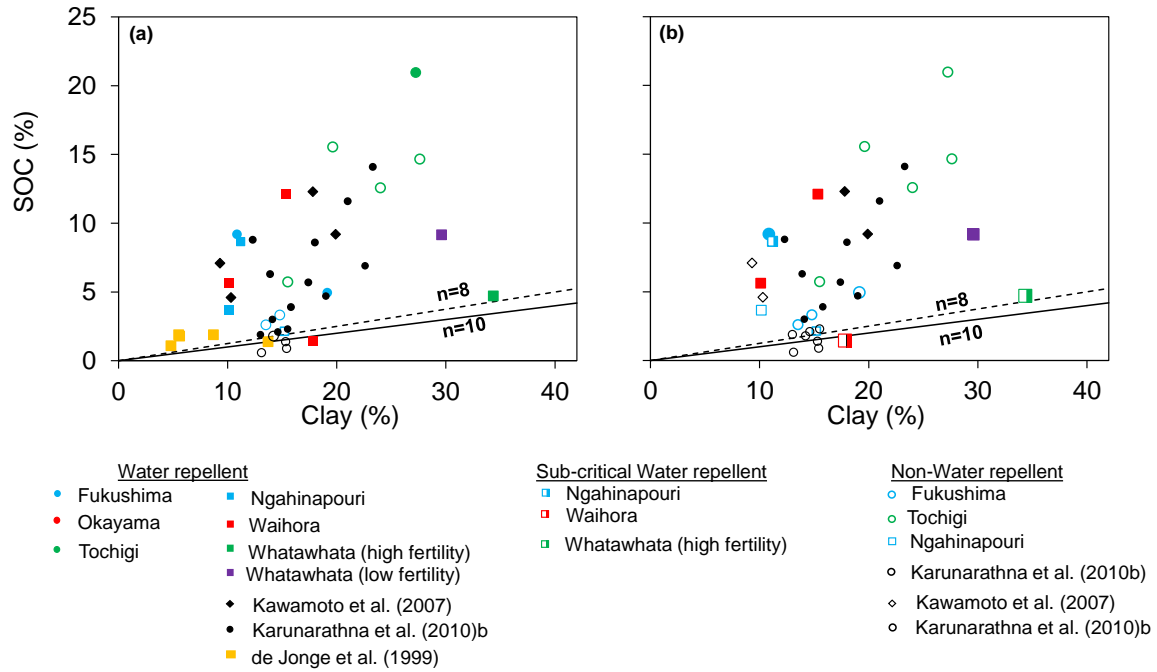
Figure 3.5 Relationship between clay and soil organic carbon (SOC) contents (Dexter et al, 2008) of water repellent (closed symbols), sub-critical water repellent (half-closed symbols) and non-water repellent soils (open symbols) (a) based on $CA_{i\text{-max}}$, and (b) based on $CA_{i\text{-AD}}$.

3.3.3   Derivation of soil water repellency parameters from SWRCC

It is time-consuming and cumbersome to estimate the full SWRCC for a water-repellent soil sample. Therefore, it is important to establish relationships between SWR parameters and other, easier to measure soil properties such as SOC contents.

Four SWRCC parameters were introduced: (i) area under the curve ($S_{WR(\theta)}$); (ii) θ at the maximum SWR ($\theta_{WR\text{-}max}$), (iii) θ where SWR ceased ($\theta_{non\text{-}WR}$), and (iv) the maximum SWR ($CA_{i\text{-max}}$). Figure 3.7 shows these SWR parameters schematically for a water-repellent soil, namely the Fukushima soil collected at 0–5 cm depth.

The calculated SWR parameters $S_{WR(\theta)}$, $\theta_{WR\text{-}max}$, $\theta_{non\text{-}WR}$ and $CA_{i,\,max}$ for the JP and NZ soils are presented as a function of the SOC content (%) in Fig. 3.8. Similar analyses were conducted by Regalado and Ritter (2005), Kawamoto et al. (2007) and de Jonge et al. (1999). The team of de Jonge et al. (1999) found a positive correlation ($r = 0.79$) between the area under the curve and the soils' organic carbon content. Kawamoto et al. (2007) concluded that the

relationship between the water-repellency parameters and the SOC contents is linear, but in their study, the measured maximum SOC was 12.3 %. In our study, the soil samples from Tochigi and Okayama had SOC contents between 20 and 26%. The linear relationship proposed by Kawamato et al. (2007) was thus, as expected, not confirmed by our results. Instead we introduced a Langmuir type equation (Eq. 3.2) to fit the data and we are able to use it with SOC-rich soil samples, or apply to a wide range of SOC contents:

$$P = P_{max}(SOC/k_{soc} + SOC) \qquad (3.2)$$

where P is the SWR parameter value (either $S_{WR(\theta)}$ [Eq. 4], $\theta_{WR\text{-}max}$ [Eq. 5] or $\theta_{non\text{-}WR}$ [Eq. 6]), P_{max} is the maximum value of the respective calculated SWR parameter values, SOC is the soil organic carbon content in percentage, %, and k_{soc} is half the SOC saturation at $P = 0.5 * P_{max}$. According to the Langmuir fitting, the following equations were found for the different SWR parameters and k_{soc} was fixed for all measured parameters as 4 % of SOC:

$$S_{WR(\theta)} = 0.78/ (4.0 + SOC) \ (r^2 = 0.60) \qquad (3.3)$$

$$\theta_{WR\text{-}max} = 0.32/ (4.0 + SOC) \ (r^2 = 0.53) \qquad (3.4)$$

$$\theta_{non\text{-}WR} = 0.49/ (4.0 + SOC) \ (r^2 = 0.70) \qquad (3.5)$$

However, $CA_{i, max}$ did not show a significant relationship with increasing SOC (%) ($r^2 = 0.03$; Fig 8d). Doerr et al. (2000) and Ellerbrock et al. (2005) found that SWR was not correlated with the total amount of organic matter. The Langmuir-type model covers the wide range of SOC soils (organic matter highly rich soils) and can be used to predict the SWR parameters or vice versa.
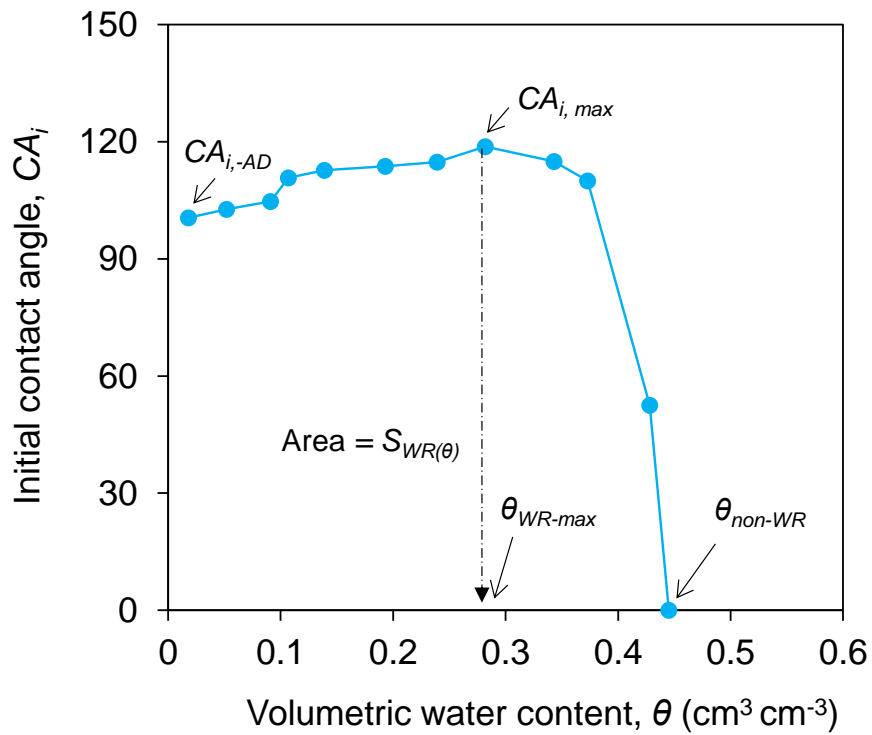
Figure 3.6 Schematic diagram showing the water repellency parameters derived using the soil water repellency characteristics curve (SWRCC): the area under the curve ($S_{WR(\theta)}$), the maximum soil-water contact angle ($CA_{i,\ max}$), and the water contents at $CA_{i,\ max}$ (θ_{WR-Max}) and at non-water repellency (θ_{non-WR}) after the maximum water repellency was reached.
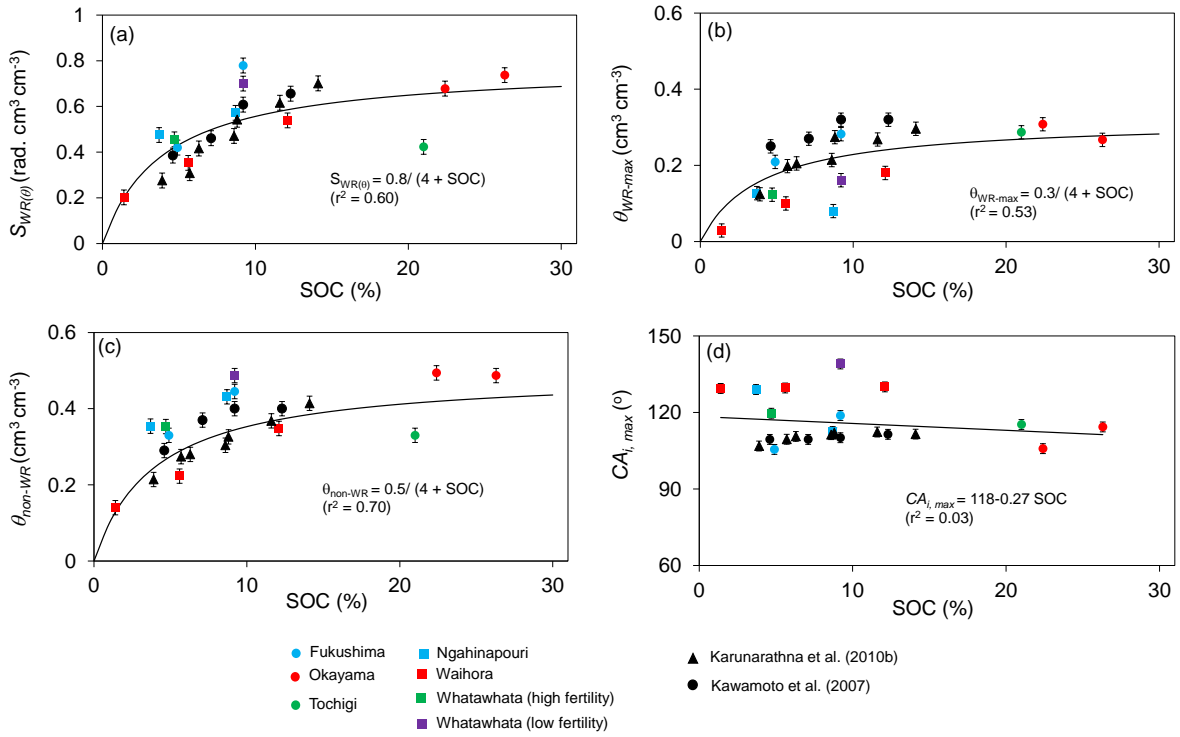
Figure 3.7 Relationship between calculated water repellency indices and SOC (%). Data points were fitted by a Langmuir type equation; P = P$_{max}$ (SOC/k$_{soc}$ + SOC) where P is parameter value, P$_{max}$ is maximum parameter value and k$_{soc}$ is half SOC saturation at P = 0.5*P$_{max}$.

3.4 Conclusions

The variation of SWR for all water-repellent soil samples with SOC contents ranging from 1.4 to 26.3%, was measured using the WDPT, MED and SDM methods at different θ. The combination of the three methods was useful to understand the persistence and degree of SWR for each soil type at different SOC. MED and SDM angles agreed well at average measurements and SDM is a more sensitive measure than MED at high SWR. In addition SDM characterizes sub-critical SWR. The *Dexter index* of 8 (*n* = 8) successfully differentiated water-repellent and non-repellent soils at the maximum water repellency, *CA$_{i\text{-max}}$*. But, the *Dexter index* was limited to differentiating water-repellent from non-repellent soil samples at air-dried conditions. Four SWR parameters were determined from the SWRCCs. They are (i) area under the curve (*S$_{WR(θ)}$*); (ii) θ at the maximum SWR (*θ$_{WR\text{-max}}$*), (iii) θ where SWR ceased (*θ$_{non\text{-WR}}$*), and (iv) the maximum SWR (*CA$_{i\text{-max}}$*). The relationships between these SWR parameters and SOC, % were characterized by fitting a Langmuir type equation: *P = P$_{max}$ (SOC/k$_{soc}$ + SOC)*.

This Langmuir type model covers the wide range of SOC soils to predict the SWR parameters or vice versa.

3.5 References

Arye, G., Nadav, I., Chen, Y., 2007. Short-term Reestablishment of Soil Water Repellency after Wetting: Effect on Capillary Pressure–Saturation Relationship. Soil Sci. Soc. Am. J. 71(3): 692.

Bachmann, J., Horton, R., van der Ploeg, R. R., Woche, S., 2000. Modified sessile drop method for assessing initial soil–water contact angle of sandy soil. Soil Sci. Soc. Am. J. 64: 564-567.

Ball, B.C., Campbell, D.J, Hunter, E.A., 2000. Soil compactability in relation to physical and organic properties at 156 sites in U.K. Soil Tillage Res. 57: 83–91.

Bisdom, E.B.A., Dekker, L.W., Schoute, J.F., 1993. Water repellency of sieve fractions from sandy soils and relationships with organic material and soil structure. Geoderma 56: 105–118.

Buczko, U., Bens, O., 2006. Assessing soil Hydrophobicity and Its variability through the soil profile using two different methods. Soil Sci. Soc. Am. J. 70: 718-727.

Carrillo, M.L.K., Letey J., Yates, S.R., 1999. Measurement of initial soil-water contact angle of water repellent soils. Soil Sci. Soc. Am. J. 63: 433–436.

Chau, H.W., Biswas, A., Vujanovic, V., Si, B.C., 2014. Relationship between the severity, persistence of soil water repellency and the critical soil water content in water repellent soils. Geoderma, 221-222: 113-120.

Clothier, B.E., Vogeler, I., Magesan, G.N., 2000. The breakdown of water repellency and solute transport through a hydrophobic soil. J. Hydrol. 231-232: 255-264.

de Jonge, L.W., Jacobsen, O.H., Moldrup, P., 1999. Soil water repellency: Effects of water content, temperature, and particle size. Soil Sci. Soc. Am. J. 63:437–442.

de Jonge, L.W., Moldrup, P., Schjønning, P., 2009. Soil Infrastructure, Interfaces and Translocation Processes in Inner Space ("Soil-it-is"): towards a road map for the constraints and crossroads of soil architecture and biophysical processes. Hydrol. Earth Syst. Sci. Discuss. 6(2): 2633–2678.

DeBano, L.F., 2000. Review: Water repellency in soils: a historical overview. Journal of hydrology, 231-232: 4-32.

Dekker, L.W., Doerr, S.H., Oostindie, K., Ziogas, A.K., Ritsema, C.J., 2001. Water repellency and critical soil water content in a dune sand. Soil Science Society of America Journal 65, 1667–1674.

Deurer, M., Müller, K., Van Den Dijssel, C., Mason, K., Carter, J., Clothier, B.E., 2011. Is soil water repellency a function of soil order and proneness to drought? A survey of soils

under pasture in the North Island of New Zealand. European Journal of Soil Science 62:765-779.

Dexter, A.R., Richard G., Arrouays, D., Czyz, E.A., Jolivet, C., Duval, O., 2008. Complexed organic matter controls soil physical properties. Geoderma 144: 620–627. doi:10.1016/j.geoderma.2008.01.022.

Doerr, S.H., Shakerby, R.A., Dekker, L.W., Ritsema, C.J., 2006. Occurrence, prediction and hydrological effects of water repellency amongst major soil and land-use types in a humid temperate climate. 57 (5): 741-754.

Doerr, S.H., Shakesby, R.A., Walsh, R.P.D., 2000. Soil water repellency: its causes, characteristics and hydro-geomorphological significance. Earth-Science Reviews 51: 33–65.

Durner, W., 1994. Hydraulic conductivity estimation for soils with heterogeneous pore structure. Water Resour. Res. 30:211–223.

Ellerbrock, R.H., Gerke, H.H., Bachmann, J., Goebel M.-O., 2005. Composition of organic matter fractions for explaining wettability of three forest soils. Soil Science Society of America Journal 69, 57–66.

Hallett, P.D., Ritz K., Wheatley, R.E., 2001. Microbial derived water repellency in golf course soil. Intl. Turfgrass Soc. Res. J. 9: 518-524.

Horne, D. J., McIntosh, J.C., 2000. Hydrophobic compounds in sands in New Zealand: Extraction, characterization and proposed mechanisms for repellency expression. J. Hydrol. 231–232: 35–46.

Jordán, A., Zavala, L.M., Nava, A.L., Alanís, N., 2009. Occurrence and hydrological effects of water repellency in different soil and land use types in Mexican volcanic highlands. Catena 79:60–71. doi: 10.1016/j.catena.2009.05.013.

Karunarathna, A.K., Moldrup, P., Kawamoto, K., de Jonge, L.W., Komatsu, T., 2010a. Two-region model for soil water repellency as a function of matric potential and water content. Vadose Zone J. 9: 719-730. Doi:10.2136/vzj2009.0124.

Karunarathna, A.K., Moldrup, P., Kawamoto, K., de Jonge, L.W., Komatsu, T., 2010b. Beta model for soil water repellency as a function of matric potential and water content. Vadose Zone J. 9: 719-730. Doi:10.2136/vzj2009.0124.

Kawamoto, K., Moldrup, P., Komatsu, T., de Jonge, L.W., Oda, M., 2007. Water repellency of aggregate size fractions of a volcanic ash soil. Soi Sci. Soc. Am. J. 71 (6):1658-1666.

Kettler, T. A., Doran, J.W., Gilbert, T.L., 2001. Simplified Method for Soil Particle-Size Determination to Accompany Soil-Quality Analyses. *Publications from USDA-ARS / UNL Faculty.* Paper 305.

King, P.M., 1981. Comparison of methods for measuring se- verity of water repellence of sandy soils and assessment of some factors that affect its measurement. Aust. J. Soil Res., 19, 275–285.

Lamparter, A., Bachmann, J., Goebel, M.-O., Woche, S.K., 2009. Carbon mineralization in soil: Impact of wetting–drying, aggregate on and water repellency. Geoderma 150:324–333. doi:10.1016/j.geoderma.2009.02.014.

Leelamanie, D.A.L., Karube, J. 2007. Effects of organic compounds, water content and clay on the water repellency of a model sandy soil. Soil Sci. Plant Nutr., 53: 711-719.

Leelamanie, D.A.L., Karube, J., 2014. Water stable aggregates of Japanese Andisol as affected by hydrophobicity and drying temperature. J. Hydrol. Hydro mech., 62 (2): 97–100.

Martínez-Zavala, L., Jordán-López, A., 2009. Influence of different plant species on water repellency in Mediterranean heathland soils. Catena, 76: 215–223. doi: 10.1016/j.catena.2008.12.002.

Ma'shum, M., Farmer, V., 1985. Origin and assessment of water repellency of a sandy South Australian soil. Aust J Soil Res, 23:623–6.

McIntosh, J.C., Horne, D.J., 1994. Causes of repellency: I. The nature of the hydrophobic compounds found in a New Zealand development sequence of yellow–brown sands. Proceedings of the 2nd National Water Repellency Workshop, 1–5 August, Perth, Western Australia: 8–12.

Müller, K., Deurer, M., Jeyakumar, P., Mason, K., van den Dijssel, C., Green, S., Clothier, B., 2014a. Temporal dynamics of soil water repellency and its impact on pasture productivity. Agricultural Water Management 143: 82–92.

Müller, K., Deurer, M., Kawamoto, K., Kuroda, T., Subedi, S., Hiradate, S., Komatsu, T., Clothier, B.E., 2014b. A new method to quantify how water repellency compromises soils' filtering function. Eur J Soil Sci 65:348–359.

Müller, K., Deurer, M., Slay, M., Aslam, T., Carter, J.A., Clothier, B.E., 2010. Environmental and economic consequences of soil water repellency under pasture. Proceedings of the New Zealand Grassland Association, 72: 207–210.

Neris, J., Tejedor, M., Rodríguez, M., 2013. Effect of forest floor characteristics on water repellency, infiltration, runoff and soil loss in Andisols of Tenerife (Canary Islands, Spain). Catena 108: 50–57. doi: 10.1016/j.catena.2012.04.011.

Nowak, E., Robbins P., Combes, G., 2013. Measurements of contact angle between fine, non-porous particles with varying hydrophobicity and water and non-polar liquids of different viscosities. Powder Technol 250: 21–32.

Regalado, C.M., and Ritter, A., 2005. Characterizing Water Dependent Soil Repellency with Minimal Parameter Requirement. Soil Sci. Soc. Am. J. 69 (6): 1955-1966.

Regalado, C.M., Ritter, A., de Jonge, L.W., Kawamoto, K., Komatsu T., Moldrup P., 2008. Useful soil-water repellency indices: Linear correlations, Soil Sci., 173, 747–757.

Resurreccion, A.C., Moldrup, P., Kawamoto, K., 2008. Variable Pore Connectivity Factor Model for Gas Diffusivity in Unsaturated, Aggregated Soil. Vadose Zone Journal 7: 397, doi: 10.2136/vzj2007.0058.

Rodríguez-Alleres, M., Benito, E., de Blas, E., 2007. Extent and persistence of water repellency in north-western Spanish soils. Hydrol. Process. 21: 2291–2299.

Roy, J.L., McGill W.B., 2002. Assessing soil water repellency using the molarity of ethanol droplet (MED) test. Soil Sci. 167: 83–97.

Schipper, L.A., Dodd, M., Fisk, L.M., Power, I., Paranzee, J., Arnold, G. C., 2009. Trends in soil carbon and nutrients of hill-country pastures receiving different phosphorus fertilizer loadings for 20 years. Biogeochemistry 104: 35-48.

Schnabel, S., Pulido-Fernández, M., Lavado-Contador, J.F., 2013. Soil water repellency in rangelands of Extremadura (Spain) and its relationship with land management. Catena 103: 53–61.

Subedi, S., Kawamoto, K., Jayarathna, L., Vithanage, M., Moldrup, P., de Jonge, L.W., Komatsu T., 2012. Characterizing time dependent contact angle for sands hydrophobized with oleic and stearic acids. Vadose zone Journal, 11 (1), doi:10.2136/vzj2011.0055.

Täumer, K., Stoffregen, H., Wessolek, G., 2005. Determination of repellency distribution using soil organic matter and water content. Geoderma 125: 107–115.

Urbanek, E., Hallett, P., Feeney, D., Horn, R., 2007. Water repellency and distribution of hydrophilic and hydrophobic compounds in soil aggregates from different tillage systems. Geoderma, 140: 147–155.

USS Working Group WRB. 2006. World Reference Base for Soil Resources 2006. A framework for international classification, correlation and communication. 2nd edition. World Soil Resources Reports 103 FAO, Rome.

Van Genuchten, M., 1980. A closed-form equation for predicting the hydraulic conductivity of unsaturated soils. Soil Science Society of America Journal 44: 892–898.

Van't Woudt, B.D., 1959. Particle coatings affecting the wettability of soils. Journal of Geophysical Research 64: 263–267.

Vogelmann E.S., Reichert, J.M., Prevedello, J., Consensa, C.O.B., Oliveira, A.É., Awe, G.O., Mataix-Solera, J., 2013. Thresholdwater content beyondwhich hydrophobic soils become hydrophilic: The role of soil texture and organic matter content. Geoderma, 209-210: 177-187.

Wallis, M.G., Horne, D.J., 1992. Soil water repellency. Adv. Soil Sci. 20: 91– 146. doi:10.1007/978-1-4612-2930-8_2.

Wraith, J. M., and Or, D. 1998. Nonlinear parameter estimation using spread sheet software. J. Nat. Resour. Life Sci. Educ. 27:13–19.

Chapter 4

4. CHEMICAL CHARACTERIZATION (C, N, O) OF WATER REPELLENT SOIL SURFACE USING XPS MEASUREMENTS.

ABSTRACT

Soil water repellency (SWR) is a phenomenon that will reduce the soil water infiltration. Generally, the presence of soil organic carbon and moisture contents will govern the degree of SWR. Therefore, understanding of surface chemical properties are important to understand the parameters controlling the SWR. Objectives of this study are to (i) assess the carbon (C), nitrogen (N) and oxygen (O) relative atomic concentration of soil grain surface, (ii) find the relationship between soil water repellency parameters and CNO composition. Fourteen soil samples were selected from Japanese forest and New Zealand pasture soils. The degree of SWR was measured using the sessile drop method. Air-dried and 2-mm sieved soil samples (~1.0 mg) were used for the XPS measurements. For each soil sample the relative C, O, and N concentration was calculated by using the peak area of each 1s orbital spectra. Peak separations were done to estimate $C^{[o]}$, $C^{[+1]}$, $C^{[+2]}$ and $C^{[+3]}$ for each soil sample. The results show higher concentration of $C^{[o]}$ (C-C or C-H functional groups) than concentrations of the other oxidation states in water repellent soil. Sub-critical water repellent soil samples showed higher concentration of $C^{[+1]}$ (C-O or C-N functional groups) than of other oxidation states. The calculated SWR parameters were plotted with measured relative atomic concentration of C, O % and C/N ratio. Results revealed high SWR at high C/N ratio (determined by XPS) and show a liner regression ($r^2 = 0.72$) between C/N and the volumetric water content at maximum SWR (θ_{WR-max}). Soil was not water repellent at the high atomic concentration of O (> 65 %) and low C (< 35 %) combination.

4.1 Introduction

Soil water repellency (SWR) is a significant phenomenon in less disturb soil and high organic matter rich soil that could lead to less infiltration rate or increase soil surface runoff (Chau et al., 2014; Doerr et al., 2006, 2000). Most of the research work has been done to estimate the SWR and very limited number of research work has been done to characterize the chemical composition of water repellent soils. Presently, there are some techniques available to measure surface chemical compositions and among them X-ray photoelectron spectroscopy (XPS) techniques (Monteil-Rivera et al., 2000) is precise to use with some limitations. The XPS is a technique for analyzing the surface chemistry of a material (Jansen and van Bekkum, 1995; Watts and Wolstenholme, 2003; Yamashita and Hayes, 2008). XPS can measure the elemental composition (Gerin et al., 2003), empirical formula, chemical state and electronic state of the elements within a solid (Gerin et al., 2003; Jansen and van Bekkum, 1995; Yamashita and Hayes, 2008).

Soil water repellency is mainly occurred as a result of organic matter coating (Karunarathna et al., 2010; Kawamoto et al., 2007; Leelamanie and Karube, 2007). Therefore, assessment of surface composition is important than bulk analysis with respect to the SWR. Nuclear Magnetic Resonance (NMR) is an absorption spectroscopic method close to infrared and ultraviolet spectroscopy (Hiradate, 2004; Hiradate et al., 2006). In the NMR, ground and powdered sample are used to obtain the NMR spectrum. But in the XPS technique, we can use either original samples itself or ground samples. So, the grains surface measurements are important to understand the enrichment of elements at the surface of the soil grains (Kobayashi and Matsui, 2006). The XPS techniques is used to detect the surface chemical composition by obtain the spectra of the soil grain surface elements and restricted to measure the depth of < 10 nm (2-3 atomic layers) from the soil surface (Gerin et al., 2003; Yuan et al., 1998).

In this study, surface soil organic carbon (C), soil organic nitrogen (N) and oxygen (O) relative atomic concentration were estimated since we assumed the there is a direct of C % to SWR. In chapter 3, concluded that bulk SOC has an effect on SWR parameters and all parameters come to saturate after 4% SOC. Therefore, in this study detailed analysis has been performed to identify the key functional groups depending on C-oxidation states (Gerin et al., 2003). Table 4.1 shows the specific binding energy with respect to type of carbon. This will to find the functional groups which are causing to SWR.

Table 4.1 Types of carbon (functional groups) which represent the specific binding energy in spectrum (Gerin et al., 2003) of XPS.

Type of carbon	Valence notation	Binding energy (eV)
C-C, C-H	$C^{[o]}$	284.8[a]
C-O, C-N	$C^{[+1]}$	286.4
C=O, O-C-O	$C^{[+2]}$	287.9
O=C-O, O=C-N, CO$_3$=	$C^{[+3]}$	289.3

Objectives of this study are to (i) assess the carbon (C), nitrogen (N) and oxygen (O) relative atomic concentration of soil grain surface, (ii) find the relationship between SWR parameters and CNO composition.

4.2 Materials and Methods

4.2.1 Soil sampling and soil properties

Soil samples were selected from Japan (JP) and New Zealand (NZ) at different soil sampling depths. The sites in JP were located in Nishigo, Fukushima (0-5, 5-10, 10-15 cm), Hiruzen, Okayama (0-3, 3-6 cm) and Nikko, Tochigi (0-5, 5-34 cm), and in NZ: Ngahinapouri, Waikato (0-5, 5-10, 10-20), Waihora, Waikato (0-5, 5-10) and Whatawhata, Waikato (0-12 cm for high fertility and low fertility sites).

Selected soil samples for different depths were air-dried and sieved, < 2.0 mm. The total carbon (C) and total nitrogen (N) for each depths were measured by CN-analyzer (FLASH 2000 CHNS/O Analyzers, Thermo Scientific, Thermo Fisher Scientific, Inc. (NYSE:TMO)). Measured C and N are tabulated in Table 4.2. All other soil properties for selected soil samples were mentioned in Chapter 3.

4.2.2 Measurements of soil water repellency

The degree of SWR of each soil samples were measured using sessile drop method (SDM) (Bachmann et al., 2000) with respect to the volumetric water content (θ) and known as soil

water repellency characteristic curve (SWRCC). Soil samples were prepared with different θ from field water content to air-dry condition by 60ºC oven drying for different time-intervals following the (Kawamoto et al., 2007)) methodology. The repack soil-column for each soil depth samples were prepared with field dry bulk densities for SDM measurements as explained in chapter 3.

4.2.3   X-ray photoelectron spectroscopy measurements and analysis

X-ray photoelectron spectroscopy (XPS) spectra were recorded on the XPS (AXIS NOVA, Kratos analytical Ltd.) using a monochromatic Al Kα X-ray source (hv = 1486.6 eV) at an electric current of 15 mA and a voltage of 20 kV (300 W). The picture of the AXIS Nova is shown in Fig. 4.1a. Soil samples were loaded in sample plate as shown in Fig. 4.1b and then sample plates was transferred to sample chamber (Fig. 4.1c).

Air-dried and 2-mm sieved soil samples (~1.0 mg) was packed into a sample holder having a diameter of 5 mm and depth of 3 mm, which was fixed on the surface of a stainless steel plate (Fig. 1b) by carbon conductive adhesive double-sided tape. Vacuum pressure was maintained at 10^{-6} to 10^{-7} Pa during measurement.

Fig. 4.2 shows the experimental procedure how to obtain the high resolution XPS spectrum by following step one and step two. In the step one, wide spectra were recorded for each visible line at 1 eV per step, analyzer pass energy of 160 eV, and the time for one scan was 300 ms. Since, we were interested only C, N and O peaks, the narrow spectrum was recorded for each visible line at 0.1 eV per step, analyzer pass energy of 40eV, and the time for one scan was 298 ms to have a high resolution element peaks. Correction of binding energy was made relative to the C-C/C-H signal at 284.8 eV (Table 4.1) in the C 1s spectra measured simultaneously. Data manipulation including integration and background subtraction was accomplished on a Comprehensive Analysis Center for Science, Saitama University, Japan installed with data treatment software (Kratos VISION 2). The contents of carbon, nitrogen, and oxygen were calculated as relative ratio (atomic %) of the three elements by using peak area of each 1s orbital. The peak area was estimated from removing the background with straight-line method. Finally, the carbon spectrum was separated to estimate relative distribution of each functional group (Amelung et al., 2002; Gerin et al., 2003; Watanabe et al., 2014) (*see* Table 4.1).
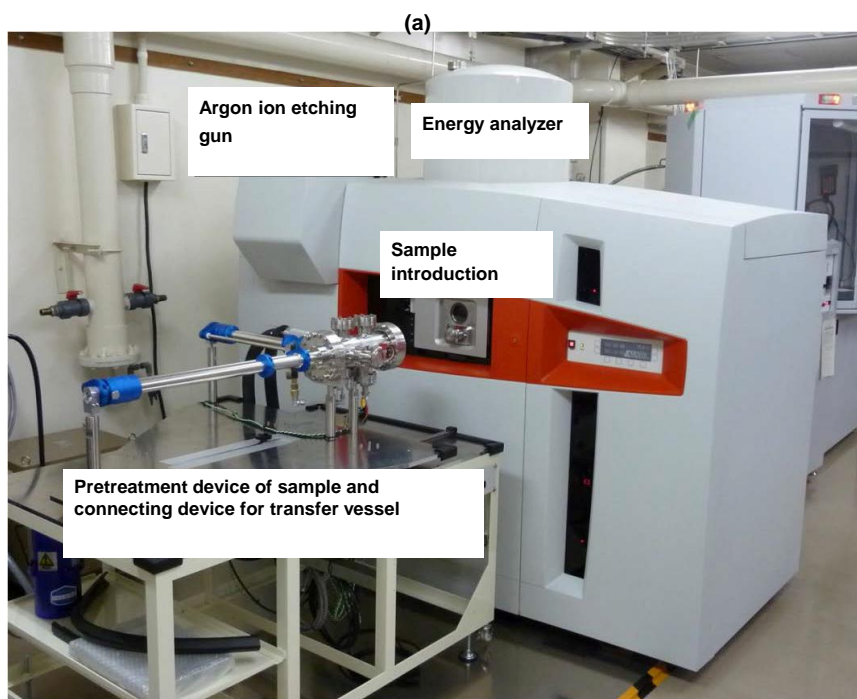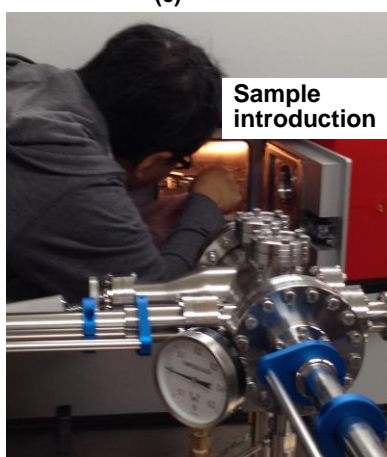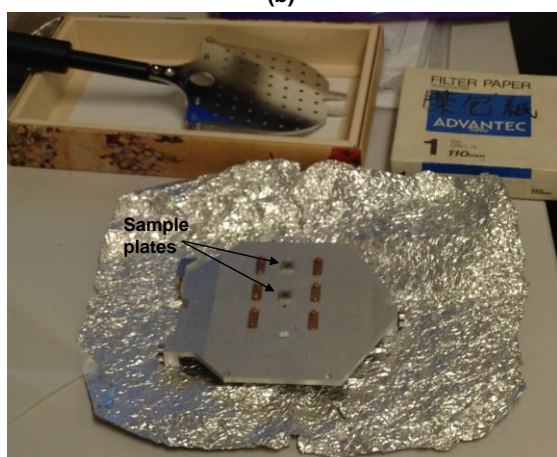
Figure 4.1 (a) Automated x-ray photoelectron spectrometer at Comprehensive Analysis Center for Science, Saitama University, Japan (AXIS NOVA, Kratos analytical Ltd.), (b) sample plates and (c) sample introduction to x-ray photoelectron spectromet

Table 4.2 Soil sampling sites details and chemical composition by CN analyzer (FLASH 2000 CHNS/O Analyzers, Thermo Scientific, Thermo Fisher Scientific, Inc. (NYSE:TMO)) and XPS (AXIS NOVA, Kratos analytical Ltd.) surface measurements.

| Sample location	Soil depth (cm)	Sample ID	Bulk analysis (CN analyzer)			Surface analysis (XPS): Relative atomic concentration (%)				$CA_{i,\,max}$	$CA_{i,\,AD}$	Soil water repellency				
			C (%)	N (%)	C/N	C	N	O	C/N			Based on $CA_{i,\,AD}$	Based on $CA_{i,\,max}$	$S_{WR(\theta)}$	$\theta_{WR\text{-}max}$	$\theta_{non\text{-}WR}$
Nishigo, Fukushima	0-5	Fk1	9.2	0.6	14.8	53.4	3.1	43.5	17.40	119	100	WR	WR	0.78	0.28	0.44
	5-10	Fk2	4.9	0.3	15.3	54.5	2.8	42.7	19.30	105	-	NWR	WR	0.42	0.21	0.33
	10-15	Fk3	3.3	0.3	10.5	30.3	2.8	67	11.00	0	-	NWR	NWR	-	-	-
Hiruzen, Okayama	0-3	Ok1	26.3	1.4	19.3	55.3	2.7	42.0	20.26	114	103	WR	WR	0.74	0.27	0.49
	3-6	Ok2	22.4	1.2	19.1	54.7	3.0	42.3	18.42	116	94	WR	WR	0.68	0.31	0.49
Nikko, Tochigi	0-5	To1	21	1.2	17.8	46.5	2.8	50.7	16.73	115	-	NWR	WR	0.42	0.29	0.33
	5-34	To2	15.6	0.8	20.1	46.3	2.8	50.9	16.54	0	-	NWR	NWR	-	-	-
Ngahinapouri, Waikato	0-5	Ng1	8.7	0.6	15.3	51.8	4.7	43.6	11.10	119	71	sub-WR	WR	0.57	0.08	0.43
	5-10	Ng2	3.7	0.4	9.4	49.5	4.8	45.7	10.30	122	-	NWR	WR	0.48	0.13	0.35
	10-20	Ng3	2.2	0.4	9.8	48	4.8	47.2	10.10	123	-	NWR	NWR	-	-	-
Waihora, Waikato	0-5	Wh1	12.1	0.6	20.9	53.9	3.6	42.5	15.02	129	109.7	WR	WR	0.54	0.18	0.35
	5-10	Wh2	5.6	0.4	12.3	51.0	3.8	45.2	13.34	131	113.7	WR	WR	0.35	0.10	0.22
Whatawhata, Waikato	0-12 (High fertility)	W-H	4.7	0.5	8.9	33.9	2.7	63.5	12.70	123	76.7	sub-WR	WR	0.45	0.12	0.35
	0-12 (Low fertility)	W-L	9.2	1.2	7.9	45.6	3.1	51.3	14.50	136	111.3	WR	WR	0.70	0.16	0.49
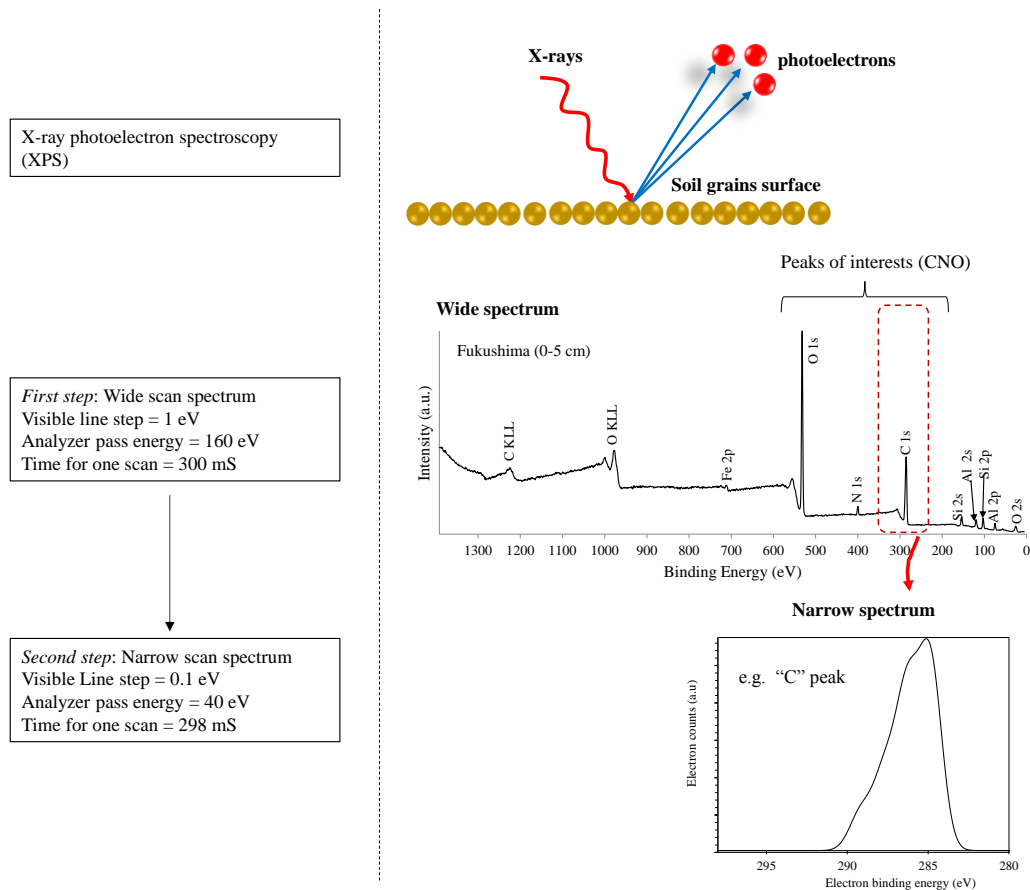
Figure 4.2 X-ray photoelectron spectroscopy wide and narrow spectrum recording procedure with high resolution and details of specific experiments condition.

4.3 Results and Discussion

4.3.1 Estimation of soil-water-repellency parameters

The measured SWR for soil samples at different volumetric water content are shown in Fig. 4.3. At the air dry soil, except Fukushima (5-10 cm) and Tochigi 0-5 cm all others are water-repellent. In Fig. 4.3, blue and red circles are marked the air-dry and maximum SWR respectively. Based on air–dry and maximum soil water repellency, soils samples were grouped into three classes as water-repellent ($CA_i > 90^o$), non-repellent ($CA_i = 0^o$) and sub-critical water-repellent ($0^o < CA_i < 90^o$). Table 4.2 shows the soils sample's classes according to the degree of water repellency.
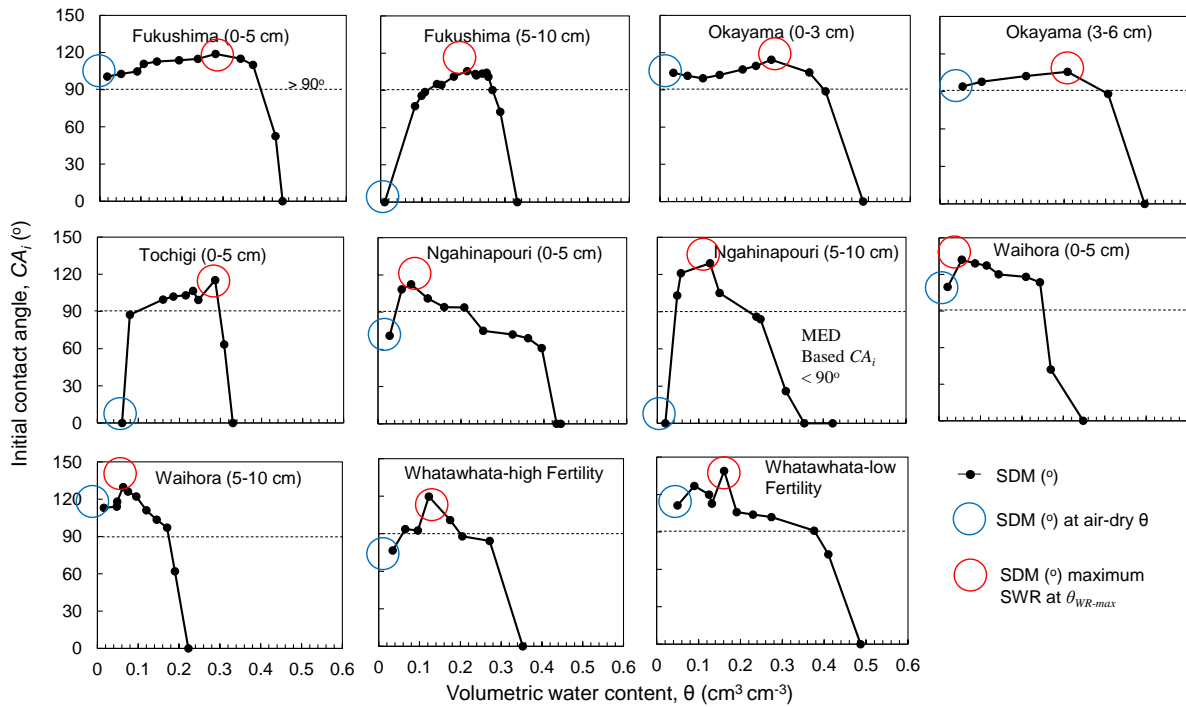
Figure 4.3 Measured soil-water initial contact angle by sessile drop method (SDM) for water repellent soils with changing volumetric water content.

Soil water repellency parameters were calculated for SDM results as (i) area under the curve ($S_{WR(\theta)}$); (ii) θ at the maximum SWR ($\theta_{WR\text{-}max}$), (iii) θ where SWR ceased ($\theta_{non\text{-}WR}$), and (iv) the maximum SWR ($CA_{i\text{-}max}$) and values are shown in Table 4.2.

4.3.2 The XPS analysis

The XPS wide spectrum for Nishigo, Fukushima is shown in Fig. 4.4. All other sample's spectrum are shown in *Appendix A*. In the wide spectrum, we are interested on C1s, O1s and N1s peaks to find relationships between SWR parameters and CNO contents by XPS. Figure 4.5 shows the variation of C, N, and O for all soil samples and each element ratio. Water-repellent soils from Andosols (both JP and NZ) are having high C, low N and low O. The Ngahinapouri samples which belong to sub-critical water-repellency are having high C, high N and very low O. Those samples having a high content of O are non-repellent (Fig. 4.5a, b and c). Figures 4.5d, e and f shows the element ratios and it is agree to conclude that high C/N and high N/O soil samples are water-repellent.
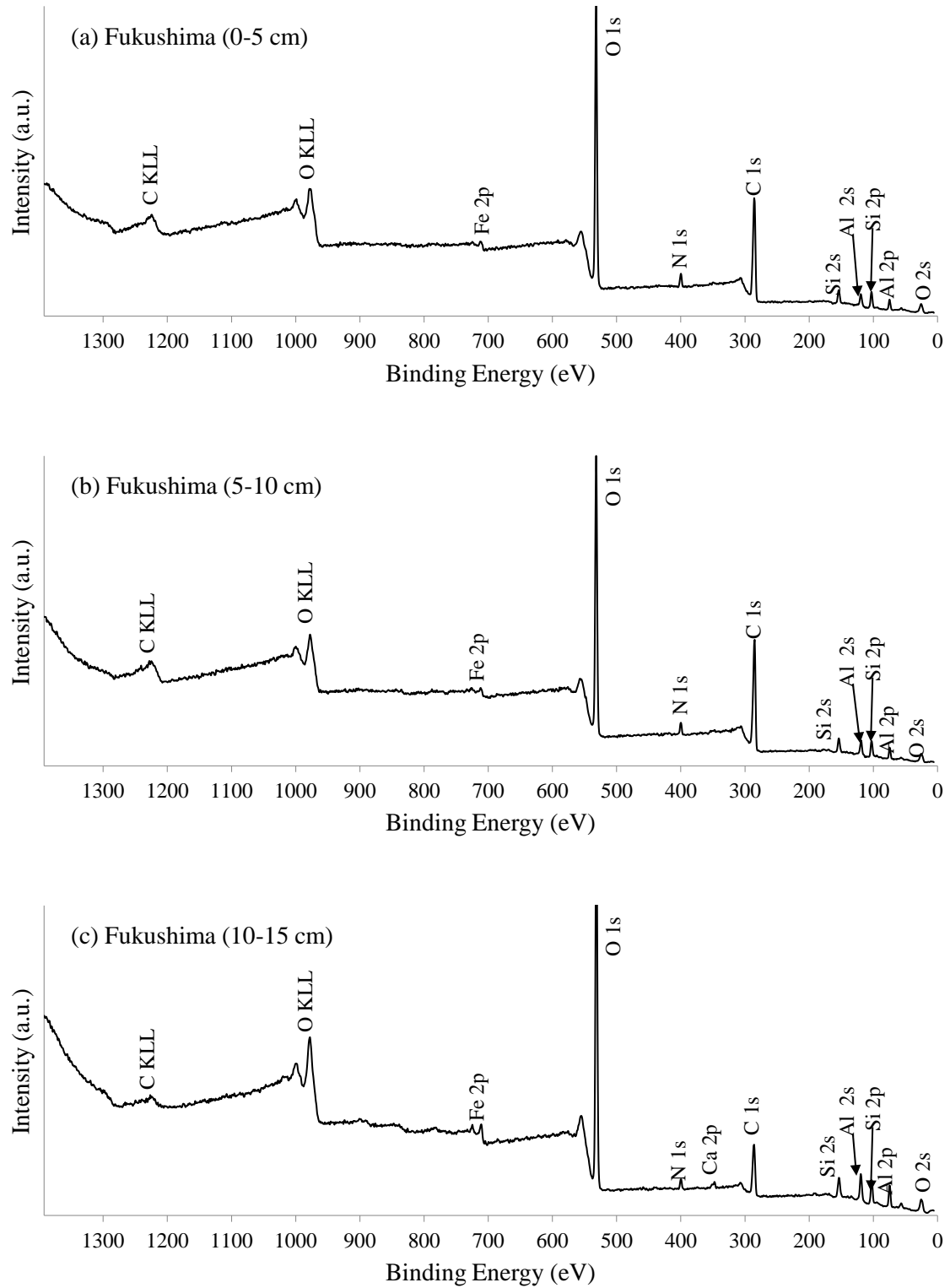
68

Figure 4.4 Wide spectrum for Nishigo, Fukushima (a) 0-5 cm depth, (b) 5-10 cm depth and (c) 10-15 cm depth soil samples to show measured peak for each elements abundances.
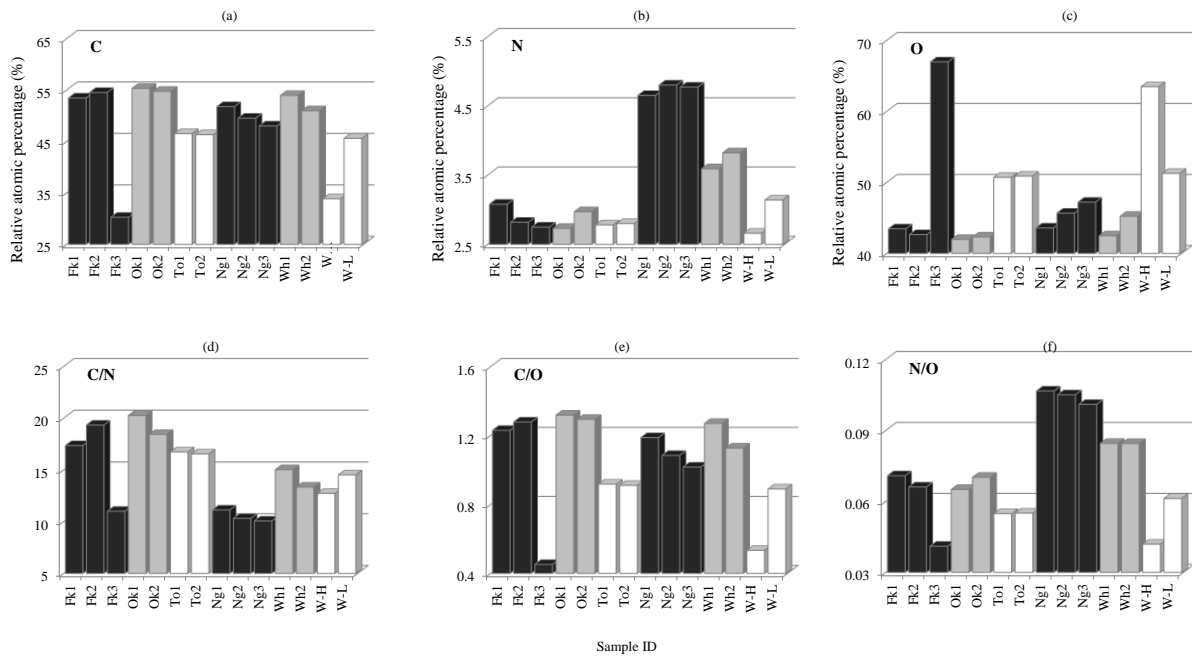
Figure 4.5 Relative atomic concentration (%) of (a) C, (b) N and (c) O for 14 soil samples, (d) C/N, (e) C/O and (f) N/O which calculated from C1s, N1s and O1s.

The measured SWR parameters plotted as a function of each interested elements concentration and C/N ratio. Figure 4.6 shows the regression analysis of each SWR parameters with the calculated C %, N %, O % and C/N ratio, Results revealed high SWR at high C/N ratio (determined by XPS) and show a liner regression ($r^2 = 0.72$) between C/N and the volumetric water content at maximum SWR ($\theta_{WR\text{-}max}$).
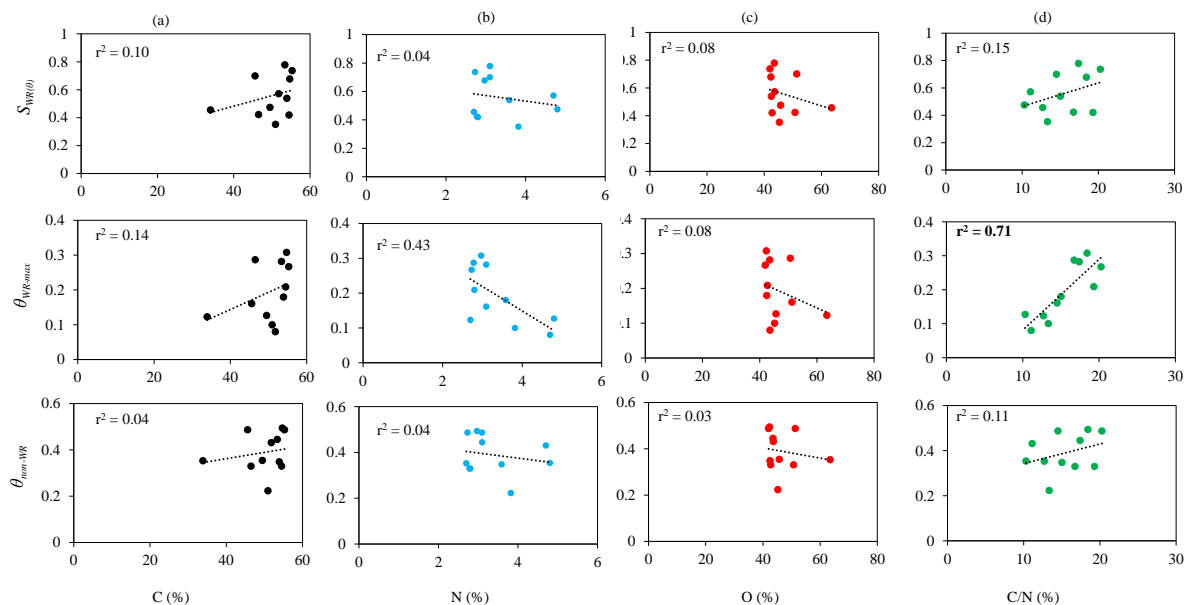
Figure 4.6 Correlation between SWR parameters to (a) C, (b) N, (c) O, and (d) C/N for all 14 soil samples.

Some of the publications have mentioned the organo-complex (Amelung et al., 2002; Dexter et al., 2008) with some soil mineral ions such as Fe^{+2}/Fe^{+3} and Al^{+3} are also causing the soil grains surface properties. In our study, specifically C1s atomic concentration and C-peak separations have been estimated by assuming those elements were directly correlate to the SWR. The very high C, % by XPS than bulk SOC content has resulted in the study of (Gerin et al., 2003). Fig. 4.7a shows the relationship between surface and bulk carbon concentration and Fig. 4.7b shows the relationship between surface C/N ratio and bulk C/N ratio observed for JP and NZ soil samples. The similar results were obtained by (Gerin et al., 2003) and it can be compared the relative amount of C with absolute amount of C.
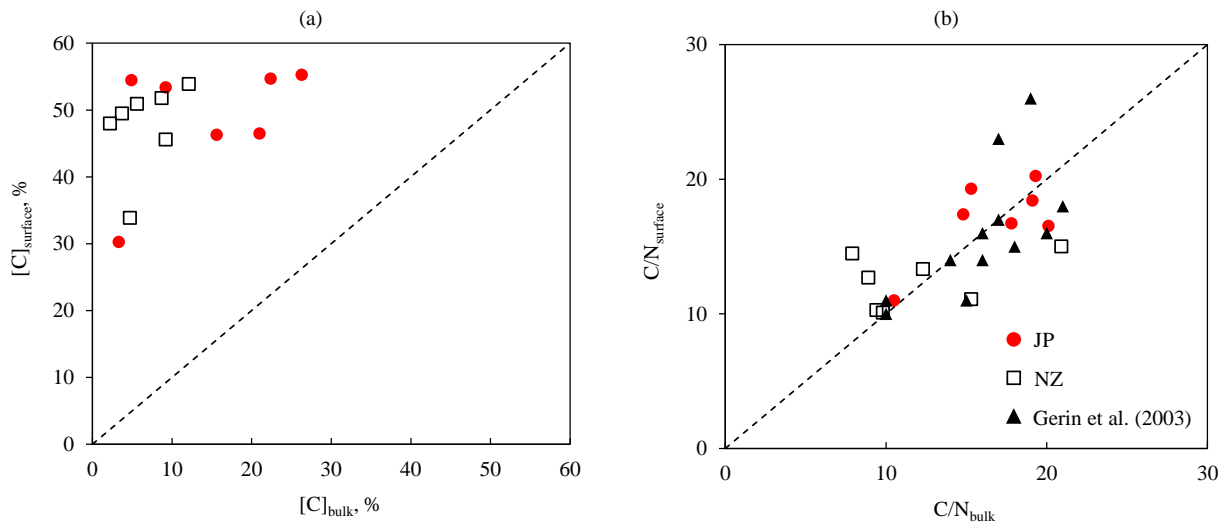
Figure 4.7 (a) Relationship between surface and bulk carbon concentration and (b) Relationship between surface and bulk carbon concentration to nitrogen ratios observed for JP and NZ soil samples.

Figure 4.8 shows the carbon spectra obtained by XPS analysis of the (Fig. 4.8a) JP-Andosols (Fk1) and (Fig. 4.8b) NZ-Cambisols (W-H) for relative distribution of carbon atoms in chemical functions corresponding to the $C^{[o]}$, $C^{[+1]}$, $C^{[+2]}$, and $C^{[+3]}$ oxidation states.
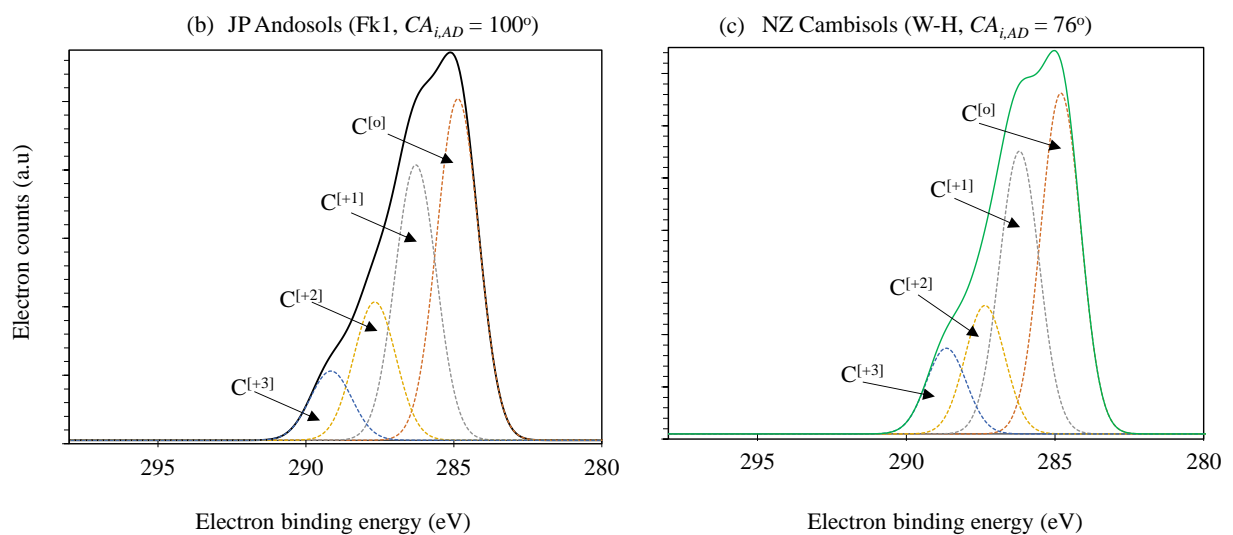

Figure 4.8 (a) decomposition of carbon spectrum of Andosols at each oxidation states and (b) decomposition of carbon spectrum of cambisols at each oxidation states which showing the distribution of chemical functions.

Each measured C-peaks were plot against to the sample sites to find relationship with SWR (Fig. 4.9). It shows that high $C^{[o]}$ in water repellent soil than that of other states, and also a sub-critical water repellent soil samples shows the high $C^{[+1]}$ than other oxidation states.
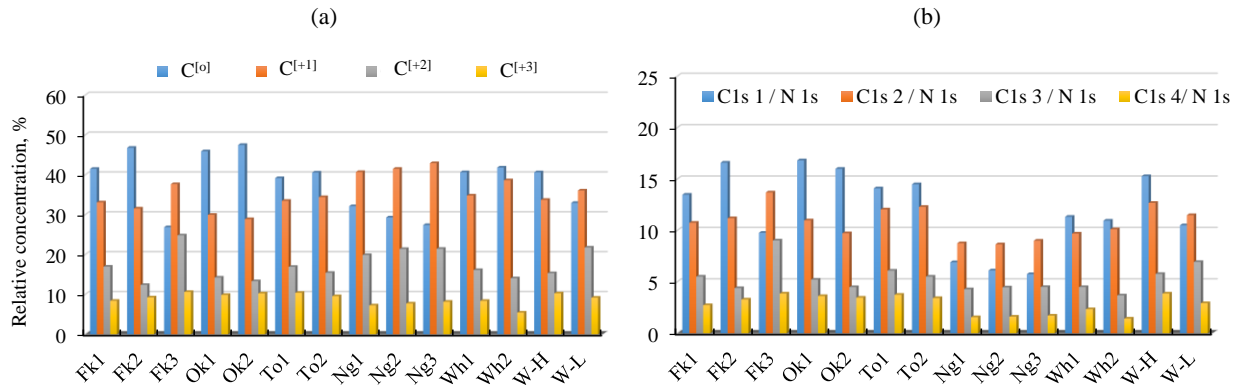

Figure 4.9 (a) Relative abundance of Carbon oxidation states ($C^{[o]}$, $C^{[+1]}$, $C^{[+2]}$ and $C^{[+3]}$) for different soil samples and (b) C/N ratios for each oxidation states.

4.4 Conclusions

Air-dried and 2-mm sieved soil samples (~1.0 mg) were used for X-ray photoelectron spectroscopy (XPS) measurements. Each soil samples were calculated the relative C, O and N concentration by using peak area of each 1s orbital spectra. Peak separations were done to estimate $C^{[o]}$, $C^{[+1]}$, $C^{[+2]}$ and $C^{[+3]}$ for each soil sample. The results show higher concentration of $C^{[o]}$ (C-C or C-H functional groups) than concentrations of the other oxidation states in water repellent soil. Sub-critical water repellent soil samples showed higher concentration of $C^{[+1]}$ (C-O or C-N functional groups) than of other oxidation states. The calculated SWR parameters were plotted with measured relative atomic concentration of C, O % and C/N ratio. Results revealed high SWR at high C/N ratio (determined by XPS) and show a liner regression (r^2 = 0.72) between C/N and the volumetric water content at maximum SWR (θ_{WR-max}). Soil was not water repellent at the high atomic concentration of O (> 65 %) and low C (< 35 %) combination.

4.5 References

Amelung, W., Kaiser, K., Kammerer, G., Sauer, G., 2002. Organic carbon at soil particle surfaces—evidence from x-ray photoelectron spectroscopy and surface abrasion. Soil Sci. Soc. Am. J. 66, 1526. doi:10.2136/sssaj2002.1526.

Bachmann, J., Ellies, A., Hartge, K.H., 2000. Development and application of a new sessile drop contact angle method to assess soil water repellency. J. Hydrol. 231–232, 66–75. doi:10.1016/S0022-1694(00)00184-0.

Chau, H.W., Biswas, A., Vujanovic, V., Si, B.C., 2014. Relationship between the severity, persistence of soil water repellency and the critical soil water content in water repellent soils. Geoderma 221–222, 113–120. doi:10.1016/j.geoderma.2013.12.025.

Dexter, A.R., Richard, G., Arrouays, D., Czyż, E.A., Jolivet, C., Duval, O., 2008. Complexed organic matter controls soil physical properties. Geoderma 144, 620–627. doi:10.1016/j.geoderma.2008.01.022.

Doerr, S.H., Shakesby, R.A., Dekker, L.W., Ritsema, C.J., 2006. Occurrence, prediction and hydrological effects of water repellency amongst major soil and land-use types in a humid temperate climate. Eur. J. Soil Sci. 57, 741–754. doi:10.1111/j.1365-2389.2006.00818.x.

Doerr, S.H., Shakesby, R.A., Walsh, R.P.D., 2000. Soil water repellency: its causes, characteristics and hydro-geomorphological significance. Earth-Sci. Rev. 51, 33–65. doi:10.1016/S0012-8252(00)00011-8.

Gerin, P. a., Genet, M. j., Herbillon, A. j., Delvaux, B., 2003. Surface analysis of soil material by X-ray photoelectron spectroscopy. Eur. J. Soil Sci. 54, 589–604. doi:10.1046/j.1365-2389.2003.00537.x.

Hiradate, S., 2004. Speciation of aluminum in soil environments. Soil Sci. Plant Nutr. 50, 303–314. doi:10.1080/00380768.2004.10408483

Hiradate, S., Hirai, H., Hashimoto, H., 2006. Characterization of allophanic Andisols by solid-state 13 C, 27 Al, and 29 Si NMR and by C stable isotopic ratio, δ 13 C. Geoderma 136, 696–707.

Jansen, R.J.J., van Bekkum, H., 1995. XPS of nitrogen-containing functional groups on activated carbon. Carbon 33, 1021–1027. doi:10.1016/0008-6223(95)00030-H

Karunarathna, A.K., Moldrup, P., Kawamoto, K., de Jonge, L.W., Komatsu, T., 2010. Two-Region Model for Soil Water Repellency as a Function of Matric Potential and Water Content. Vadose Zone J. 9, 719. doi:10.2136/vzj2009.0124.

Kawamoto, K., Moldrup, P., Komatsu, T., de Jonge, L.W., Oda, M., 2007. Water Repellency of Aggregate Size Fractions of a Volcanic Ash Soil. Soil Sci. Soc. Am. J. 71, 1658. doi:10.2136/sssaj2006.0284.

Kobayashi, M., Matsui, H., 2006. Surface chemical composition of soil aggregates as a controlling factor of water repellency of forest soils. Jpn. J. Soil Sci. Plant Nutr. Jpn.

Leelamanie, D. a. L., Karube, J., 2007. Effects of organic compounds, water content and clay on the water repellency of a model sandy soil. Soil Sci. Plant Nutr. 53, 711–719. doi:10.1111/j.1747-0765.2007.00199.x.

Monteil-Rivera, F., Brouwer, E.B., Masset, S., Deslandes, Y., Dumonceau, J., 2000. Combination of X-ray photoelectron and solid-state 13C nuclear magnetic resonance spectroscopy in the structural characterisation of humic acids. Anal. Chim. Acta 424, 243–255. doi:10.1016/S0003-2670(00)01139-9.

Watanabe, A., Tsutsuki, K., Inoue, Y., Maie, N., Melling, L., Jaffé, R., 2014. Composition of dissolved organic nitrogen in rivers associated with wetlands. Sci. Total Environ. 493, 220–228. doi:10.1016/j.scitotenv.2014.05.095.

Watts, J.F., Wolstenholme, J., 2003. An Introduction to Surface Analysis by XPS and AES. Introd. Surf. Anal. XPS AES John F Watts John Wolstenholme Pp 224 ISBN 0-470-84713-1 Wiley-VCH May 2003 -1.

Yamashita, T., Hayes, P., 2008. Analysis of XPS spectra of Fe2+ and Fe3+ ions in oxide materials. Appl. Surf. Sci. 254, 2441–2449. doi:10.1016/j.apsusc.2007.09.063.

Yuan, G., Soma, M., Seyama, H., Theng, B.K.G., Lavkulich, L.M., Takamatsu, T., 1998. Assessing the surface composition of soil particles from some Podzolic soils by X-ray photoelectron spectroscopy. Geoderma 86, 169–181. doi:10.1016/S0016-7061(98)00049-4.
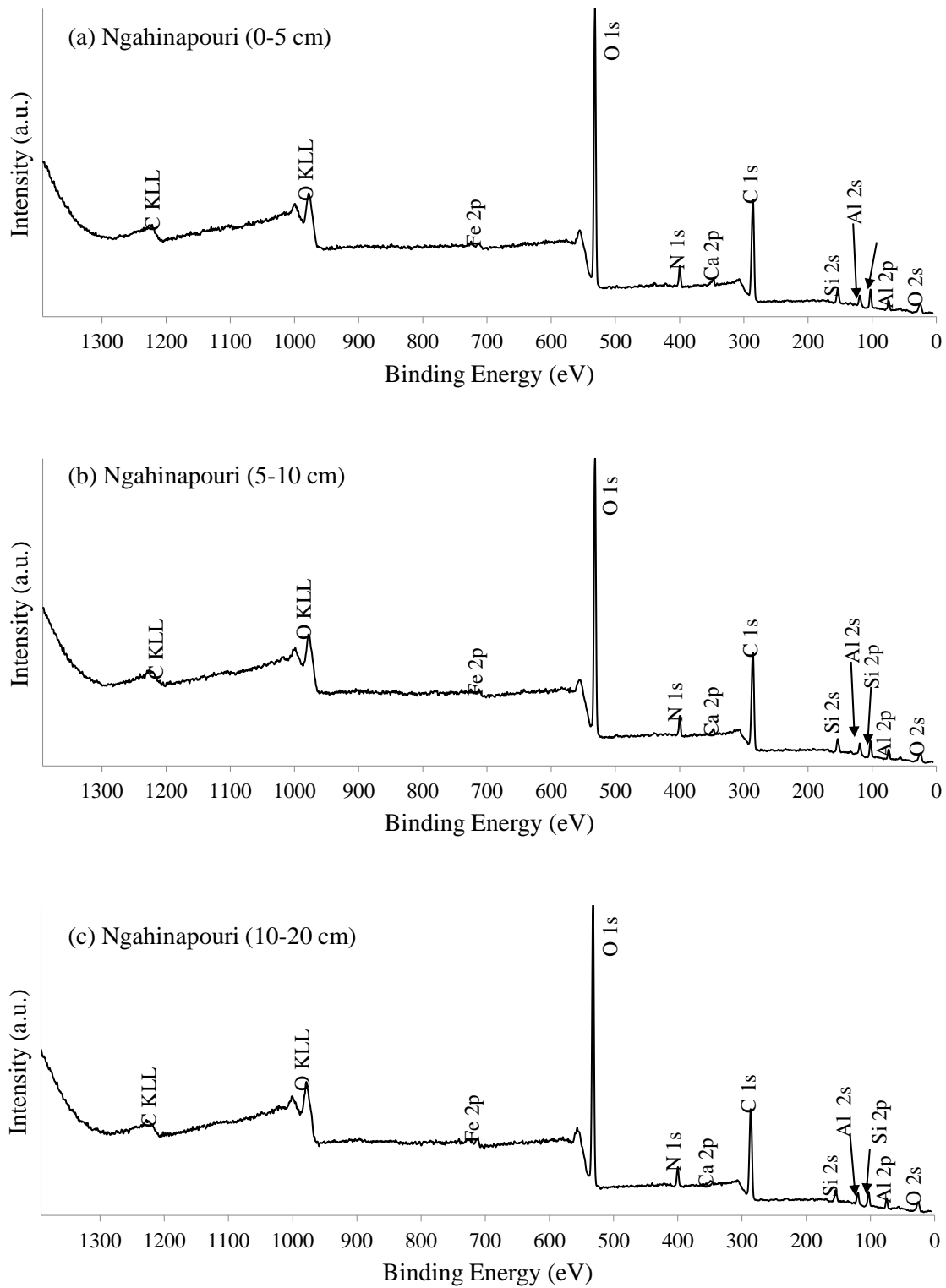
APPENDIX

A: Wide spectrum for Hiruzen, Okayama (a) 0-3 cm depth and (b) 3-6 cm depth soil samples
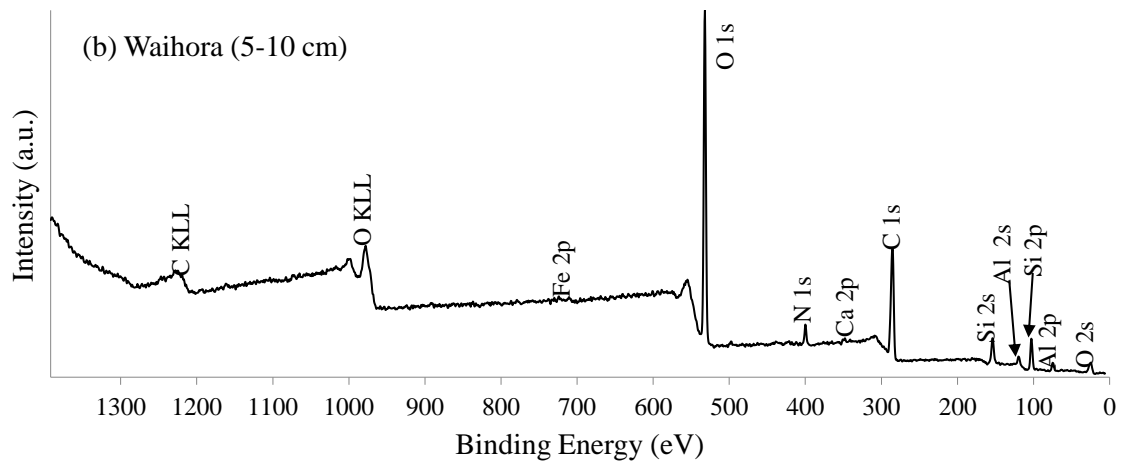

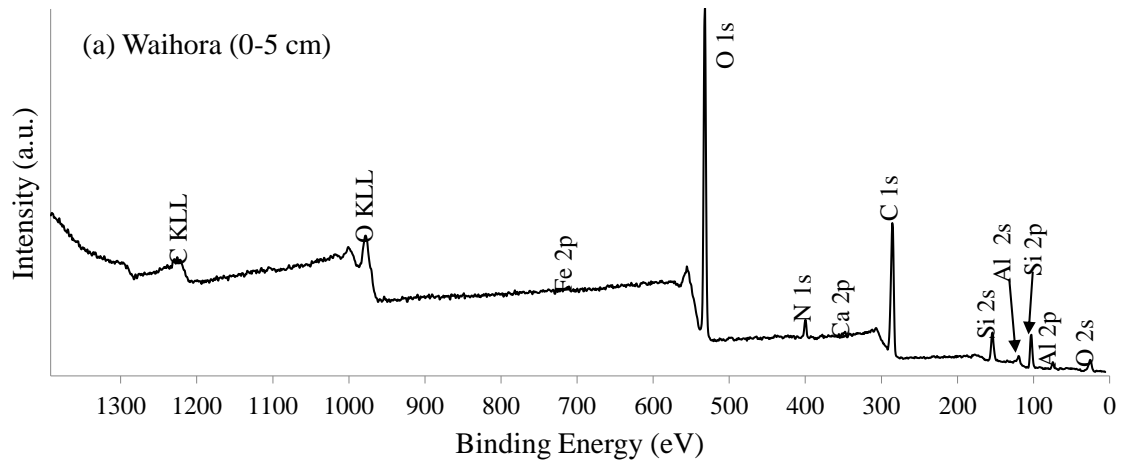(a) Okayama (0-3 cm)

(b) Okayama (3-6 cm)
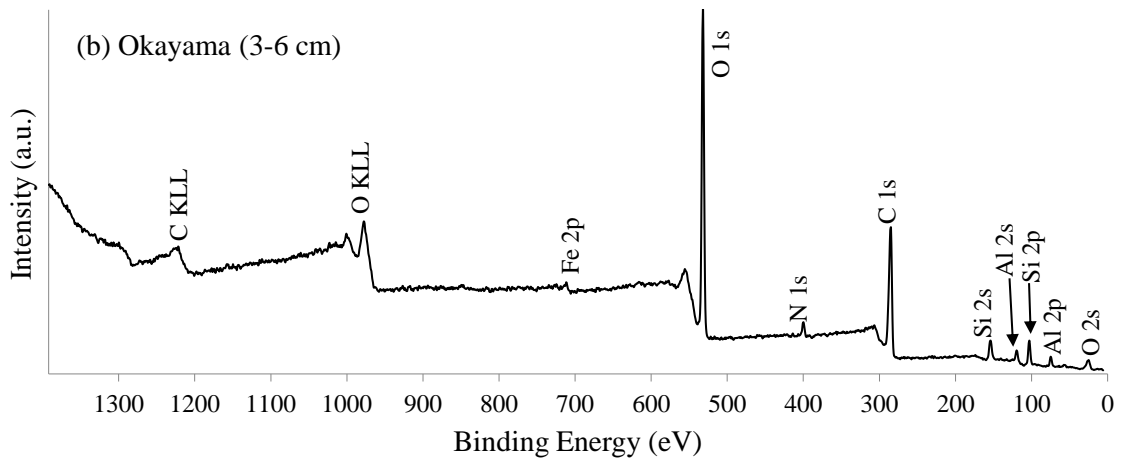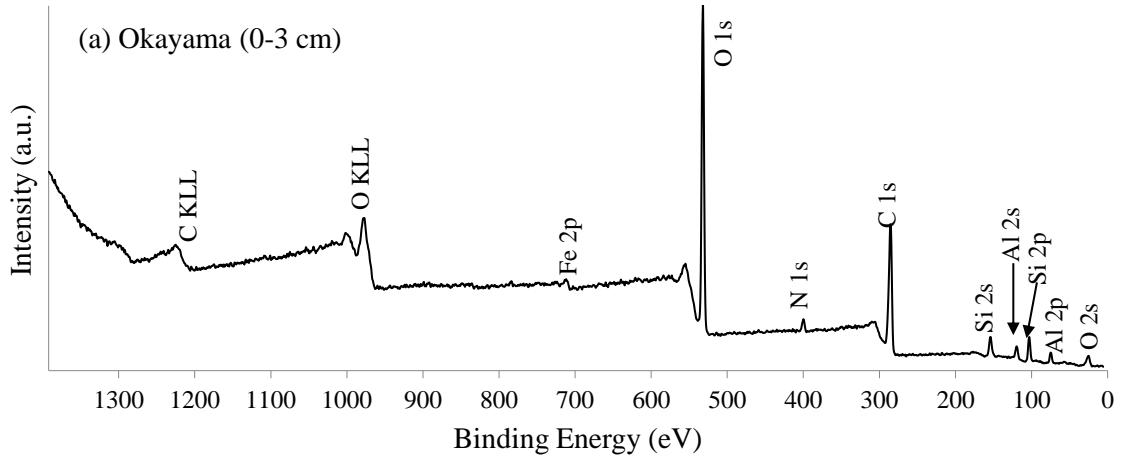
B: Wide spectrum for Nikko, Tochigi (a) 0-5 cm depth and (b) 5-34 cm depth soil samples.
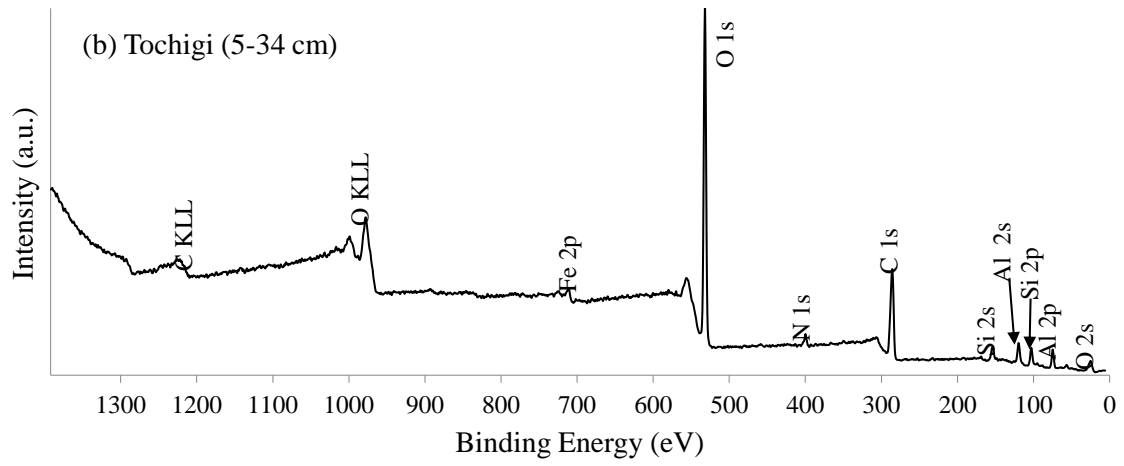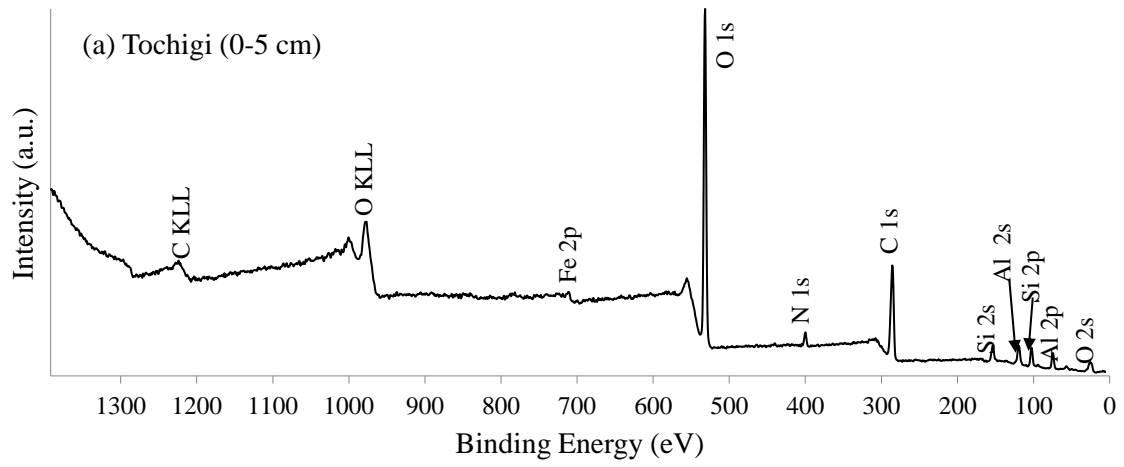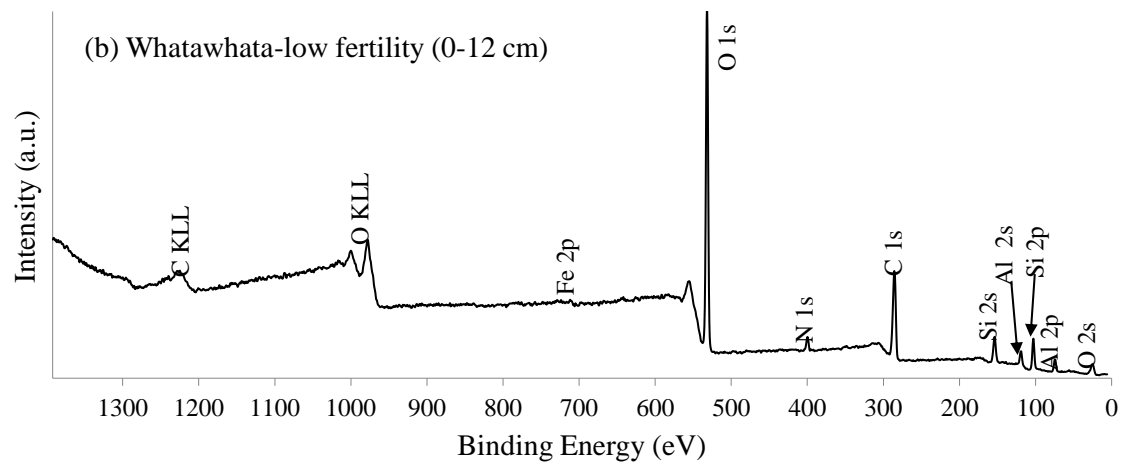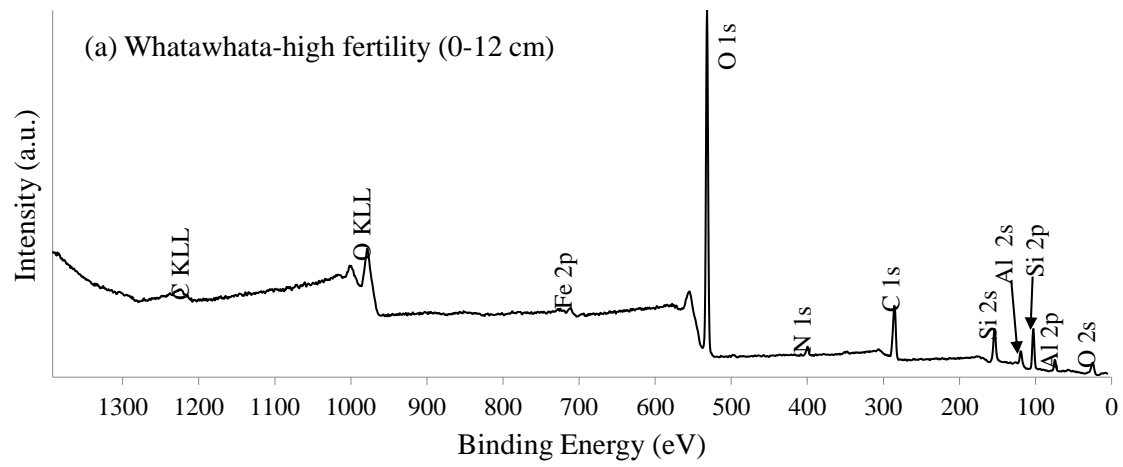
C: Wide spectrum for Ngahinapouri, Waikato (a) 0-5 cm depth, (b) 5-10 cm, and (c) 10-20 cm depth soil samples.

D: Wide spectrum for Waihora, Waikato (a) 0-5 cm and (b) 5-10 cm depth soil samples.

E: Wide spectrum for Whatawhata, Waikato (a) 0-12 cm, high fertility site and (b) 0-12 cm, low fertility site, soil samples.

Chapter 5

5. SUMMARY, CONCLUSIONS AND PERSPECTIVES

This study was done to characterize the soil water repellency for Japanese and New Zealand volcanic ash soils and for hydrophobized sand grains. In addition to that, chemical characterization of water repellent soils were evaluated using X-ray photoelectron spectroscopy. Mainly the Chapter 1 discuss the applicability of this water repellency phenomena to control water infiltration into solid waste landfill site by developing a capillary barrier cover system as an earthen cover system.

In Chapter 2, studied the grain hydrophobicity using six different grains with different geometries and sizes were used to prepare dry hydrophobized grains by mixing with different contents of oleic acid (OA) as a HA. Wet hydrophobized grains were prepared by adjusting the water content (θ_g; kg kg^{-1}) of dry hydrophobized grains. To characterize the water repellency (WR) of dry and wet hydrophobized grains, initial solid-water contact angles (α_i) were measured using the sessile drop method (SDM). Pearson correlation analysis was performed to identify correlations between proposed WR indices and basic grain properties. Results showed that WR indices correlated well to d_{50} and coefficient of uniformity (C_u) and regression equations for WR indices were obtained as functions of d_{50} and C_u ($r^2 > 0.7$).

In Chapter 3, studied the relationship between the degree of SWR and the soil volumetric water content (θ) can be described by the soil water repellency characteristics curve (SWRCC). In this study, six sites were selected from Japan (forest) and New Zealand (pasture). Different soil horizons were sampled with soil organic carbon contents ranging between 1 and 26%. We found that applying the *Dexter index* to separate water repellent soil from non-water repellent soil was successful only at the maximum SWR. Based on the SWRCCs, the following SWR parameters were introduced: (i) area under the curve ($S_{WR(\theta)}$); (ii) θ at maximum (θ_{WR-max}) and minimum (θ_{non-WR}) SWR, and (iii) maximum SWR (CA_{i-max}). Langmuir type equations provided the best fit for SWR parameters as a function of SOC with regression coefficients between 0.5 and 0.7.

In Chapter 4, studied the mainly the water repellent and non-water repellent soil to assess the soil surface composition of carbon, nitrogen and oxygen for Japan and New Zealand soils. The wide spectrum was recorded for all soil samples and then obtained high resolution narrow spectrum to measure the relative atomic concentration of C, N and O in 1s orbital. The measured surface soil compositions of C and C/N specifically effects on degree of SWR.

5.2 Conclusions

- Relationships between the WR indices and basic grain properties such as d_{50} and coefficient of uniformity (C_u), both in the cases of natural grains (non-round), dry and wet, hydrophobized grains highly useful for optimal material/grain selection when developing and designing hydrophobized capillary barrier cover systems.

- The combination of the three SWR methods was useful to understand the water drop persistence and degree of SWR for each soil type at different SOC and additionally SDM helps to find sub-critical SWR. The clay /SOC ratio was limited to differentiating water repellent from non-water repellent soil samples at air-dried conditions. The relationships between SWR parameters and SOC, % were introduced by fitting to Langmuir type equation:

- The calculated SWR parameters were plotted with C %, O % and C/N ratio, results reveled that high SWR at high C/N ratio (by XPS) and also positive correlation (+ 0.72) with volumetric water content at maximum SWR (θ_{WR-max}). Soil does not show water repellent at high atomic concentration of O1s and low C1s combination.

5.3 Perspectives

We found that fine and middle sand fractions are optimized to produce the hydrophobized sands. It should design a small-scale hydrophobized capillary barrier cover system to study the field-scale performance. A sand-witch type small CBCS layer can be introduce as an alternative final cover system. Evaluation of the CBCS performance should be conducted in terms of water balance study, hydraulic properties such as hydraulic conductivity variation.

Performance evaluation of the CBCS should covered different climatic regions. In Sri Lanka, spatial distribution of rain fall is very high. Wet zone is receiving > 2500 mm of average annual precipitation. Therefore, CBCS design requirement may be varied for dry zone and wet zone. To find the optimum condition we have to undergo field experiments at which areas having high rainfall and less rain fall. Additionally, characterization of hydrophobicity for locally available sands types has to be evaluated with different type of hydrophobic agents (low –cost and locally available).

PUBLICATIONS

Journal Articles

Wijewardana, Y.N.S, Kawamoto, K, Moldrup, P, Komatsu, T, Kurukulasuriya, L.C, Priyankara, N.H. (2015). Characterization of water repellency for Hydrophobized grains with Different Geometries and Sizes. *Environmental Earth Sciences* (*Accepted;* DOI: 10.1007/s12665-015-4565-6)

Wijewardana, Y.N.S., Muller, K., Kawamoto, K., Clothier, B., Komatsu, K., Hiradate, S., Moldrup, P., de Jonge, L.W. (2015). Soil water repellency characteristics curves for soil profiles with organic carbon gradients (*Manuscript prepared to submit Geoderma*).

Peer reviewed proceedings

Wijewardana, Y.N.S., K. Kawamoto, S. Subedi, P. Moldrup, S. Hamamoto, and T. Komatsu. 2013. Effect of water film thickness on the degree of water repellency for hydrophobized sand grains. Proceedings of the International Symposium on Advances in Civil and Environmental Engineering Practices for Sustainable Development (ACEPS 2013), 176-182, ISSN 2279-1329 (Oral. 27 September, 2013. Galle, Sri Lanka)

Wijewardana, Y.N.S., K. Kawamoto, T. Komatsu, S. Hamamoto, S, Subedi and p. Moldrup. 2013. Characterization of time-dependent contact angles for oleic acid mixed sands with different particle size fractions. Unsaturated soils: Research and apllications-n. Khalili, A. Russell and A. Khoshghalb (eds) (UNSAT 2014), 255-260, ISBN 978-1-138-00150-3 (Oral. 27 September, 2013. Galle, Sri Lanka)

Wijewardana, Y. N. S, K. Kawamoto, L. C. Kurukulasuriya, N. H. Priyankara, A. M. N. Alagiyawanna, M. I. M. Mowjood, M. Vithanage and G. B. Herath. Selection of Suitable Grain Materials for Development of Hydrophobized Capillary Barrier Cover Systems. Proceedings of the Special Session on Urban Water Environment: Monitoring & Management Solid Waste Management, Vol 5: 109-115. *5th International Conference on Sustainable Built Environment 2014 Kandy, Sri Lanka,* 12, 13 & 14th December 2014 ISBN: 978 – 955 – 589 – 187 – 5.

International conference abstract

WIJEWARDANA, Senani, KAWAMOTO, Ken, MULLER, Karin, CLOTHIER, Brent, HIRADATE, Syuntaro, KOMATSU, Toshiko, MOLDRUP, Per. Characterization of water repellency parameters in soil water repellency characteristic curves for JP and NZ soils. Japan Geoscience Union Meeting 2014. 28 April-2 May at Pacific Yokohama, Kanagawa, Japan.

Syuntaro Hiradate, Ken Kawamoto, Nadeeka Senani Wijewardana, Karin Müller, Per Møldrup, Brent Clothier, Toshiko Komatsu. Orientation of functional groups of soil organic matter on the surface of water repellent soils determined by pulse saturation magic angle spinning (PSTMAS) nuclear magnetic resonance (NMR) spectroscopy. Geophysical Research abstracts, Vol. 16 EGU2014-13697, 2014, EGU General Assembly 2014.

K. Müller, K. Kawamoto, R. Simpson, K. Mason, C. van den Dijssel, Y.N.S. Wijewardana, S. Hiradate, T. Komatsu, B.E. Clothier, Soil water repellency impacts runoff and phosphorous losses. NZ Society of Soil Science Conference "Soil Science for Future Generations" 1 - 4 December 2014 - The University of Waikato, Hamilton.

H. Kuroki, Y. N. S. Wijewardana, K. Kawamoto, K. Müller, S. Hiradate, H. Maki, T. Komatsu, and B. Clothier. Mass transport parameters in gaseous and aqueous phases for water repellency affected agricultural soil. NZ Society of Soil Science Conference "Soil Science for Future Generations" 1 - 4 December 2014 - The University of Waikato, Hamilton.

KUROKI, Hisanabu., WIJEWARDANA, Senani, KAWAMOTO, Ken, HIRADATE, Syuntaro, MULLER, Karin, CLOTHIER, Brent, KOMATSU, Toshiko, MAKI, Hiroyuki. (2015). Consideration of various factors on the expression of soil water repellency. Japan Geoscience Union Meeting 2015. 24th to 28 May, 2015at Makuhari, Chiba, Japan.